Cooperative Diversity Techniques for Future Wireless Communications Systems

Submitted to the School of Engineering in fulfillment of the academic requirements for the degree of Doctor of Philosophy in Electronic Engineering

at the

UNIVERSITY OF KWAZULU-NATAL

By

Jules Merlin Mouatcho Moualeu, BSc.Eng., MSc.Eng.

School of Engineering

University of KwaZulu-Natal

Durban, South Africa

Cooperative Diversity Techniques for Future Wireless Communications Systems

Submitted by Jules Merlin Mouatcho Moualeu

in fulfillment of the requirements for the degree of

Doctor of Philosophy

Professor Hongjun Xu

Thesis Supervisor

Professor Fambirai Takawira

Thesis Co-Supervisor

University of KwaZulu-Natal

2013

March 10, 2013

Dedication

TO GOD BE THE GLORY.

Abstract

Multiple-input multiple-output (MIMO) systems have been extensively studied in the past decade. The attractiveness of MIMO systems is due to the fact that they drastically reduce the deleterious effects of multipath fading leading to high system capacity and low error rates. In situations where wireless devices are restrained by their size and hardware complexity, such as mobile phones, transmit diversity is not achievable. A new paradigm called cooperative communication is a viable solution. In a cooperative scenario, a single-antenna device is assisted by another single-antenna device to relay its message to the destination or base station. This creates a virtual multiple-input multiple-output (MIMO) system.

There exist two cooperative strategies: amplify-and-forward (AF) and decode-and-forward (DF). In the former, the relay amplifies the noisy signal received from the source before forwarding it to the destination. No form of demodulation is required. In the latter, the relay first decodes the source signal before transmitting an estimate to the destination. In this work, focus is on the DF method. A drawback of an uncoded DF cooperative strategy is error propagation at the relay. To avoid error propagation in DF, various relay selection schemes can be used. Coded cooperation can also be used to avoid error propagation at the relay. Various error correcting codes such as convolutional codes or turbo codes can be used in a cooperative scenario. The first part of this work studies a variation of the turbo codes in cooperative diversity, that further reduces error propagation at the relay, hence lowering the end-to-end error rate. The union bounds on the bit-error rate (BER) of the proposed scheme are derived using the pairwise error probability via the transfer bounds

and limit-before-average techniques. In addition, the outage analysis of the proposed scheme is presented. Simulation results of the bit error and outage probabilities are presented to corroborate the analytical work. In the case of outage probability, the computer simulation results are in good agreement with the the analytical framework presented in this chapter.

Recently, most studies have focused on cross-layer design of cooperative diversity at the physical layer and truncated automatic-repeat request (ARQ) at the data-link layer using the system throughput as the performance metric. Various throughput optimization strategies have been investigated. In this work, a cross-relay selection approach that maximizes the system throughput is presented. The cooperative network is comprised of a set of relays and the reliable relay(s) that maximize the throughput at the data-link layer are selected to assist the source. It can be shown through simulation that this novel scheme outperforms from a throughput point of view, a system throughput where the all the reliable relays always participate in forwarding the source packet.

A power optimization of the best relay uncoded DF cooperative diversity is investigated. This optimization aims at maximizing the system throughput. Because of the non-concavity and non-convexity of the throughput expression, it is intractable to derive a closed-form expression of the optimal power through the system throughput. However, this can be done via the symbol-error rate (SER) optimization, since it is shown that minimizing the SER of the cooperative system is equivalent to maximizing the system throughput. The SER of the retransmission scheme at high signal-to-noise ratio (SNR) was obtained and it was noted that the derived SER is in perfect agreement with the simulated SER at high SNR. Moreover, the optimal power allocation obtained under a general optimization problem, yields a throughput performance that is superior to non-optimized power values from moderate to high SNRs.

The last part of the work considers the throughput maximization of the multi-relay adaptive DF over independent and non-identically distributed (i.n.i.d.) Rayleigh fading channels, that integrates ARQ at the link layer. The aim of this chapter is to maximize the system

throughput via power optimization and it is shown that this can be done by minimizing the SER of the retransmission. Firstly, the closed-form expressions for the exact SER of the multi-relay adaptive DF are derived as well as their corresponding asymptotic bounds. Results showed that the optimal power distribution yields maximum throughput. Furthermore, the power allocated at a relay is greatly dependent of its location relative to the source and destination.

Declaration

I, _____, declare that:

(i) The research reported in this thesis, except where otherwise indicated, is my original work.

(ii) This thesis has not been submitted for any degree or examination at any other University.

(iii) This thesis does not contain other persons' data, pictures, graphs or information, unless specifically acknowledged as being sourced from other persons.

(iv) This thesis does not contain other persons' writings, unless specifically acknowledged as being sourced from other researchers. Where other written sources have been quoted, then:

  (a) Their words have been re-written but the general information attributed to them has been referenced;

  (b) Where their exact words have been used, their writing has been placed inside quotation marks, and referenced.

(v) Where I have reproduced a publication of which I am an author, co-author or editor, I have indicated in detail which part of the publication was actually written by myself alone and have fully referenced such publication.

(vi) This thesis does not contain text, graphics or tables copied and pasted from the internet unless specifically acknowledged, the source being detailed in the thesis and in the References section.

Signed: _____

As the candidate's supervisor, I agree to the submission of this thesis

Signed: _____

Name: _____ Date: _____

Acknowledgments

This thesis would not have be completed without the guidance, support and valuable comments of my supervisor Professor Hongjun Xu. I would also like to express my appreciation to my co-supervisor Professor Fambirai Takawira, director of the Centre for Radio Access and Rural Technologies (CRART) for giving me the opportunity to pursue my studies under his supervision and the financial support he has provided throughout the duration of this work. I am most grateful to Professor Walaa Hamouda for his patience and giving me the opportunity to work under his guidance. His valuable comments, constructive criticism and everlasting support have greatly contributed towards the completion of this work and more importantly shaped my research abilities and growth. I am also thankful to Dr. Telex Ngatched for insight on many aspects of my work and the discussions we have had on several occasions. He was always there to provide advice, to encourage me and boost my confidence during tough times.

I am also indebted to my parents for their sacrifice from the day I came in this world and always believing in me. Many thanks to my uncle Dr. Jean-Michel Tchuenche who has been a role model, my brothers and sister for their constant encouragement and endless support throughout this research work. I could not end without thanking my lovely fiancée Nina who has always been there to support me, as well as my parents-in-law for their immense support, encouragement and everlasting love.

Finally, special thanks also go Ali Faraj from the Wireless Communications Research Lab

at Concordia University and Dieter Duyck from the DIGCOM Research Group at Ghent University, for the various discussions we have had on some aspects of my work, as well as my colleagues Rudy Pillay, Seare Rezenom, Farzad Ghayour, John Msumba, Remmy Musumpuka, Ilesanmi Oluwafemi, Chrispin Mulangu, Gbolahan Aiyetoro for the interesting discussions on various topics. I would also like to thank my flatmates and friends William and Renée for their friendship and the time we have shared throughout this journey. Finally, I would like to express my gratitude to Professor Jules-Raymond Tapamo and his wife for always welcoming me in their home and for their support since I started my tertiary studies.

Contents

List of Figures

List of Tables

List of Symbols

b	Number of bits per symbol
d	Hamming distance
d_f	Free Hamming distance
d_{ij}	Distance between node i and node j
$C(\bullet)$	Instantaneous capacity
D	Destination node
$\mathbb{E}\langle\bullet\rangle$	Statistical average operator
erfc	Complementary error function
E_b	Signal transmitted energy per bit
E_s	Signal transmitted energy per symbol
E_1	Recursive systematic convolutional encoder 1
E_2	Recursive systematic convolutional encoder 2
f	Trade-off parameter for listening-transmit time
$f_X(\bullet)$	Probablity density function of random variable X
$F_X(\bullet)$	Cumulative density function of random variable X
${}_1F_1(\bullet,\bullet;\bullet)$	Confluent Hypergeometric function

${}_2F_1(\bullet,\bullet,\bullet;\bullet)$	Gauss Hypergeometric function
$\Gamma(\bullet)$	Gamma function
$\Gamma(\bullet,\bullet)$	Upper incomplete Gamma function
$\mathcal{G}$	Generator polynomial
$\mathcal{H}$	Hessian Matrix
$h_{_{SD}}$	Complex fading channel coefficient from source node to destination node
$h_{_{SR}}$	Complex fading channel coefficient from source node to relay node
$h_{_{RD}}$	Complex fading channel coefficient from relay node to destination node
m_{sd}	Nakagami-m fading parameter of the source-to-destination link
m_{sr}	Nakagami-m fading parameter of the source-to-relay link
m_{rd}	Nakagami-m fading parameter of the relay-to-destination link
π	Interleaver
K	Packet length
$L(x)$	Log-likelihood ratio
M	Modulation order
$\mathcal{M}_X(\bullet)$	Moment generating function of random variable X
η	System throughput
$n_{_{SD}}$	Additive white Gaussian noise from source node to destination node
$n_{_{SR}}$	Additive white Gaussian noise from source node to relay node
$n_{_{RD}}$	Additive white Gaussian noise from relay node and destination node
N_0	Noise power spectral density
$\overline{P}_b$	Average bit error probability

P_{sd}	Transmitted power from source node to destination node
P_{sr}	Transmitted power from source node to relay node
P_{rd}	Transmitted power from relay node to destination node
P_{out}	Outage probability
$P\left(d\right)$	Average pairwise error probability
$Q(\bullet)$	Gaussian Q-function
R	Relay node
R_c	Code rate
S	Source node
γ	Instantaneous signal-to-noise ratio
$\bar{\gamma}$	Average signal-to-noise ratio
$\varphi(\bullet, \bullet)$	Lower incomplete Gamma function
y_{SD}	Received signal from source node to destination node
y_{SR}	Received signal from source node to relay node
y_{RD}	Received signal from relay node to destination node
$\mid \bullet \mid$	Cardinality
Θ	Set of indices of cooperative relays
σ_{sd}^2	Noise variance from source node to destination node
σ_{sr}^2	Noise variance from source node to relay node
σ_{rd}^2	Noise variance from relay node to destination node

List of Acronyms

ACK positive acknowledgement

AF amplify-and-forward

AMC adaptive modulation and coding

ARQ automatic-repeat request

AWGN additive white Gaussian noise

BER bit-error rate

BPSK binary phase shift keying

BSC binary symmetric channel

CDF cumulative density function

CRC cyclic redundancy check

CSI channel state information

dB decibels

DF decode-and-forward

EPA equal power allocation

EXIT extrinsic mutual information transfer

FEC forward-error correction

FER frame-error rate

FDM frequency division multiplexing

FG factor graph

i.i.d. independent and identically distributed

i.n.i.d. independent and non-identically distributed

4G fourth generation

LDPC low-density parity-check

LLR log-likelihood ratio

MAP maximum *a posteriori* probability

MIMO multiple-input multiple-output

MISO multiple-input single-output

MRC maximum ratio combiner

MGF moment generating function

NACK negative acknowledgement

OPA optimal power allocation

PEP pairwise error probability

PER packet-error rate

PDF probability density function

M-QAM M-ary Quadrature Amplitude Modulation

PCCC parallel concatenated convolutonal code

RC rate-compatible

RCPC rate-compatible puntured convolutional

RSC recursive systematic convolutional

RF radio frequency

RV random variable

SER symbol-error rate

SDF soft decode-and-forward

SISO single-input single-output

STBC space-time block code

STC space-time codes

SNR signal-to-noise ratio

TAS transmit antenna selection

TCC turbo coded cooperation

TDMA time division multiple access

TDM time division multiplexing

Chapter 1

Introduction

1.1 Research Motivation

Over the past decade, there has been a significant growth in the demand for high data rates and uninterrupted connectivity in wireless communications systems, in order to support various applications that include video, voice, e-mail, file transfer, internet access, to name a few. Future wireless applications face many challenges that need to be addressed. One of them is bandwidth which is a scarce resource as its availability to a service provider is often limited since the use of radio spectrum is allocated and controlled in most countries by governement regulatory bodies. Another challenge is the improvement of the battery life for wireless devices. In order to achieve that and to keep the devices as small as possible, minimum power is required. From the challenges mentioned above, the designers are faced with a difficult task, that is, to achieve high data rates while utilizing a reasonable allotment of the spectrum. Transmitting over a reliable channel in a wireless environment is a challenge, unlike the wired channel. This is due to the fact that, the wireless channel is an unpredictable and difficult communications medium. The transmission of a signal over a wireless channel is received through out-of-phase multipaths which can add constructively or destructively. When they add destrutively, they cause deep attenuation in the received signal, resulting in

severe degradation of the system performance (error probability). This deep attenuation in the received signal is referred to as *fading*.

One of the most efficient and powerful techniques to increase robustness against fading or accomplish reliable communication over a wireless channel is called *diversity*. The idea behind this technique is that, the receiver sees multiple, independent faded copies of the transmitted signal. In this case, the probability that all the replicas undergo deep fades is very small; having said that, at least one of the replicas will be received correctly. There are various forms of diversity [1]- [4]: time diversity, frequency diversity, spatial diversity, modulation diversity, etc. In time diversity, the signal is modulated through different periods of time, whereas in frequency diversity, the signal is transmitted through different carriers. Spatial or antenna diversity represents a very effective method to combat the deleterious effects of fading. In the latter, the signal is transmitted or received using multiple antennas. These antennas (transmitter or receiver) should be separated by a few wavelengths for the multiple replicas of the transmitted signal to undergo independent fading. Such systems often referred to as multiple-input multiple-output (MIMO) systems [5]- [6] have proved to be an effective way to improve capacity and provide diversity gain, resulting in much more reliable wireless transmission compared to single-input single-output (SISO) systems. To further improve the system performance, Alamouti [7] and Tarokh *et al.* [8] proposed other diversity techniques using suitably designed transmitted signals at the multi-antenna transmitter. The resulting technique is referred to as space-time coding.

However, multiple antennas cannot be deployed in scenarios where terminals are limited by their size or hardware constraints. In order to overcome these limitations, a novel approach termed *cooperative communications* [9]- [13] has been proposed as a viable solution for the high-data rate coverage required in future wireless applications, including wireless sensor networks, fourth generation (4G) cellular networks, broadband wireless channels. In cooperative diversity networks, several terminals form a distributed MIMO system. A source node broadcasts a message to a set of relay nodes that appear in the vicinity, and in turn those

relays forward the source message to the destination node. The destination nodes combine the signal from the direct transmission (source to destination) and the signals transmitted from the relay nodes. Laneman [13] and Nabar [15] have shown that the occurrence of errors at the relay nodes greatly degrades the end-to-end performance. If the source-to-relay links are good, perfect detection is possible at the relay nodes and full diversity is maintained. However, worse source-to-relay links will result in poor detection at the relays. Various methods exist in the literature to avoid error propagation. In coded cooperation [18]- [19], there is no attempt to correct the erroneous message when error detection occurs. This motivates the development of a coded system in user cooperation to avoid error propagation, thus enhancing the end-to-end system performance. Furthermore, cross-layer designs that integrate cooperative diversity at the physical layer and truncated automatic-repeat request (ARQ) at the link layer have been investigated in [20]- [22]. In most cases, all the reliable relays participate in the retransmission. Selecting all the reliable relays to retransmit does not necessarily yield an optimal throughput at the link layer. This is a problem addressed in this dissertation.

1.2 Thesis Contributions

The main contributions in this thesis are summarized in this section:

1.2.1 Multi-relay Turbo-Coded Cooperative Diversity Networks over Nakagami-m Fading Channels

In this Chapter, the performance of turbo codes in multi-relay cooperative diversity networks over slow independent and identically distributed (i.i.d.) and independent and non-identically distributed (i.n.i.d.) Nakagami-m fading channels with positive fading severity index is studied. In the proposed scheme, all the relays dedicate a certain amount of time to listen to the information bits sent by the source prior to performing decoding. Only

the error-free relays are able to retransmit to the destination in the second time slot the parity or punctured bits. Union bounds on the bit-error rate (BER) using the transfer function bounding and the limit-before-average techniques are derived. Furthermore, the asymptotic behaviour of the system at high signal-to-noise ratio (SNR) using the pairwise error probability (PEP) is examined. A closed-form analytical expression of the outage probability for various numbers of relays and different fading parameters is also derived. Its asymptotic behavior suggests that the achievable diversity order depends on the number of cooperating relays and/or fading severity indices. Finally, simulation and analytical results are presented for performance evaluation of the proposed scheme.

1.2.2 Cross-layer Relay Selection Scheme for Cooperative Networks

In this Chapter, a cross-layer relay selection approach that maximizes the link-layer throughput is proposed. In this approach, the set of reliable relays that participate in the retransmission phase are the ones that provide maximum link-layer throughput and this set is determined at the destination via an exhaustive search. A joint optimization of packet length and constellation size for the proposed scheme is also investigated. The results show that the proposed approach (CROSS-layer) which assigns transmission to relays that see better channel conditions outperforms the PHY-layer approach used for comparison, in terms of throughput performance. Moreover, the CROSS-layer approach is more attractive since it incurs less bandwidth penalty than the PHY-layer approach does. This can be explained by noting that in CROSS-layer not all the reliable relays are used during every retransmission whereas in PHY-layer all the reliable relays always participate in the retransmission.

1.2.3 Cross-layer Throughput Maximization via Power Optimization in Cooperative Networks

In this Chapter, cross-layer design including a relay selection at the physical layer combined with truncated ARQ at the data-link layer in order to improve the system bandwidth efficiency and the overall throughput is investigated. In the sequel, it is shown that the overall throughput is dependent on the SER of the retransmission where minimizing the SER greatly improves the throughput. Prior to formulating the optimization problem, an asymptotic SER for the best DF relay selection is derived that will enable evaluation of the optimal allocated power at the source and best relay for different modulation schemes through a general optimization problem. It is shown that the asymptotic SER of the retransmission derived in this Chapter, is in perfect agreement with our simulations. In addition, the throughput performance with optimal power allocation is superior to the one with non-optimized power values from moderate to high SNR.

1.2.4 Power Assignment in Multi-relay Adaptive DF Cooperative Networks

A power assignment scheme in multirelay adaptive DF cooperative-diversity networks over non-identical Rayleigh fading channels, that integrates truncated ARQ at the link layer is investigated. At the cooperative level, only the reliable relays participate in the retransmission phase if necessary. In this Chapter, the aim is to maximize the system throughput via power optimization and it is shown that this can be done by minimizing the SER of the retransmission. The closed- form expressions for the exact SER of the multi-relay adaptive DF over non-identical Rayleigh fading channels as well as the asymptotic bounds for the SER are derived. Results show that the analytical bounds for the SER corroborate the simulated SER at high SNR and maximum throughput is achieved through optimal power allocated at the source and various reliable relays.

1.3 Thesis Organization

The rest of the thesis is organized as follows. Chapter 2 presents a review of cooperative diversity, turbo codes and retransmission protocols. First, the two main cooperative strategies are described. A brief discussion on some cooperative protocol based on the first and second time slots transmission is also presented. In Chapter 3, a variation of the conventional turbo coded cooperation (TCC) in a multi-relay environment over slow independent and identically distributed (i.i.d.) and independent and non-identically distributed (i.n.i.d.) Nakagami-m fading channels is proposed. Assuming binary phase shift keying (BPSK) transmission, the union bounds on the BER on one hand and the exact outage probability on the other hand are derived. Simulation results are presented to verify the accuracy of the proposed analytical work. Chapter 4 investigates the cross-layer relay selection scheme for cooperative networks. In this scheme, the criterion for relay selection is throughput based, that is, the selected relays are the ones that maximize the link-layer throughput. In Chapter 5, throughput maximization via power optimization of the best relay is studied. An asymptotic expression for the SER of the best relay DF cooperative network is derived and is shown to yield tight bounds with the exact SER at high SNR. For this reason, a power optimization problem is formulated using the the derived asymptotic SER as the objective function. In Chapter 6, the multi-relay adaptive relay scenario with non-identical fading channels is presented. Closed-form expressions for the exact and asymptotic SER of the scheme under study for various modulation levels are derived. Morever, power optimization on the reliable relays is studied and results show that the relays that are closer to the source than the destination are allocated more power than their counterparts which are closer to the destination. Finally conclusions are drawn in Chapter 7 and future work is presented.

1.4 Published/Submitted Work

- J. M. Moualeu, W. Hamouda, H. Xu, and F. Takawira, "Cross-layer Relay Selection Criterion for Cooperative-Diveristy Networks," in Proc. *IEEE International Conference on Communications (ICC'12)*, Ottawa, Canada, 10–15 June, 2012.

- J. M. Moualeu, W. Hamouda, H. Xu, and F. Takawira, "Power Assignment in Multi-relay Adaptive DF Cooperative Networks," in Proc. *IEEE Global Telecommunications Conference (GLOBECOM'12)*, Anaheim, California, 03–07 December, 2012.

- J. M. Moualeu, W. Hamouda, H. Xu, and F. Takawira, "Multi-relay Turbo-Coded Cooperative Diversity Networks over Nakagami-m Fading Channels," Accepted for publication in the *IEEE Transactions on Vehicular Technology*.

- J. M. Moualeu, W. Hamouda, H. Xu, and F. Takawira, "Performance of Distributed Turbo-Coded Cooperative Networks with Multiple Dual-Hop Relays over Nakagami-m Fading Channels," Accepted for presentation at the *IEEE Wireless Communications and Networking Conference (WCNC'13)*, Shanghai, China, 07–10 April, 2013.

Chapter 2

Literature Review

2.1 General Background of Cooperative Diversity Networks

Cooperative diversity allows for single-antenna devices often limited by their size, to share their antennas and mimic a MIMO system. In a given network, most transmissions can be overheard by peers due to the broadcast nature of the wireless medium. This is done at no additional costs: transmission power and bandwidth. Moreover, a given destination combines the signals from the different nodes that have undergone independent channel fading statistics. Figure 2.1 illustrates a cooperative diversity scenario. The communication takes place in two time slots, since the relay cannot operate in full duplex, that is, it cannot transmit and receive simultaneously. In the first time slot, the source node (S) transmits its information bits to the destination node (D). A relay node (R) that belongs to the network, may overhear S and provides D with another version of the original signal through different channel fading coefficients.

There are two main cooperative relaying strategies: AF [14] and DF [12]. In the AF mode, the relay node amplifies the signal received from the source node and retransmits it

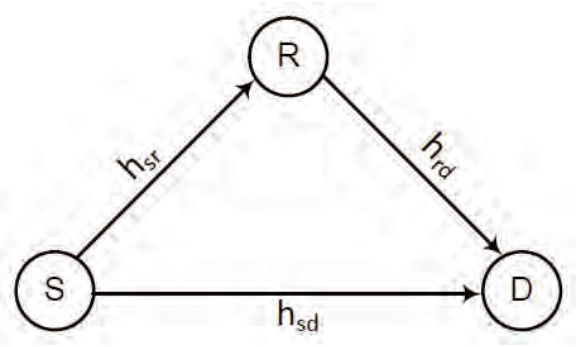

Figure 2.1: Cooperative diversity network.

to the destination. The amplified signal and the ampified noise form the retransmitted signal. The destination will combine the retransmitted signal and the information sent by the source in order to decide on the transmitted information. Despite the noise amplification at the relay, – more errors are expected at the destination – the destination is still able to correctly decode since it sees two independently faded versions of the original signal. This strategy is also known as analog relaying or non-regenerative relaying. For DF, the relay decodes the source message prior to retransmitting a new version to the destination. This strategy is also referred to as digital relaying or regenerative relaying. Both relaying strategies are depicted in Figure 2.2. Although the AF strategy is attractive due to to its simplicity and low computational complexity compared to DF, its practical implementation is not easy to achieve for the following reasons [23]:

- A large amount of data storage is required in time division multiplexing (TDM).

- In the case of frequency division multiplexing (FDM), expensive and complex tranceivers are needed.

For the above-cited reasons, DF is preferred in the studies in this thesis.

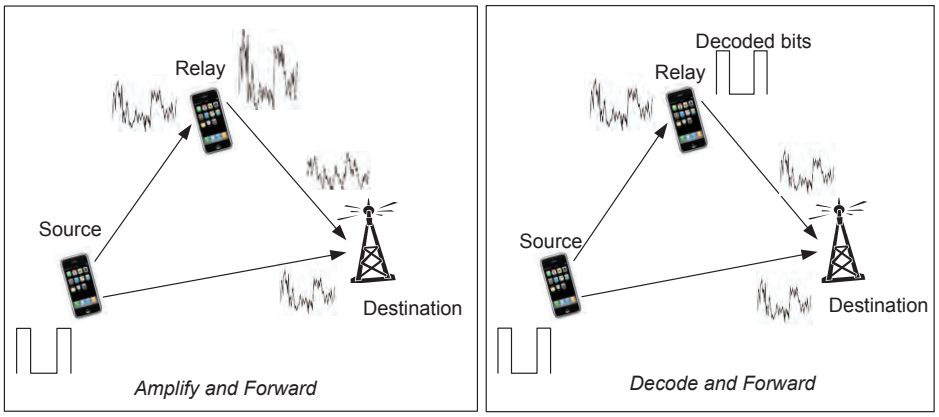

Figure 2.2: Cooperative relaying strategies: AF and DF.

2.2 Relaying Protocols

There are three time division multiple access (TDMA)-based cooperative protocols that have been discussed extensively in the existing literature since they provide some diversity gains [13], [15]. These protocols are named Protocol I, II and III. Because of the half-duplex nature of the relay node, each protocol is divided into two phases: the broadcasting phase or phase 1 and the cooperative phase or phase 2. These protocols are illustrated in Figure 2.3 shown in the next page.

2.2.1 System model

- **Protocol I**. Also known as *non-orthogonal* protocol, this protocol was proposed in [15]. In the DF mode, the source broadcasts to the relay and destination nodes during phase 1. The received signals y_{sr} at the relay, and y_{sd_1} destination during the the broadcasting phase are given respectively by

$$y_{sr} = h_{sr}x + n_{sr}, \tag{2.1}$$

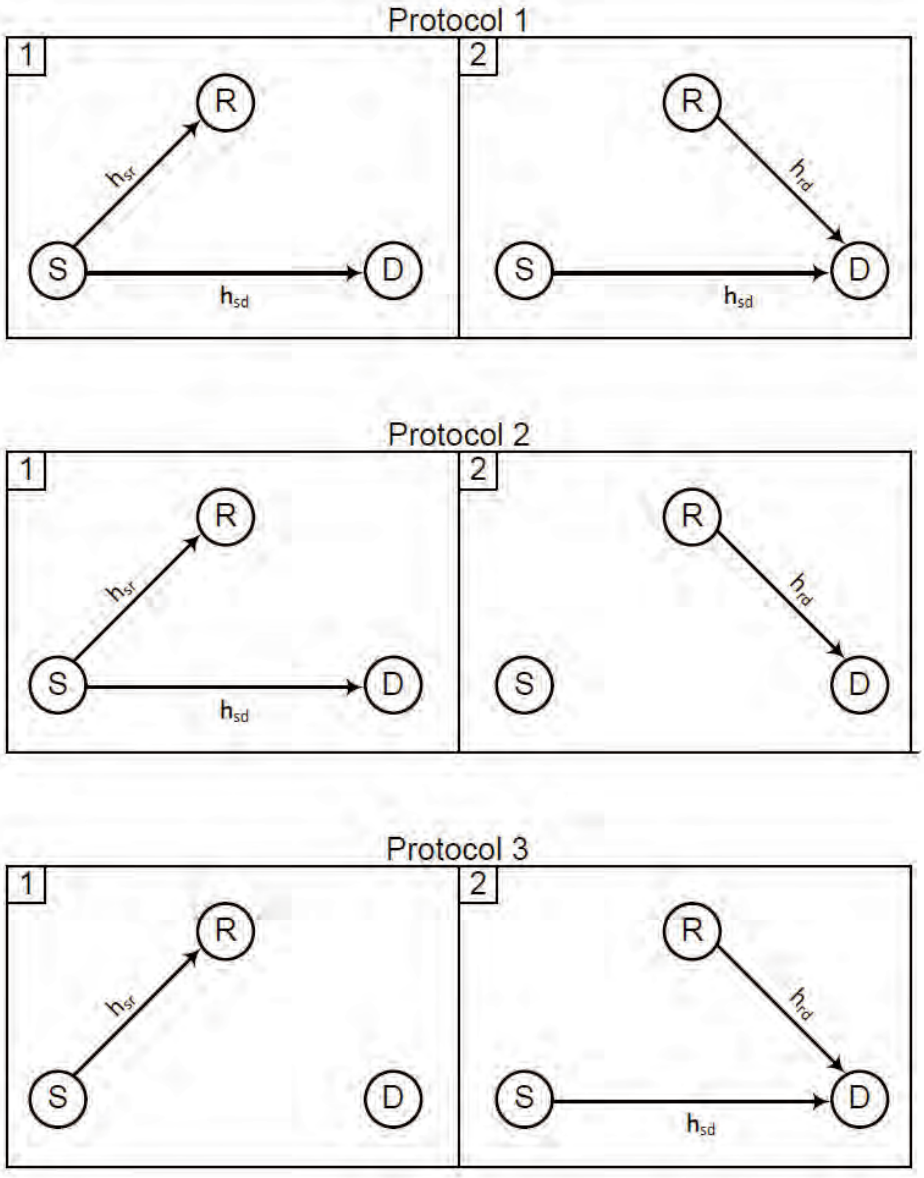

Figure 2.3: Cooperative Protocols.

and

$$y_{sd_1} = h_{sd}x + n_{sd_1}, \tag{2.2}$$

where x is the source transmitted bit/symbol, h_{sd} and h_{sr} are the complex fading channel coefficients with unit variance for $S-D$ link and $S-R$ link, respectively, n_{sd_1} and n_{sr} are the complex additive white Gaussian noise (AWGN) with zero mean and

variance $N_0/2$ per dimension for $S-D$ link in the first time slot and $S-R$ link. In phase 2, after decoding the source signal at the relay, the received signals y_{sd_2} and y_{rd} at the destination prior to combining during the cooperative phase are given by

$$y_{sd_2} = h_{sd}x + n_{sd_2}, \tag{2.3}$$

and

$$y_{rd} = h_{rd}\hat{x} + n_{rd}, \tag{2.4}$$

where $\hat{x}$ is the decoded version of the original bit/symbol at the destination, h_{rd} is the complex fading channel coefficient with unit variance for the $R-D$ link, n_{sd_2} and n_{rd} are the complex AWGN and are modelled as i.i.d. circularly symmetric complex Gaussian random variables of variance with zero mean and variance $N_0/2$ per dimension for $S-D$ link in the phase 2 and $R-D$ link.

- **Protocol II**. This protocol is referred to as *orthogonal* protocol [13]. The source transmits to the relay and destination in the first time slot, for the DF mode. The received signals at the relay and destination in the first time slot are similar to (2.1) and (2.2), respectively. The relay decodes the source message and transmits to the destination in the second time slot. The signal received from the relay at the destination is identical to (2.4).

- **Protocol III**. This protocol was first proposed in [25]. In the first phase, the source transmits to the relay. The received signal may be given by (2.1). After decoding at the relay, the source and the relay transmit to the destination in the second time slot as given by (2.3)-(2.4), respectively.

2.2.2 Simulation results

In order to evaluate the performance, simulation results of the aforementioned protocols using BPSK are presented. It is assumed that perfect channel state information (CSI) is known at the receiver, that is, R has knowledge of the channel coefficients for the $S - R$ link, and D knows the channel coefficients of the $S - D$ and $R - D$ links. The channels are assumed to be quasi-static, namely, the channels are fixed within one frame, but vary independently from one frame to the next one. In this section, all the protocols operate in the DF mode.

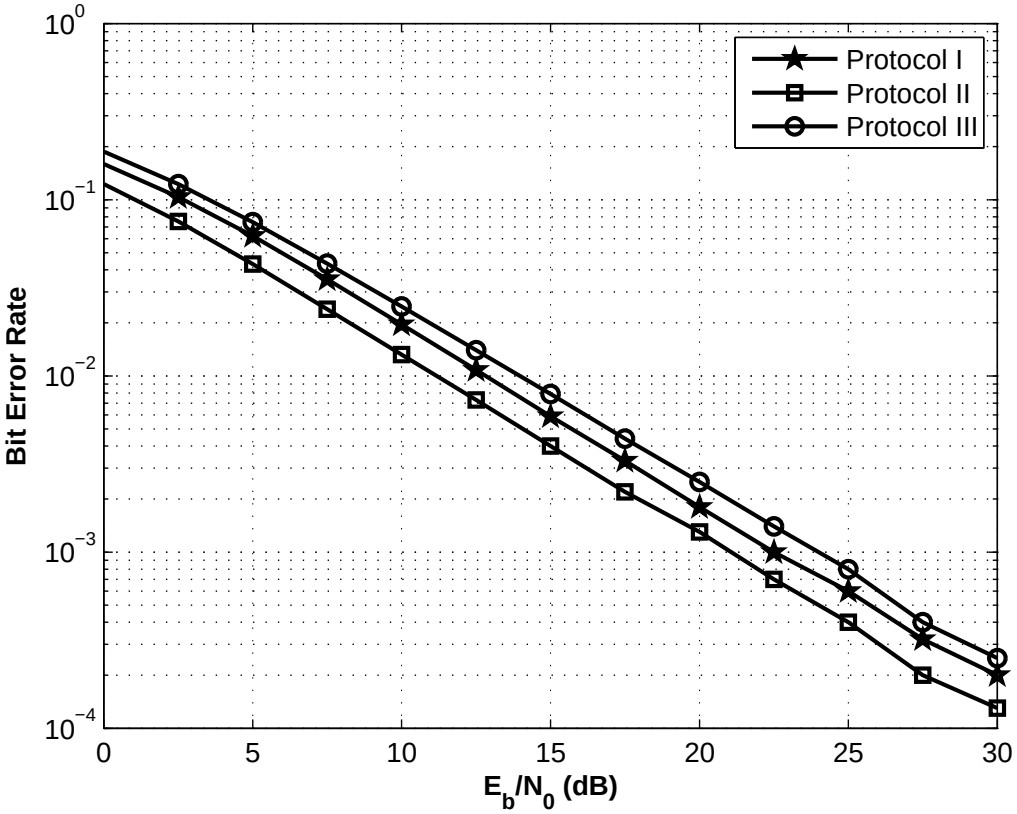

Figure 2.4: BER comparison for Protocols I, II and III in the DF mode with errors at the relay.

In Figure 2.4, the BER performance of all three protocols with the effects of errors at the relay are evaluated through simulations. It is noted that Protocol II outperforms the

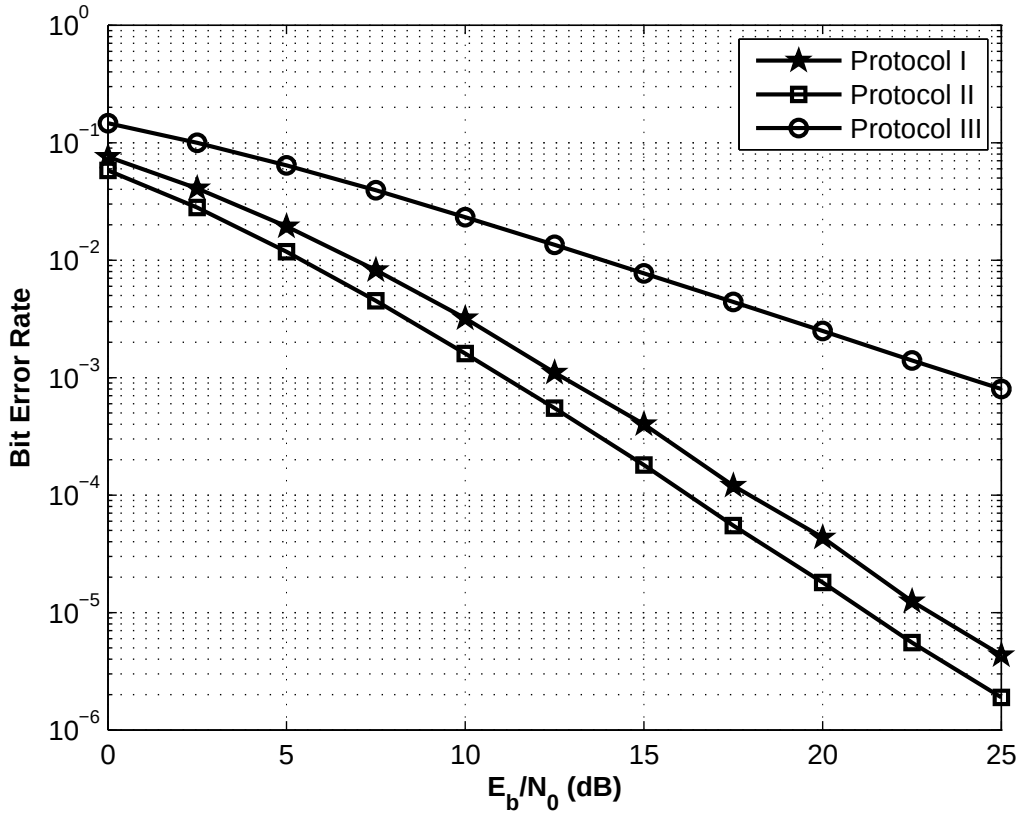

Figure 2.5: BER comparison for Protocols I, II and III in the DF mode without errors at the relay.

Protocol I and Protocol III by 1.5decibels (dB) and 3dB at 3×10^{-4}, respectively. Moreover, the diversity order in all three protocols is 1. This shows that error propagation at the destination leads to performance degradation.

Figure 2.5 depicts BER comparisons for all three protocols. In this figure, the relay is considered to be error free. This is only practical when the relay operated at high SNR or when there is no fading in the $S - R$ link. Protocol II outperforms both protocols I and III. At 10^{-3}, the gains of Protocol II over Protocol I and Protocols III are 2dB and 12dB, respetively. It is also noted that Protocols I and II achieve full diversity. In both the scenarios presented here, it can be noted that Protocol II presents the best performance in terms of error rate.

2.3 Coded Cooperation

The performance of an uncoded DF cooperative scenario degrades significantly. This is due to the effects of error propagation at the relay. In the previous section, it was shown through computer simulations that, when the relay is error free, its performance improves in terms of error rates, and full diversity is achieved. On the other hand, in a practical scenario whereby the relay transmits erroneous bits/symbols to the destination, the system performance degrades drastically.

The scenario with error-free relay is ideal and its occurrence in practice is minimal. A new technique termed *coded cooperation* that integrates channel with cooperative signaling has been proposed recently. This concept was introduced by Hunter *et al.* [18] and [26] where they used rate-compatible puntured convolutional (RCPC) codes with an error detection scheme cyclic redundancy check (CRC) codes at the relay node. The proposed coding scheme proves to be efficient for a cooperative framework as large gains are achieved over a non-cooperative scenario while maintaining the same transmit power, bandwidth and rate. However, they did not analytically show that the proposed scheme achieves a second-order diversity. The authors in [27] suggested an analytical framework on the frame-error rate (FER) that depicts the full-diverity order of coded cooperation. Janani *et al.* [19] proposed a coded cooperation scheme with a different channel coding from [26]. They investigated the application of turbo codes in coded cooperation and showed through a careful design that turbo codes naturally fit in this framework. Along the same lines, punctured turbo codes in a cooperative framework with a strict decoding constraint is studied in [28]. In [29], Stefanov and Erkip develop a cooperative framework that integrates space-time codes (STC).

Since coded cooperation proposed in [26] represents the core of a part of this thesis, it is worth revisiting. In what follows, the principles of the coded cooperation framework as presented in [26] are discussed.

A cooperative scenario of source, relay and destination is considered. The source has K information bits per block which is appended with a CRC code, and N coded bits per block given by $N = K/R$ where R is the channel code rate. The transmission of the N coded bits takes place in two consecutive time slots or frames. The transmitted codeword of length N is divided into two sub-codewords of length N_1 and N_2, where $N_1 + N_2 = N$. In the first time slot, a sub-codeword of length N_1 given by $N_1 = K/R_1$ – where R_1 is the channel code rate in the first frame– is broadcast by the source and received by the destination as well as the relay. Error detection which is determined by the use of a CRC code, is performed at the relay. If the relay decodes the source message correctly, it will compute the remaining N_2 bits of N coded bits, prior to forwarding to the destination in the second time slot. Otherwise, the source itself will transmit its own additional parity N_2 bits to the destination. It should be mentioned that the roles of the source and the relay can be used interchangeably. Figure 2.6 illustrates the transmission of a coded cooperation scheme, where in the broadcasting phase of the first frame, user 1 and user 2 bits are of length N_1 bits, whereas in the second frame, user 1 and user 2 bits are of length N_2 bits. A total of N bits is always transmitted by each user over the two time slots. Furthermore, each user transmits on orthogonal channels in order to enable the destination to detect each user separately.

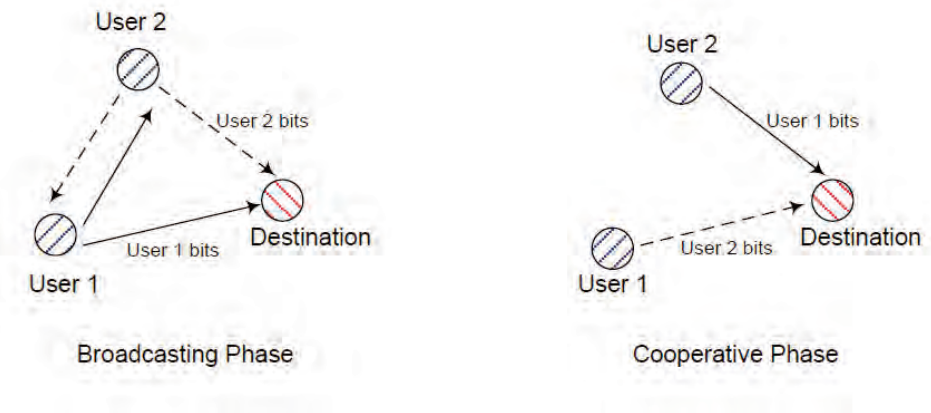

Figure 2.6: Coded-cooperative transmission scheme.

In general, coded cooperation can integrate virtually various channel coding schemes such

as block or convolutional code or a combination of both. The partition of the code bits in each time frame could be done through product codes, punctured codes or some forms of concatenation. Hunter and Nosratinia [26] proposed a coded cooperation implementation with RCPC codes [30]. The puncturing matrix that corresponds to R_1 is used to form the codeword for the first frame. The bits punctured in the first frame are transmitted by the relay as additional parity bits provided the source-to-relay link is reliable.

In a two-user cooperative scenario, each user acts independently without knowledge of the partner decoding status. This results in four cooperation cases for the transmission of the second frame. Figure 2.7 illustrates all the cooperative cases for the second frame based on the partner decoding status, determined by the use of CRC.

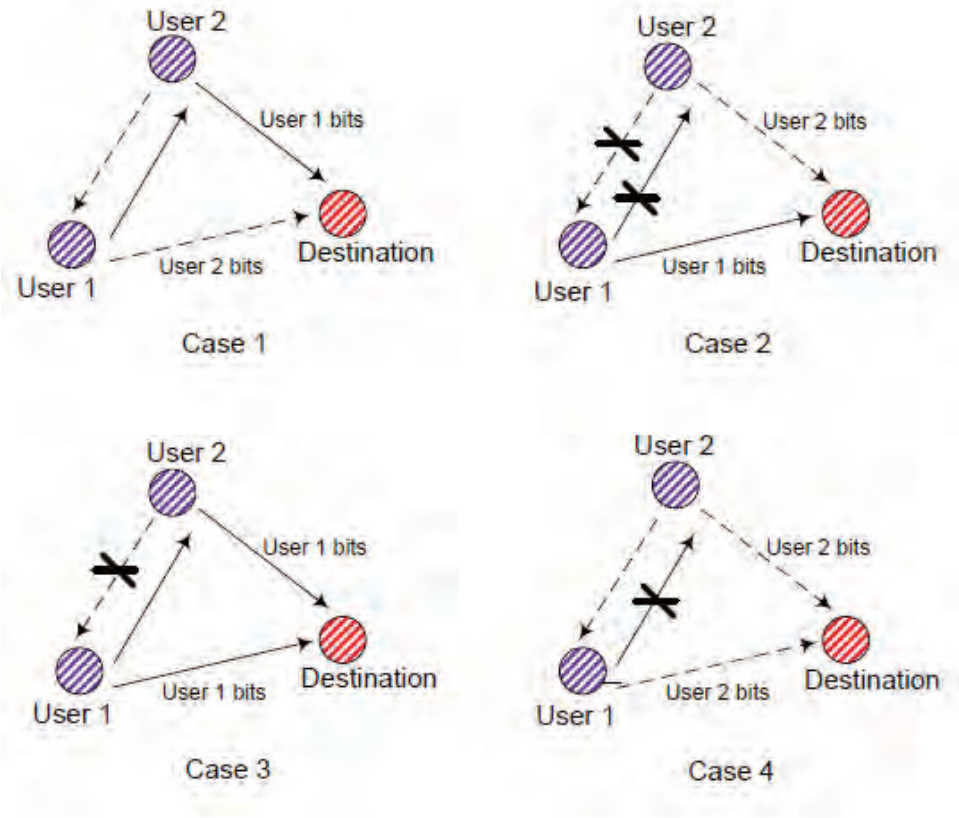

Figure 2.7: Cooperative cases based on the partner decoding status.

In case 1, each user detects its partner's first frame correctly, and hence will transmit

the partner's second frame. As a result, full cooperative diversity is achieved for both users. In case 2, neither user correctly decodes its partner's first frame. Consequently, both users will transmit their own second frame resulting in a non-cooperative scenario. No diversity is achieved for any of the users. In case 3, User 1 decodes User 2's first frame unsuccessfully, but User 2 decodes User 1's first frame correctly. In the second time slot, both users will transmit User 1's frame. At the destination, User 1's frames (first and second) are optimally combined and decoded. In this case, User 1 benefits from cooperation. Case 4 is similar to Case 3, with the roles of both users interchanged.

Until recently, most of the works on cooperative diversity with channel coding schemes such as convolutional codes [18] have been implemented. However, Boutros *et al.* [31] showed that these codes have an error probability that increases logarithmically with the block length and are far from approaching the outage limits of relay channels. In order to approach the capacity limits, the error probability should be independent of the block length. A solution is to use outage-achieving codes such as turbo codes and low-density parity-check (LDPC) codes. Recently, turbo codes and LDPC codes have been implemented in cooperative diversity in [19] and [32] respectively (and the references therein). In this work, focus is on the implementation of turbo codes in coded cooperation. Turbo codes seem to be a natural fit in cooperative communications since their constituents can be sent independently through the user and its partner(s). In the following section, a background on turbo codes is studied as this will further improve understanding of the subject and how it is implemented in cooperative diversity. But prior to that, it is worth presenting a brief review for LDPC-coded relay cooperation since this topic has now become a very attractive research area. The intention here is not to revisit LDPC codes, but to briefly introduce them.

2.3.1 LDPC-coded cooperation

Introduced in 1962 by Gallager in his PhD thesis, LDPC (See [33], [34]) are a class of linear error-correcting block codes and are defined in terms of a sparse parity-check matrix as the

name suggests. Forgotten for over three decades by the majority of the research community, LDPC codes were rediscovered two decades ago by MacKay *et al.* [35] and Sipser *et al.* [36]. Subsequent works, for e.g. [37], have shown tremendous performance (approaching capacity limits) surpassing turbo codes for large code lengths.

Recent studies (for e.g., [32], [38]– [42]) have focused on the implementation of LDPC codes in cooperative diversity in an effort to achieve the capacity limits for the relay channels. A brief literature survey of LDPC coded cooperation is presented here:

1. Methods aimed at designing LDPC codes for each factor graph (FG) are developed in [32] based on FG decoupling and successive decoding schemes. Furthermore, relay and destination operations as tantamount to virtual multiple-input single-output (MISO) and MIMO systems are formulated and a binary symmetric channel (BSC) model for the relay output node. Using extrinsic mutual information transfer (EXIT) chart technique, the performance analysis ofthe LDPC-coded relay system is also derived.

2. In [38], the authors considered the design of LDPC for cooperative relay systems for half-duplex mode. In their work, the ensemble design of rate-compatible LDPC codes is used as a formulation for the code design problem in half-duplex relay channels. Moreover, a density evolution method with a modified Gaussian approximation is developed in an effort to accurately predict the ensemble performance. A density evolution is defined as an algorithm for computing the threshold (minimum channel SNR for which the iterative algorithm converges) of LDPC codes with iterative decoding [43].

3. Bilayer graphically code structures are specially designed for relay generated parity bits in order to achieve the theoretical capacity limits for DF relaying strategy [39]. This work is restricted to Gaussian relay channels at low SNRs for which binary linear codes are suitable. Two forms of bilayer codes that approach theoretical DF rate for a wide range of channel parameters are proposed. These codes are: the bilayer-expurgated and

bilayer-lengthened codes. The authors showed that the rate of such properly designed bilayer LDPC codes tightly approach the theoretical DF rate limit.

4. The capability of near-capacity achieving LDPC codes is exploited to design coding schemes for relay channels in [40]. Both full-duplex and half-duplex are considered. The convergence behavior of the LDPC-coded system over ergodic and non-ergodic fading channels is analyzed based on the average mutual information. Both simulated and theoretical convergence show that the proposed LDPC-coded scheme closely approaches the ergodic information rates and achieves the near-capacity achieving performance over wireless relay channels.

5. In [41], the use of rate-compatible (RC)-LDPC codes in soft decode-and-forward (SDF) protocol over half-duplex relay channel is considered. Two challenges that stem from the use of RC-LDPC codes under SDF scheme are addressed: (a) the soft-reencoding of the additional parity bits at the relay, and (b) the precise computation of the log-likelihood ratio (LLR) of the received signal at the destination under the SDF scheme. The soft-decoding and soft-reencoding algorithms for the proposed RC-LDPC codes allowing the relay to forward soft messages to the destination when the relay fails to decode the source message. Moreover, a novel method referred to as soft fading, is proposed to compute the LLR of the received signal at the destination for the SDF scheme.

6. Chakrabarti *et al.* [42] proposed LDPC code designs based on the information theoretic random coding scheme for half-duplex decode-and-forward relaying. Also, the exact relationships that the component LDPC code profiles in the relay coding scheme must satisfy are derived.

2.4 Background on Turbo Codes

Also referred to as parallel concatenated convolutonal code (PCCC), turbo codes proposed by Berrou *et al.* [44] were received with skepticism in the research community due to their performance very close to the Shannon limit (within 0.7dB) for AWGN channels. The genesis of concantated codes dates back to the work of [45] where the design of long codes without excessive computations at the decoder was addressed. This concatenation code [45] is also referred to as serially concatenated code. In the early '90s Berrou, Glavieux and Thitimajshima [44] proposed a practical near-Shannon limit error coding technique known as turbo codes. The encoder of the proposed scheme is made up of two recursive systematic convolutional (RSC) codes aligned in parallel. Figure 2.8 shows the encoder structure of a rate 1/2 RSC encoder with a generator polynomial $\mathcal{G}(1, 17/13)$ in octal form and memory length $m = 3$. In the above-mentioned structure, the bits are forwarded by a shift register denoted D_{sr} with a delay of one unit time. The code is systematic since the encoded input is included in the output. Furthermore, the code is referred to as recursive because the current bits are fed back to the input to compute the new memory bits. Unlike in conventional codes, where the encoders which are terminated at the *zero* state by inputting 0s at the end of the tail of the trellis, this is not always the case for the turbo encoder. This is due to the fact that the constituent encoders are recursive. In [44], there is no reference as to how both encoders are terminated. Driving both encoders into the all-zero state simultaneously is hard to achieve due to the interleaver preceding the second encoder. Thus, it is common to terminate the first encoder in the all-zero state while the second encoder is left open [46].

2.4.1 Turbo encoder

The turbo encoder as depicted in Figure 2.9 is a parallel concatenation of two RSC encoders. Because the encoders are systematic, the input sequence (original) is part of the output sequence. The same information bits of block size N are encoded by the first

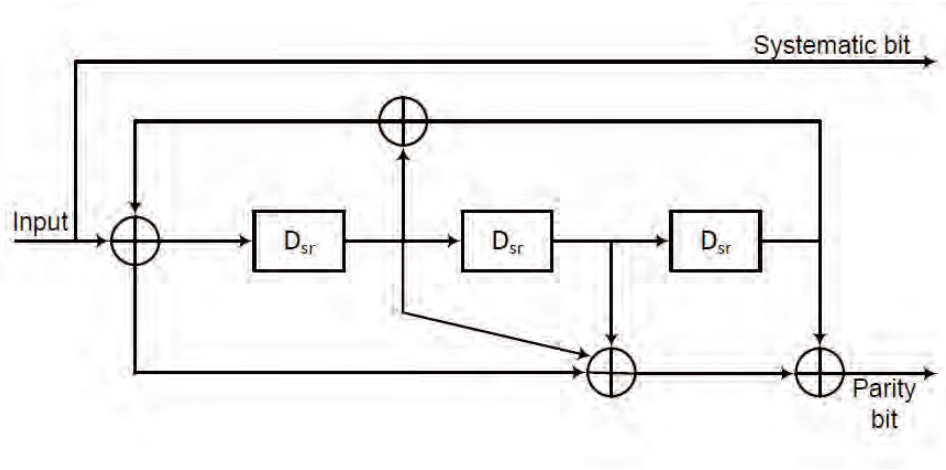

Figure 2.8: Encoder structure of rate 1/2 recursive systematic convolutional code.

constituent encoder denoted E_1 to produce the first parity bits of the same size as the information block size. On the other hand, the information bits which enter the second constituent encoder E_2 are first interleaved prior to being encoded to yield the second parity bits. The size of the interleaver is identical to the information block size and the rate of such an encoder is 1/3. Higher rates could be obtained without changing the design of the encoder. This can be done through puncturing. It is worth noting that, the puncturer in Figure 2.9 is optional. In the sequel, the constituents of a turbo encoder are briefly described.

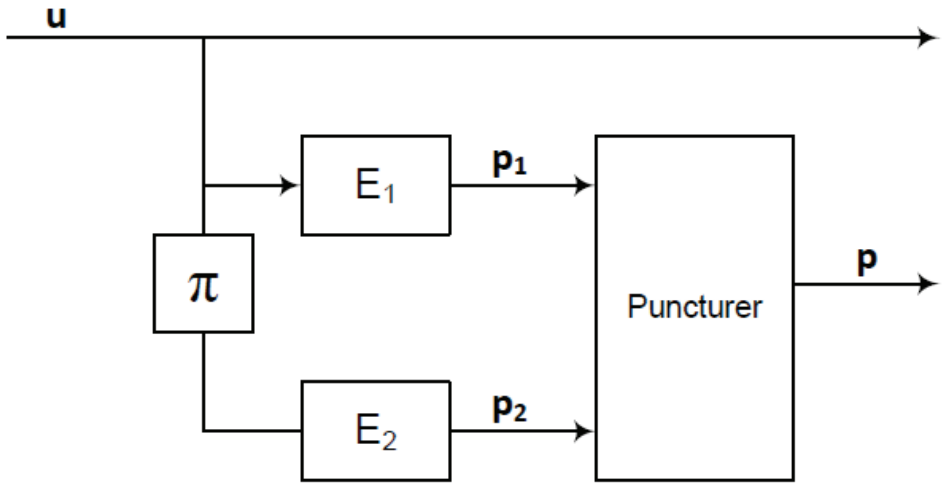

Figure 2.9: Turbo encoder.

2.4.1.1 Recursive systematic encoder

As shown in Figure. 2.8, the constituent encoders are convolutional codes in a systematic structure (the uncoded information bits appear in the output data sequence) and feedback form or recursive since the current memory bits are fed back to the input to compute the new memory bits. The generator polynomial describing the constituent encoder is $\mathcal{G}(1, 17/13)$ in octal form, where 17 represents the feedforward path and 13 the feedback path. This can also be written as $\left(1, \frac{1+D_{sr}+D_{sr}^2+D_{sr}^3}{1+D_{sr}+D_{sr}^3}\right)$, where D_{sr} denote the delay operator (shift register) and D_{sr}^k is a delay of k symbol times. For this encoder, two output data sequences for an input sequence are obtained. Hence the code rate is $R_c = \frac{1}{2}$.

2.4.1.2 Interleaver

An interleaver is a device used to scramble or permute the symbols (bits) in a random sequence. It is mostly used in situations where burst errors occur, to protect the data by spreading the errors in a systematic pattern. An interleaver is also used to lower the number of low-weight sequences, by increasing the Hamming distance of codewords. In the case of the turbo encoder, an information sequence with low weight is interleaved to produce large-weight sequence in the second encoder, hence improving the performance.

2.4.1.3 Puncturer

The puncturer is used to increase the rate of the system. This is done by periodically deleting some selected bits from the codewords. As shown in Figure. 2.9, puncturing is applied to the parity bits which are generated by the two RSC encoders. For example, an information sequence of size N with two parity bits of length N respectively yields an overall code rate of $R_c = \frac{1}{3}$. If a puncturer is employed to periodically delete $\frac{N}{2}$ bits from each parity bits, the resulting code rate is $R_c^{'} = \frac{1}{2}$.

2.4.2 Iterative decoder of the PCCC

Figure 2.10 shows the iterative decoder of the PCCC. It uses a modified version of the maximum *a posteriori* probability (MAP) algorithm first proposed by [47]. The authors in [47] applied the algorithm to feedforward convolutional codes whereas Berrou *et al.* modified it for recursive convolutional codes. Before describing the turbo decoder, some terms that are useful in the decoding process are explained.

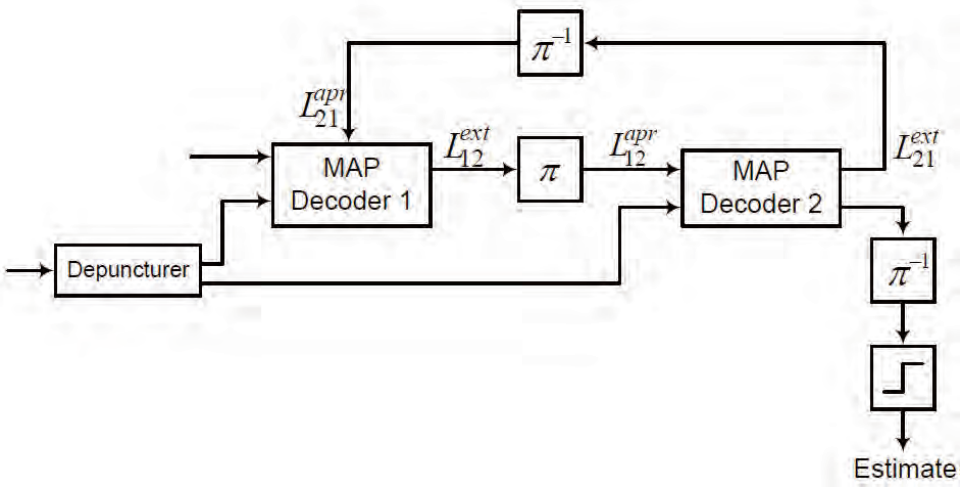

Figure 2.10: Iterative decoder of turbo codes.

The a priori information about a random variable (RV) x can be given by the LLR of x with *a priori* probability $p(x)$ as

$$L(x) = \log\left(\frac{p(x=+1)}{p(x=-1)}\right). \tag{2.5}$$

A decision to decode the transmitted signal x is made by the decoder on the *a posteriori* LLR of x. If $\mathrm{P}(x=-1|y) > \mathrm{P}(x=+1|y)$, the decoder will decide in favour of $x=-1$ and $x=+1$ otherwise. The *a posteriori* LLR value of x given the received signal y given by

$$L(x|y) = \log\left(\frac{\mathrm{P}(x=+1|y)}{\mathrm{P}(x=-1|y)}\right). \tag{2.6}$$

The latter term provides valuable information on the transmitted signal x. The sign of the term in (2.6) tells about the hard decison on x, whereas its magnitude provides the reliability of the decision. The larger the magnitude of (2.6), the greater the certainty of the decision.

The constituent decoders are soft-input soft-output decoders using the MAP algorithm and linked by an interleaver in a similar fashion to the encoder structure. The first component decoder is used to decode the sequence of bits from the first encoder whereas the second decoder corresponds to the second constituent encoder. The turbo decoder operates iteratively by exchanging valuable information about the bits between the component decoders. This valuable information is called extrinsic information and is based on the *a-priori* information and the received sequence.

2.4.3 Performance of turbo codes in AWGN

The performance of turbo codes depends on many parameters such as: interleaver size, type of interleaver, number of decoding iterations, generator polynomial or constraint length, puncturing pattern on the parity bits. The BER performance of turbo codes using BPSK in AWGN when varying some parameters are presented. Unless otherwise indicated, the following parameters are used in the simulations: interleaver size $N = 1024$, $\mathcal{G}(1, 17/13)$ in octal form with memory length $m = 3$ and a total of 8 iterations. It is worth mentioning that the turbo code parameters used in these simulations differ from [44], but present the same characteristics. The intention here is just to show the effects of various parameters on the turbo codes performance.

In Figure. 2.11, the BER performance of turbo codes with various interleaver sizes is presented. It can be noticed that as the interleaver size increases, the performance improves drastically. In this scenario, only $N = 128$, $N = 512$ and $N = 1024$ are presented.

Figure. 2.12 shows the BER performance of the PCCC for various numbers of iterations performed by the decoding algorithm. It is clear that the number of iterations affects the performance of turbo codes. It can be noted that the coding gain for 1 or 2 iterations to 8

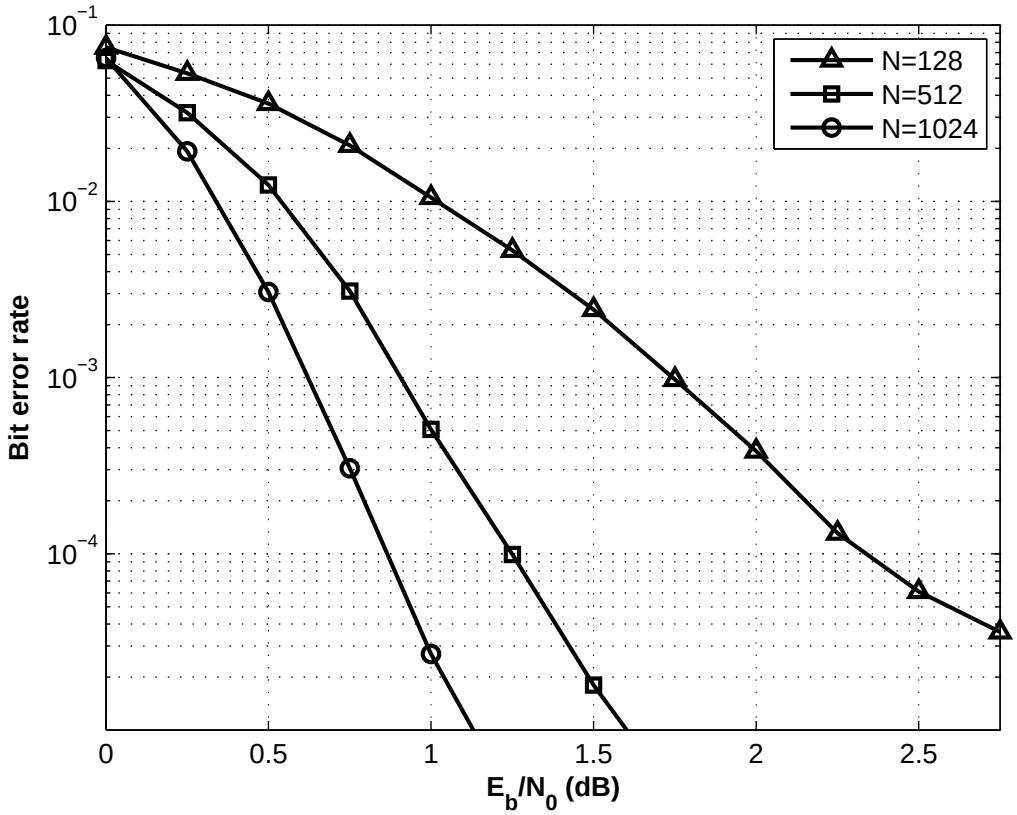

Figure 2.11: BER performance of turbo codes as the interleaver size varies

iterations is substantial. But the coding gain between 8 iterations and 12 iterations becomes less significant.

2.4.4 Turbo codes in cooperative diversity

Janani *et al.* [19] proposed a cooperative scenario using turbo codes termed turbo coded cooperation. Turbo codes [44] use two RSC encoders separated by a random interleaver. The interleavers used in a cooperative scenario, that is, at the users (source and relay) and the destination are identical in their structure. Similar to [18], the first frame is broadcast by the source to its partner and the destination. The first frame of the codeword is a combination of the first RSC encoder output and the systematic bits. Following a successful decoding at the partner (Viterbi decoder is employed here), the second frame obtained by interleaving the

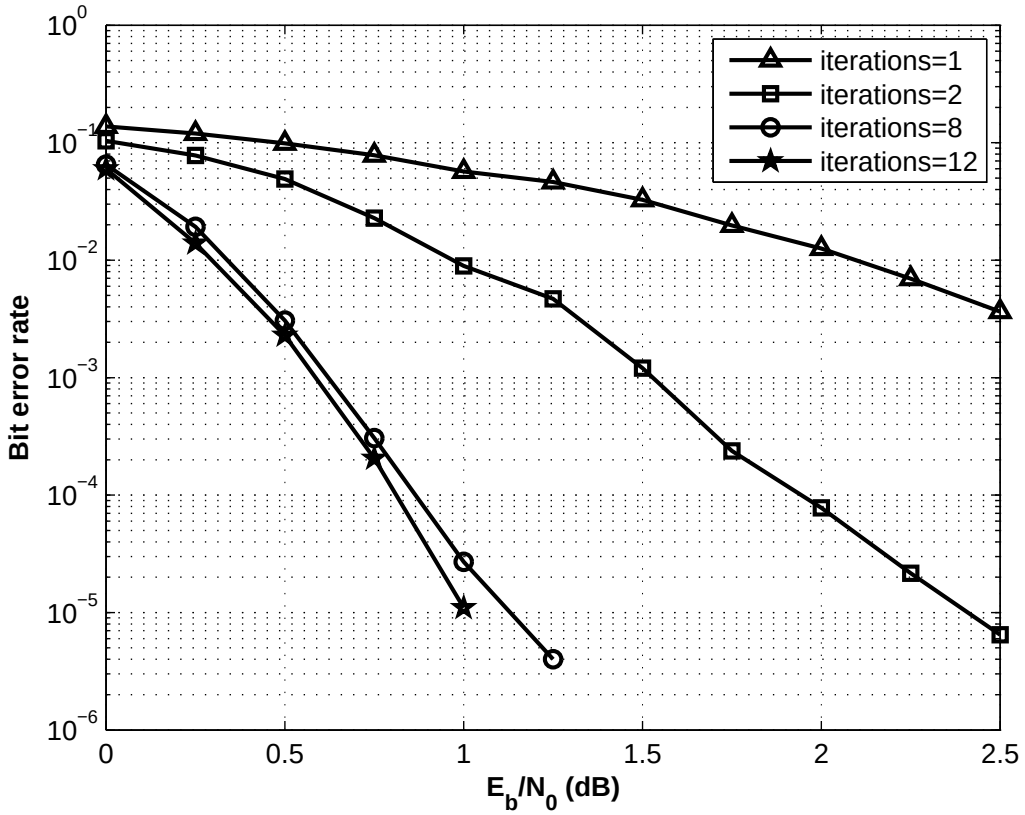

Figure 2.12: BER performance of turbo codes as a function of the number of iterations.

systematic bits and encoding through the second RSC encoder, is sent to the destination by the partner. At the destination, a low-complexity turbo decoder [44] is employed to estimate the transmitted signal.

2.5 Retransmission Protocols

Error control schemes are widely used in wireless communications to control error transmission caused by the channel noise so that information data can be transmitted reliably to the receiver. The are two basic classes of error control schemes: forward-error correction (FEC) and ARQ. The former scheme, also referred to as *channel coding* is a powerful method that improves the data reliability by introducing some redundancy in the transmitted sequence prior to transmission. It is mostly used in systems where no feedback channel

is available between the receiver and transmitter, since it corrects errors without requesting for retransmission. On the other hand, ARQ is a combination of error detection and error-free feedback. ARQ schemes require the availability of a feedback channel and provide data reliability based on the retransmission. The feedback channel is used by the receiver to notify the transmitter on the success or failure of the transmission. CRC codes are generally used for error detection at the receiver side when the decoding process takes place. If the decoding is successful, i.e. no error is detected, the receiver informs the transmitter by sending a positive acknowledgement (ACK). Otherwise, it sends a negative acknowledgement (NACK) to request retransmission. This can be repeated until the transmitted data is successfully decoded or the number of maximum retransmissions is attained. In order to minimize the buffer sizes and delays, the number of maximum retransmissions can be limited or truncated. This is generally referred to as truncated ARQ. The feedback channel is assumed to be low-rate (so that a single-parity bit can be sent) and not susceptible to errors. There exist various ARQ schemes that can be classified into two categories: basic ARQ and hybrid ARQ. Basic ARQ protocols have been widely used over the years and still emerges as the preferred ARQ schemes due to their simplicity. In the following, a brief description of the stop-and-wait ARQ scheme from a point-to-point transmission scenario is given. Furthermore, the most used standard performance metric in data error control systems known as throughput is introduced. It is defined as the ratio of the number of bits successfully received per unit time to the total number of bits transmitted per unit time [48].

2.5.1 Stop-and-wait ARQ protocol

A transmitter sends information data to a receiver and waits for the receiver to notify through a feedback channel whether the data have been successfully detected or not. In the case of positive acknowlegment or ACK (data have been succcessully received), the transmitter sends the next data sitting in the queue. Otherwise (in the case of NACK), it resends the same information data until an ACK is fed back. The stop-and-wait ARQ

suffers from long delays due to the time waiting to receive an acknowledgment and this can be very impratical in some communication networks such as satellite networks. Figure. 2.13 illustrates the stop-and-wait ARQ transmission protocol.

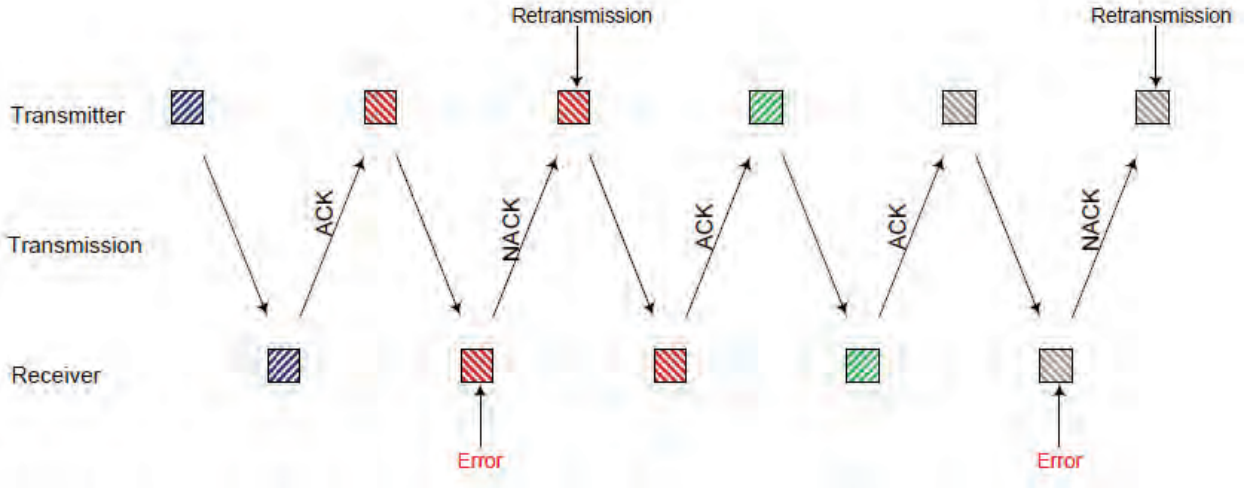

Figure 2.13: Stop-and-wait ARQ protocol.

2.5.2 Cooperative ARQ protocol

The basic idea behind ARQ protocols is that retransmission is requested by the receiver when the transmission of a packet is unsuccessful (at the receiver). Futhermore, at the data-link layer, ARQ protocols (basic and hybrid) have proved to be efficient error control schemes for data packet transmissions [48]- [50]. ARQ protocols, in the cooperative context were studied in [51]- [54] (and the references therein) in an effort to enhance system reliability over conventional multihop ARQ systems. These works have shown that cooperative ARQ networks provide better system performance in terms of delay, energy consumption and throughput in comparison to multihop ARQ networks.

2.6 Chapter Summary

In this Chapter, a general overview of cooperative communications was presented and some concepts used in the cooperative context were introduced. First of all, a detailed

background on cooperative diversity was given, ranging from the motivation (advantages over MIMO system) to cooperative protocols and techniques. The most-surveyed cooperative technique was coded cooperation (which combines channel coding and cooperative signaling), as it represents the core of a part of the thesis. Secondly, a detailed study of turbo codes in SISO systems was presented since it is later explored in the cooperative scenario. Finally, an introductory overview of retransmission protocols (widely used during the course of the thesis) for point-to-point communications was given as well as in the context of cooperative diversity networks.

Chapter 3

Distributed Turbo-Coded Cooperative Diversity with Multiple Dual-Hop Relays over Nakagami-m Fading Channels

In this chapter, the performance of turbo codes in multi-relay cooperative diversity networks is investigated over i.i.d. and i.n.i.d. slow Nakagami-m fading channels with positive fading severity index. In the proposed scheme, all the relays are equipped with error detection capabilities, and dedicate a certain amount of time to listen to the source message which is determined by a trade-off parameter denoted f, whereas the destination receives the entire codeword (systematic and parity bits) sent by the source during the first phase. In this work, it is assumed that $f = 0$ which is tantamount to the relays receiving the noisy systematic bits only. In the second phase, only the error-free relays are able to retransmit to the destination the remainder of the source message that was not received in the previous phase, i.e., the parity bits. An optimal combiner is employed at the destination for the parity bits

sent by the source and error-free relays. The entire codeword, which consists of the noisy systematic and combined parity bits, is decoded via a turbo iterative decoder. Union bounds on the BER using the transfer function bounding and the limit-before-average techniques are derived. Furthermore, the asymptotic behaviour of the system in the high-SNR regime using the PEP is examined. In addition, a closed-form analytical expression of the outage probability for various numbers of relays and different fading parameters is derived. Its asymptotic behavior suggests that the achievable diversity order depends on the number of cooperating relays and/or fading severity indices. Finally, simulation and analytical results of both bit error and outage probabilities are presented for performance evaluation of the proposed scheme.

3.1 Introduction

Multipath propagation is one of the main limitations in wireless communications systems, since various paths have different lengths resulting in dissimilar phase differences and attenuation factors for replicas of the transmitted signals. Diversity techniques such as transmit/receive diversity are a solution to the multipath propagation problem, and can be achieved by employing multiple antennas at the transmitter and/or receiver. MIMO technology [6] has proved to be an effective method to improve capacity and reliability. However, it may not be viable due to cost, size or power limitations. In order to overcome these limitations, user cooperation [9]- [10] has been proposed as a practical solution for the high-data rate coverage required in future wireless systems.

User cooperation techniques allow single-antenna mobile terminals to share their physical resources by creating a virtual antenna array. There are two main cooperative diversity strategies: AF and DF. In the AF mode, the relay terminal (or cooperating user) amplifies the signal received from the source terminal (partner) before forwarding it to the destination terminal. On the other hand, in the DF mode, the relay terminal decodes and regenerates

the received source's information for retransmission to the destination [12]- [13]. In [13], cooperative diversity with multiple relays is investigated and the authors show that reliability and high data rate can be achieved. In the aforementioned schemes, the relay/partner terminal simply repeats the received bits.

In recent years, a novel framework that integrates channel coding with cooperative diversity and termed *coded cooperation* was introduced in [18]. Hunter *et al.* [18] proposed an efficient coding scheme by using RCPC codes for the users and CRC codes at the relay terminal. Similar to [18], the authors in [29] derived a frame-error rate (FER) for the proposed scheme and showed that full diversity can be achieved. Turbo codes have shown to be a natural fit in user cooperation [19]- [28]. Janani *et al.* [19] investigated the use of turbo codes in user cooperation in the context of original coded cooperation and space-time cooperation. In [28], the authors studied the punctured turbo-coded cooperation FER performance for a quasi-static fading channel and a strict decoding delay constraint. In [12], the authors investigated space-time cooperation for multi-relay channels whereby the decoding relays, i.e., the relays that have correctly decoded the source bits, utilize a suitable space-time code in the second time slot. They demonstrated that full spatial diversity in the number of cooperating relays can be achieved. The authors in [55] derived some analytical bounds on the outage probability for a single relay convolutional-coded cooperative network over Rayleigh fading channels. In [56], the authors proposed a convolutional-based distributed scheme reminiscent of [29] but in a multi-relay scenario and evaluated their proposed scheme both in terms of bit error and outage probabilities. In a work similar to [55], Elfituri *et al.* [56] found some approximated bounds on the BER and outage probability for a multi-relay scenario.

The above-mentioned works on coded cooperation are considered over Rayleigh fading channels. A Rayleigh fading model is practically unrealistic since it does not include the statistical characteristics of the land mobile, the complex indoor environments and ionospheric radio links. A model that gives the best fit for these characteristics is the Nakagami-m model, as it represents a generalized distribution where various fading environments (severe,

light, no fading) can be modelled. Many works consider the uncoded cooperative diversity schemes over Nakagami-m distribution [58]- [62]. In [58], Ikki and Ahmed proposed a multi-relay for an uncoded DF scheme over i.n.i.d. flat Nakagami-m fading channels. Exact and approximate closed-form expressions of the bit error, outage probabilities and channel capacity are obtained. The authors in [59] examined the SER of the uncoded DF with multiple dual-hop relay over Nakagami-m fading channels. Closed-form expressions for the SER and the outage probability were derived in [60]- [62] for uncoded DF cooperative networks.

Very few works have focused their attention on channel coding schemes with user cooperation over Nakagami-m fading channels. The work in [63] analyzes the outage probablity of a transmission protocol identical to [18] (convolutional coding) under Nakagami-m fading channels. However, no closed-form expression for the exact outage probability was derived since the integral part in the outage probability expression is not easy to evaluate. Motivated by these observations, a distributed turbo-coded system in a multi-relay cooperative network subjected to slow Nakagami-m fading channels was considered. It appears that, no work has been investigated on the integration of turbo codes in multi-relay cooperative networks over Nakagami-m fading channels and this is the gap that this thesis aspires to fill. The schemes that are closely related to this work are the ones investigated in [29], [64] and [65]. In [29], the authors considered a distributed turbo coded system in a single-relay scenario over Rayleigh fading channels, where the source and relay use the same puncturing pattern to transmit to the destination. The work in [64] is an extension of [19] to a multi-relay scenario. However, the proposed code design is dissimilar to [64], as well as the transmission protocol. Moreover, the analytical work on the BER presented in [64] appears to be incomplete and no analysis on the outage probability is studied as suggested in the paper. It is also noted that the proposed analytical work for the BER bounds presented in their work is best suited for fast fading channels. Recently, Haghighat and Hamouda [65] proposed a novel signal-processing scheme in which a single relay listens to the source for a certain amount of time and transmits for the remainder of time using a trade-off parameter

f. This parameter determines the amount of time the relay should listen and transmit. However, the complexity of the latter transmission scheme is an issue since it resembles a turbo code embedded in another turbo code, hence requiring a complex decoding process. Furthermore, the authors in [65] only considered a single-relay scenario over Rayleigh fading channels. The proposed scheme uses a less complex system from the encoding and decoding point of view in comparison to [65].

In this work, a distributed turbo-coded cooperative system where the source and relay terminals share their antenna, to create a virtual antenna array to transmit to the destination terminal is considered. It is assumed that the relays are equipped with a turbo encoder and decoder, and the source and the destination with a turbo encoder and decoder respectively. An end-to-end cooperative transmission consists of two consecutive phases. The cooperation scheme under study can be summarized as follows. In the first phase, the source after encoding and interleaving, broadcasts the entire codeword (systematic, first and second parity bits) to the destination and relays. The relays need not listen to the entire codeword prior to decoding. Only the systematic bits are received by the relays and this can be done through puncturing. Each relay uses its own turbo iterative decoder to estimate the source information bits. During the second stage, only the decoding relays transmit the first-stage punctured bits, i.e., parity bits, to the destination through orthogonal channels. The parity bits from the source and relay are optimally combined through a maximum ratio combiner (MRC) prior to entering the turbo iterative decoder at the destination. A Nakagami-m fading distribution is considered in this work. Moreover, the union bounds on the probability of bit error for both i.i.d. and i.n.i.d. slow Nakagami-m fading channels by using the transfer function bounds, and the limit-before-average technique which proves to yield tight bounds are derived. Furthermore, a closed-form analytical expression on the outage probability is derived for an arbitrary number of relays and different fading indices. This is done by evaluating the difficult integral part of the outage probability expression. Approximations of both the PEP and outage probability for the high-SNR regime are provided showing that

full diversity in the number of cooperating relays and fading parameters is achieved. The proposed system uses a trade-off parameter that corresponds to $f = 0$ in [65]. Finally, through computer simulations the effects of f on the outage probability for various values of f ranging from $[0, 1]$ are studied.

3.2 Proposed Scheme

3.2.1 System model

A multi-relay turbo-coded cooperative system transmitting over Nakagami-m fading channels is considered. In what follows, the source, the n^{th} relay and destination nodes are denoted by s, r_n, d respectively, where $n \in \{1, \cdots, L\}$ and L represents the number of cooperating relays. All nodes are equipped with a single antenna and the relays operate in half-duplex mode, i.e., they cannot receive and transmit simultaneously. It is assumed that the channels are modelled as quasi-static, i.e., the fading coefficients are constant for the entire duration of a transmission frame, but vary independently from one frame to another one. It is also assumed that all receivers perfectly know the channel statistics of the transmitter-to-receiver link. The cooperative transmission is divided into two phases and the proposed system works as follows:

1. In the first phase, the source encodes a message of length K by a turbo code of rate $R_c = \frac{1}{3}$, and starts broadasting the generated N-bit codeword. In the model, a turbo code consisting of two parallel concatenated convolutional codes separated by an interleaver is considered. It is assumed the destination listens to the entire codeword whereas the relays only listen to a fraction of the entire codeword which is assumed to be equal for all relays and given by [65]

$$N' = K + (N - K)f, \tag{3.1}$$

$0 \leq f \leq 1$ and denotes the parameter that determines the amount of time the relays listen to the destination. As previously mentioned, $f = 0$ is used in this work. Hence $N' = K$ and simply means that all the relays received the noisy systematic bits prior to decoding. The received codeword at the destination and relay nodes are given by

$$y_{sd}(1:N) = \sqrt{P_s} h_{sd} x_s(1:N) + n_{sd}(1:N), \tag{3.2}$$

$$y_{sr_n}(1:K) = \sqrt{P_s} h_{sr_n} x_s(1:K) + n_{sr_n}(1:K), \tag{3.3}$$

where $x_s(1:N)$=$\{x_s(1), \cdots, x_s(K), x_s(K+1), \cdots, x_s(N)\}$, with $x_s(1:K)$ representing the systematic bits and $x_s(K+1:N)$ the parity bits, h_{sd} and h_{sr_n} are the fading coefficients for the source-destination and source-relays links respectively, obtained from a Nakagami-m distribution with $\mathbb{E}\langle|h_{sd}|^2\rangle = 1$ and $\mathbb{E}\langle|h_{sr_n}|^2\rangle = 1$ and parameters m_{sd} and m_{sr_n} (m_{sd} and m_{sr_n} denote the Nakagami-m fading figures), P_s are the transmitted signal power at the source for the s-d and s-r$_n$ links, $n_{sd}(1:N)$ and $n_{sr_n}(1:K)$ represent the complex i.i.d. AWGN modelled as $\mathcal{CN}(0, N_0/2)$. All the relays are equipped with a turbo iterative decoder to estimate the source information bits, as well as an error detection scheme via a CRC code[1].

2. During the second phase, the decoding relays regenerate the source message and forward the punctured bits, i.e., the parity bits, to the destination. The received signal at the destination is given by

$$y_{r_nd}(K+1:N) = \sqrt{P_r} h_{r_nd} \hat{x}_s(K+1:N) + n_{r_nd}(K+1:N), \tag{3.4}$$

where $\hat{x}_s(K+1:N)$ denotes the estimated parity bits, h_{r_nd} is the fading coefficient for the relay-destination links with $\mathbb{E}\langle|h_{r_nd}|^2\rangle = 1$ and fading figure m_{r_nd}, $n_{r_nd}(K+1:N)$

[1]This is already included in the information message and as such, does not represent an additional overhead.

denotes the complex i.i.d. AWGN with zero mean and variance $N_0/2$ per dimension and P_r is the transmitted signal power at the relays for the r-d links. The parity bits from the source and the decoding relays are optimally combined by a MRC and the output of the MRC is sent to a turbo decoder. Each of the reliable relays and the source employ an interleaver as in PCCC. In what follows, we address the type of interleaver for the source and the reliable relays since the interleaver design plays a major role in turbo coded system over noisy channel. An interleaver is primarily used to create a code with good distance properties.to It is widely known that structured codes performance is not as good as random codes. There exists a fair amount of works in the literature on the design of interleavers. Among such works, [44] proposed a random interleaver that creates a code with good distance properties and reasonable complexity. In this Chapter, a random interleaver similar to [44] is used. Fig. 3.1 illustrates the proposed scheme during both phases. It is worth stressing that decoding at the destination only takes place after the second-hop transmission when at least one relay is able to correctly decode the source message. Otherwise no transmission occurs in the second phase, and in this scenario all the relays remain silent and the destination starts decoding the source message sent during the first phase.

The instantaneous received SNR at j from transmitter i is defined by

$$\gamma_{ij} = |h_{ij}|^2 \bar{\gamma}_{ij}, \tag{3.5}$$

where $\bar{\gamma}_{ij}$ denotes the average SNR between users i and j, and$|h_{ij}|^2$ is a gamma-distributed random variable (RV). The probability density function (PDF) of γ_{ij} is given by

$$p(\gamma_{ij}) = \frac{m_{ij}^{m_{ij}} \gamma_{ij}^{m_{ij}-1}}{\Gamma(m_{ij}) \bar{\gamma}_{ij}^{m_{ij}}} \exp\left(-\frac{m_{ij}\gamma_{ij}}{\bar{\gamma}_{ij}}\right), \tag{3.6}$$

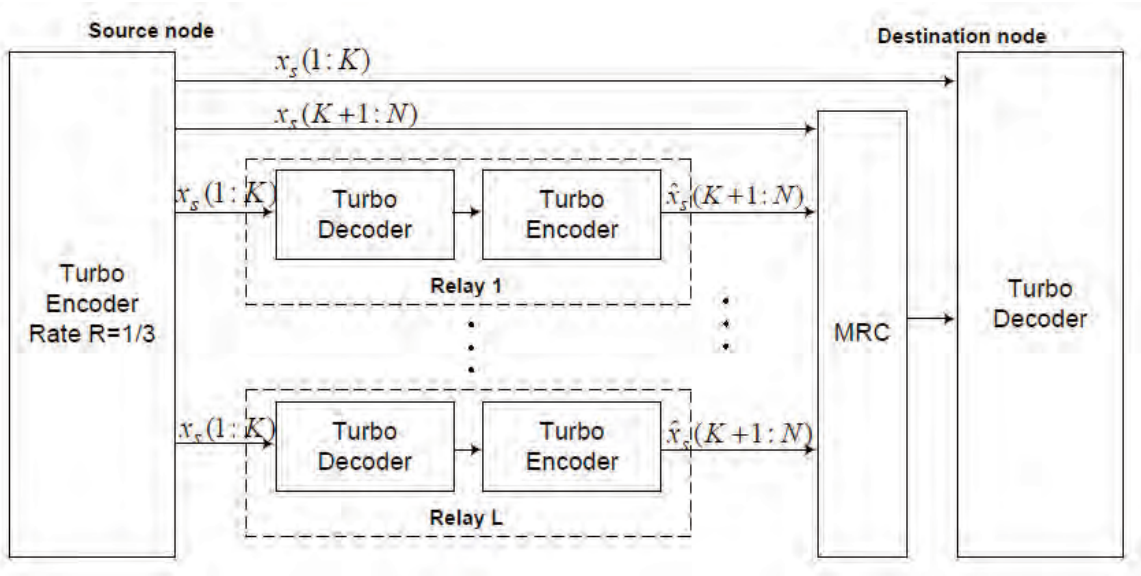

Figure 3.1: Proposed distributed turbo-coded cooperative system with L relays.

where m_{ij} denotes the fading parameter in the $i-j$ link and $\Gamma(\bullet)$ is the Gamma function defined in [75, Eq. (8.310.1)] as

$$\Gamma(x) = \int_0^\infty e^{-t} t^{x-1} \mathrm{d}t. \tag{3.7}$$

3.3 Union bounds on the Bit Error Rate

In this section, the union bounds on the BER of the proposed scheme for L relays over Nakagami-m fading are derived. In the analysis, BPSK modulation[2] is considered. The number of relays that forward to the destination during the second phase is not fixed and varies from 0 to L.

3.3.1 Pairwise error probability

The conditional PEP for a coded system is defined as the probability of selecting an erroneous codeword $\tilde{\mathbf{x}} = (\tilde{x}_1, \tilde{x}_2, \cdots, \tilde{x}_N)$ when the codeword $\mathbf{x} = (x_1, x_2, \cdots, x_N)$ is trans-

[2]This can be easily be extended to other modulation schemes, but for the sake of brevety focus is on BPSK in this Chapter.

mitted. As a baseline, a single-link transmission is considered and a coherent detection is assumed. Hence the PEP conditioned on the instantaneous SNR $\gamma = \{\gamma(1), \gamma(2), \cdots, \gamma(N)\}$ is given by [57]

$$P(\mathbf{x} \to \tilde{\mathbf{x}}|\gamma) = Q\left(\sqrt{2\sum_{i\in\xi}\gamma(i)}\right), \tag{3.8}$$

where $Q(x)$ denotes the Gaussian Q-function, $\gamma(n)$ is the instantaneous received SNR for code bit i and ξ is the set of all code bits i for which $\tilde{\mathbf{x}} \neq \mathbf{x}$ and the selection of the codeword $\tilde{\mathbf{x}}$ over $\mathbf{x}$ is called an error event. The cardinality of ξ is equal to the Hamming distance between $\mathbf{x}$ and $\tilde{\mathbf{x}}$, denoted by d. For the purpose of error analysis, consideration is given and restricted to a chosen all-zero transmitted codeword without loss of generality. Therefore, the PEP is not a function of $\tilde{\mathbf{x}}$ and $\mathbf{x}$, but rather of d and can be given by $P(d|\gamma)$ since d is typically referred to as the error event ($\mathbf{x} \neq \tilde{\mathbf{x}}$) Hamming weight.

In the proposed scheme, the number of relays that forward to the destination during the second phase varies from 0 to L, since there may be some relays that fail to correctly decode the received message sent by the source. Hence, Θ is denoted as the set of indices of cooperating relays

$$\Theta = \{k_1, k_2, \cdots, k_\vartheta\} \subset \{1, 2, \cdots, L\}, \tag{3.9}$$

where $\vartheta = |\Theta|$ denotes the cardinality of Θ.

Under the assumption that γ_{sd}, $\gamma_{sr_1}, \cdots, \gamma_{sr_L}$, $\gamma_{r_1 d}, \cdots, \gamma_{r_L d}$ are statistically independent,

the end-to-end PEP can be given by

$$P(d|\gamma_{sd},\gamma_{sr_1},\cdots,\gamma_{sr_L},\gamma_{r_1d},\cdots,\gamma_{sr_L}) = \overbrace{Q\Big(\sqrt{2d\gamma_{sd}}\Big)\cdot\prod_{j=1}^{L}Q\Big(\sqrt{2d_1\gamma_{sr_j}}\Big)}^{Pe_1}$$
$$+\underbrace{\sum_{\vartheta=1}^{L}\binom{L}{\vartheta}\Bigg(\prod_{i\notin\Theta}Q\Big(\sqrt{2d_1\gamma_{sr_i}}\Big)\Bigg)\Bigg(\prod_{i\in\Theta}1-Q\Big(\sqrt{2d_1\gamma_{sr_i}}\Big)\Bigg)\Bigg(Q\Bigg(\sqrt{2d\gamma_{sd}+\frac{1}{\vartheta}\sum_{i\in\Theta}d_2\gamma_{r_id}}\Bigg)\Bigg)}_{Pe_2}, \tag{3.10}$$

where Pe_1 denotes the probability that all the cooperating relays are unreliable, Pe_2 is the probability that some relays or all the relays are reliable and d is given by $d = d_1 + d_2$ with d_1 and d_2 denoting the fractions of the error event bits transmitted in the s-r$_n$ and r$_n$d links respectively.

The alternative representation of the Gaussian Q-function was proposed by Craig [67] and is given by

$$Q(x) = \frac{1}{\pi}\int_0^{\frac{\pi}{2}}\exp\left(-\frac{x^2}{2\sin^2\theta}\right)\mathrm{d}\theta. \tag{3.11}$$

Using (3.11), (3.10) can be rewritten as

$$P(d|\gamma_{sd},\gamma_{sr_1},\cdots,\gamma_{sr_L},\gamma_{r_1d},\cdots,\gamma_{sr_L}) = \left(\frac{1}{\pi}\int_0^{\frac{\pi}{2}}\exp\left(-\frac{d\gamma_{sd}}{\sin^2\theta}\right)\mathrm{d}\theta\right)$$
$$\times\left(\prod_{j=1}^{L}\left[\frac{1}{\pi}\int_0^{\frac{\pi}{2}}\exp\left(-\frac{d_1\gamma_{sr_j}}{\sin^2\theta_j}\right)\mathrm{d}\theta_j\right]\right)+\sum_{\vartheta=1}^{L}\binom{L}{\vartheta}\left(\prod_{i\notin\Theta}\frac{1}{\pi}\int_0^{\frac{\pi}{2}}\exp\left(-\frac{d_1\gamma_{sr_i}}{\sin^2\theta_i}\right)\mathrm{d}\theta_i\right)$$
$$\times\left(\prod_{i\in\Theta}\left[1-\frac{1}{\pi}\int_0^{\frac{\pi}{2}}\exp\left(-\frac{d_1\gamma_{sr_i}}{\sin^2\mathrm{d}\theta_i}\right)\right]\right)\left(\frac{1}{\pi}\int_0^{\frac{\pi}{2}}\exp\left(-\frac{d\gamma_{sd}+\frac{1}{\vartheta}\sum_{i\in\Theta}d_2\gamma_{r_id}}{\sin^2\theta_i}\right)\mathrm{d}\theta_i\right). \tag{3.12}$$

The average PEP can be given by

$$P(d) = \left(\frac{1}{\pi}\int_0^{\frac{\pi}{2}}\int_0^{\infty} \exp\left(-\frac{d\gamma_{sd}}{\sin^2\theta}\right) p(\gamma_{sd})\mathrm{d}\gamma_{sd}\mathrm{d}\theta\right)\left(\prod_{j=1}^{L}\left[\frac{1}{\pi}\int_0^{\frac{\pi}{2}}\int_0^{\infty} \exp\left(-\frac{d_1\gamma_{sr_j}}{\sin^2\theta_j}\right)\right.\right.$$
$$\left.\left.\times\, p(\gamma_{sr_j})\mathrm{d}\gamma_{sr_j}\mathrm{d}\theta_j\right]\right) + \sum_{\vartheta=1}^{L}\binom{L}{\vartheta}\left(\prod_{i\notin\Theta}\frac{1}{\pi}\int_0^{\frac{\pi}{2}}\int_0^{\infty} \exp\left(-\frac{d_1\gamma_{sr_i}}{\sin^2\theta_i}\right) p(\gamma_{sr_i})\mathrm{d}\gamma_{sr_i}\mathrm{d}\theta_i\right)$$
$$\times\left(\prod_{i\in\Theta}\left[1-\frac{1}{\pi}\int_0^{\frac{\pi}{2}}\int_0^{\infty} \exp\left(-\frac{d_1\gamma_{sr_i}}{\sin^2\theta_i}p(\gamma_{sr_i})\mathrm{d}\gamma_{sr_i}\mathrm{d}\theta_i\right)\right]\right)$$
$$\times\left(\frac{1}{\pi}\int_0^{\frac{\pi}{2}}\int_0^{\infty}\int_0^{\infty} \exp\left(-\frac{d\gamma_{sd}+\frac{1}{\vartheta}\sum_{i\in\Theta} d_2\gamma_{r_id}}{\sin^2\theta_i}\right) p(\gamma_{sd})p(\gamma_{r_id})\mathrm{d}\gamma_{sd}\mathrm{d}\gamma_{r_id}\mathrm{d}\theta_i\right), \quad (3.13)$$

where $p(\gamma_{sd})$, $p(\gamma_{sr_i})$ and $p(\gamma_{r_id})$ denote the PDF as given by (3.6) with the subscripts changed to the corresponding links.

Using the expression of the moment generating function (MGF) given by [57]

$$\int_0^{\infty}\exp(-s\gamma_{ij})p(\gamma_{ij})\mathrm{d}\gamma_{ij} = \left(1+\frac{s\gamma_{ij}}{m_{ij}}\right)^{-m_{ij}}, \quad (3.14)$$

and after some algebraic manipulations, (3.13) can further be given by

$$P(d) = \left(\frac{1}{\pi}\int_0^{\frac{\pi}{2}}\left(1+\frac{d\bar{\gamma}_{sd}}{m_{sd}\sin^2\theta}\right)^{-m_{sd}}\mathrm{d}\theta\right)\cdot\prod_{j=1}^{L}\left(\frac{1}{\pi}\int_0^{\frac{\pi}{2}}\left(1+\frac{d_1\bar{\gamma}_{sr_j}}{m_{sr_j}\sin^2\theta_j}\right)^{-m_{sr_j}}\mathrm{d}\theta_j\right)$$
$$+\sum_{\vartheta=1}^{L}\binom{L}{\vartheta}\left(\prod_{i\notin\Theta}\frac{1}{\pi}\int_0^{\frac{\pi}{2}}\left(1+\frac{d_1\bar{\gamma}_{sr_i}}{m_{sr_i}\sin^2\theta_i}\right)^{-m_{sr_i}}\mathrm{d}\theta_i\right)$$
$$\times\left(\prod_{i\in\Theta}1-\frac{1}{\pi}\int_0^{\frac{\pi}{2}}\left(1+\frac{d_1\bar{\gamma}_{sr_i}}{m_{sr_i}\sin^2\theta_i}\right)^{-m_{sr_i}}\mathrm{d}\theta_i\right)$$
$$\times\frac{1}{\pi}\int_0^{\frac{\pi}{2}}\left(1+\frac{d\bar{\gamma}_{sd}}{m_{sd}\sin^2\theta}\right)^{-m_{sd}}\cdot\prod_{i\in\Theta}\left(1+\frac{d_2\bar{\gamma}_{r_id}}{\vartheta m_{r_id}\sin^2\theta}\right)^{-m_{r_id}}\mathrm{d}\theta. \quad (3.15)$$

Using [57, Eqs. (5A.58)-(5A.70)] with [68, Eq. (63)] and after algebraic manipulations, a closed-form expression of (3.15) for positive m_{sd}, m_{sr_n} and m_{r_nd} can be obtained and given

by

$$
\begin{aligned}
P(d) = & \left[\frac{(d\bar{\gamma}_{sd}/m_{sd})^{\frac{1}{2}}}{2\sqrt{\pi}\left(1+\frac{d\bar{\gamma}_{sd}}{m_{sd}}\right)^{m_{sd}+\frac{1}{2}}} \cdot \frac{\Gamma(m_{sd}+\frac{1}{2})}{\Gamma(m_{sd}+1)} \cdot {}_2F_1\left(1, m_{sd}+\frac{1}{2}; m_{sd}+1; \frac{m_{sd}}{m_{sd}+d\bar{\gamma}_{sd}}\right) \right] \\
& \times \prod_{j=1}^{L} \left[\frac{(d_1\bar{\gamma}_{sr_j}/m_{sr_j})^{\frac{1}{2}}}{2\sqrt{\pi}\left(1+\frac{d_1\bar{\gamma}_{sr_j}}{m_{sr_j}}\right)^{m_{sr_j}+\frac{1}{2}}} \cdot \frac{\Gamma(m_{sr_j}+\frac{1}{2})}{\Gamma(m_{sr_j}+1)} \cdot {}_2F_1\left(1, m_{sr_j}+\frac{1}{2}; m_{sr_j}+1; \frac{m_{sr_j}}{m_{sr_j}+d_1\bar{\gamma}_{sr_j}}\right) \right] \\
& + \sum_{\vartheta=1}^{L} \binom{L}{\vartheta} \left\{ \prod_{j=\vartheta+1}^{L} \left[\frac{(d_1\bar{\gamma}_{sr_j}/m_{sr_j})^{\frac{1}{2}}}{2\sqrt{\pi}\left(1+\frac{d_1\bar{\gamma}_{sr_j}}{m_{sr_j}}\right)^{m_{sr_j}+\frac{1}{2}}} \cdot \frac{\Gamma(m_{sr_j}+\frac{1}{2})}{\Gamma(m_{sr_j}+1)} \right. \right. \\
& \left. \times {}_2\mathrm{F}_1\left(1, m_{sr_j}+\frac{1}{2}; m_{sr_j}+1; \frac{m_{sr_j}}{m_{sr_j}+d_1\bar{\gamma}_{sr_j}}\right) \right] \left. \right\} \left\{ 1 - \prod_{j=1}^{\vartheta} \left[\frac{(d_1\bar{\gamma}_{sr_j}/m_{sr_j})^{\frac{1}{2}}}{2\sqrt{\pi}\left(1+\frac{d_1\bar{\gamma}_{sr_j}}{m_{sr_j}}\right)^{m_{sr_j}+\frac{1}{2}}} \right. \right. \\
& \times \frac{\Gamma(m_{sr_j}+\frac{1}{2})}{\Gamma(m_{sr_j}+1)} \cdot {}_2F_1\left(1, m_{sr_j}+\frac{1}{2}; m_{sr_j}+1; \frac{m_{sr_j}}{m_{sr_j}+d_1\bar{\gamma}_{sr_j}}\right) \sum_{j=1}^{L} \sum_{k=1}^{m_{r_j}d} \Lambda_{kj} \\
& \times \frac{\left(\frac{d\bar{\gamma}_{sd}m_{r_jd}M}{d_2\bar{\gamma}_{r_jd}}\right)^{k-1}}{2\left(1-\frac{d\bar{\gamma}_{sd}m_{r_jd}\vartheta}{d_2\bar{\gamma}_{r_jd}m_{sd}}\right)^{m_{sd}+k-1}} \left(\sum_{l=0}^{k-1} \left(\frac{d_2\bar{\gamma}_{r_jd}m_{sd}}{d\bar{\gamma}_{sdr_jd}} - 1 \right)^{l} B_l I_l\left(\frac{d_2\bar{\gamma}_{r_jd}}{r_jd}\right) \right. \\
& \left. \left. \left. - \left(\frac{d\bar{\gamma}_{sd}m_{r_jd}\vartheta}{d_2\bar{\gamma}_{rd_j}m_{sd}}\right) \sum_{l=0}^{m_{sd}-1} \left(1-\frac{d\bar{\gamma}_{sd}m_{r_jd}\vartheta}{d_2\bar{\gamma}_{r_jd}m_{sd}}\right)^{l} C_l I_l\left(\frac{d\bar{\gamma}_{sd}}{m_{sd}}\right) \right) \right] \right\},
\end{aligned}
\tag{3.16}
$$

where ${}_2F_1(a, b; c; x)$ denotes the Gauss hypergeometric function defined in [75, Eq. (9.111)] as

$$
{}_2F_1(a, b; c; x) = \frac{\Gamma(c)}{\Gamma(b)\Gamma(c-b)} \int_0^1 \frac{t^{b-1}(1-t)^{c-b-1}}{(1-tx)^a} \mathrm{d}t, \tag{3.17}
$$

$\Gamma(y)$ denotes the gamma function, Λ_{kj}, B_l, C_l and I_l are given respectively by

$$
\Lambda_{jk} = \frac{\frac{\mathrm{d}^{m_{r_jd}-k}}{\mathrm{d}s^{m_{r_jd}-k}} \prod_{\substack{n=1 \\ n\neq j}}^{L} \left(\frac{1}{1+\frac{d_2\bar{\gamma}_{r_nd}}{m_{r_nd}\vartheta}s} \right)}{(m_{r_jd}-k)! \left(\frac{d_2\bar{\gamma}_{r_jd}}{m_{r_jd}}\right)^{m_{rd}-k}}, \tag{3.18}
$$

$$B_l = \frac{A_l}{\binom{m_{sd}+k-1}{l}}, \tag{3.19a}$$

$$C_l = \sum_{k-1}^{n=0} \frac{\binom{k}{n}}{\binom{m_{sd}+k-1}{n}} A_l, \tag{3.19b}$$

$$A_l = (-1)^{k-1+l} \frac{\binom{k-1}{l}}{(k-1)!} \prod_{\substack{n=1 \\ n \neq l+1}}^{k} (m_{sd} - k + n), \tag{3.19c}$$

and

$$I_l(x) = 1 - \sqrt{\frac{x}{1+x}} \left(1 + \sum_{n=1}^{l} \frac{(2n-1)!!}{n! 2^n (1+x)^n} \right), \tag{3.19d}$$

with $(2n-1)!!$ denoting the double factorial defined as $(2n-1)!! = 1 \times 3 \times \cdots \times (2n-1)$.

Although (3.16) yields an exact closed-form expression for the PEP and more importantly its numerical evaluation is not computationally prohibitive, it does not offer an insight into the effects of the system parameters. In what follows, the PEP is simplified as the SNR$\rightarrow \infty$. Let $\bar{\gamma}_{sd} = \bar{\gamma}_{sr_1} = \cdots = \bar{\gamma}_{sr_L} = \bar{\gamma}_{r_1 d} = \cdots = \bar{\gamma}_{r_L d} = \bar{\gamma} \rightarrow \infty$ and $\sin^2\theta \approx 1$, then (3.15) will reduce to

$$P(d) \approx \frac{1}{\pi} \int_0^{\frac{\pi}{2}} (d\bar{\gamma})^{-m_{sd}} \left(\frac{d_2}{L} \bar{\gamma} \right)^{\sum_{j=1}^{L} m_{r_j d}} \mathrm{d}\theta. \tag{3.20}$$

After some elementary integration and manipulation, the PEP can be expressed as

$$P(d) \approx \frac{1}{2} d^{-m_{sd}} \left(\frac{d_2}{L} \right)^{-\sum_{j=1}^{L} m_{r_j d}} \bar{\gamma}^{-\left(m_{sd} + \sum_{j=1}^{L} m_{r_j d}\right)}. \tag{3.21}$$

The PEP expression in (3.21) shows that the diversity order of the system is $m_{sd} + \sum_{j=1}^{L} m_{r_j d}$.

3.3.2 Transfer function bounds

The weight distribution is essential in deriving the union bounds on the error rates of a given code. However, for a turbo code with a given interleaver, it is exceedingly difficult to obtain making it impractical. This is due to the fact that, the redundant bits generated by

the second interleaver are dependent on the input word and the manner in which the bits are interlaced. A viable solution to this approach is an exhaustive search over all possible cases, but for long interleavers it proves to be computationally intensive. In [69]- [70], the average weight distribution for turbo codes for a given length using the transfer bounds technique is proposed. However, the computation method in [70] allows for more accurate numerical results. In this work, the method proposed in [70] is used.

3.3.2.1 Weight enumerators

The state transition for the $(1, \frac{17}{13})_8$ code fragment used in this work – where the subscript 8 denotes the octal representation – can be shown in Fig. 3.2.

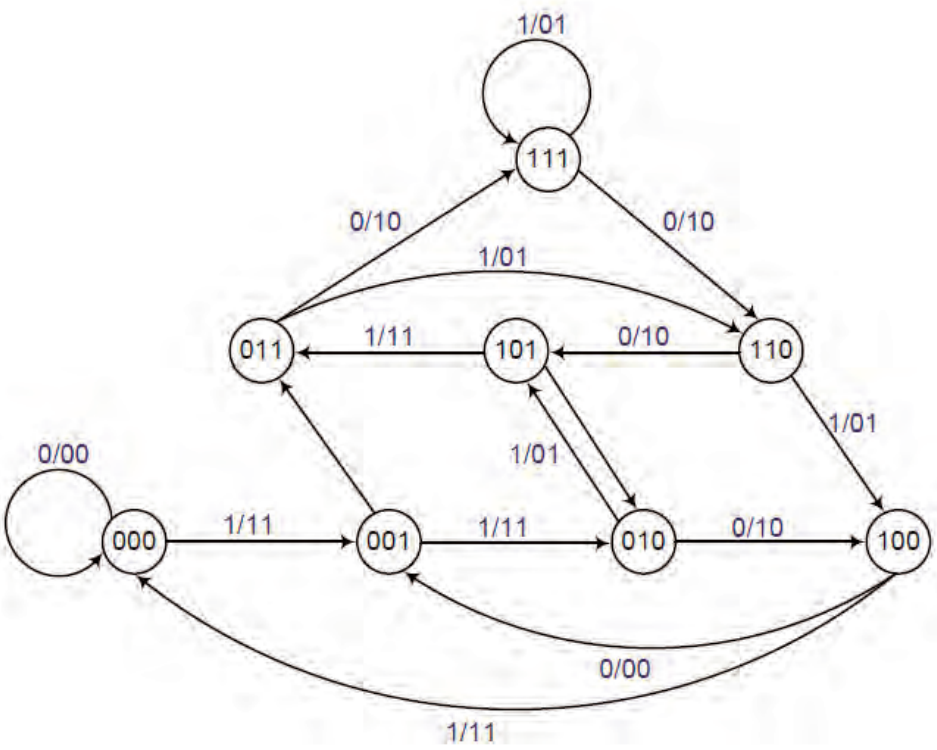

Figure 3.2: State transition diagram of $\left(1, \frac{17}{13}\right)$ code fragment in octal form.

The labels of the transition between the states represent the input information bit (systematic bit) and the output bits. Following the method in [70], a state transition can be

obtained using Fig. 3.2 and is given by

$$\mathbf{A}(\mathbf{J},\mathbf{I},\mathbf{D}) = \begin{pmatrix} J & JID & 0 & 0 & 0 & 0 & 0 & 0 \\ 0 & 0 & JID & J & 0 & 0 & 0 & 0 \\ 0 & 0 & 0 & 0 & JD & JI & 0 & 0 \\ 0 & 0 & 0 & 0 & 0 & 0 & JI & JD \\ JID & J & 0 & 0 & 0 & 0 & 0 & 0 \\ 0 & 0 & J & JID & 0 & 0 & 0 & 0 \\ 0 & 0 & 0 & 0 & JI & JD & 0 & 0 \\ 0 & 0 & 0 & 0 & 0 & 0 & JD & JI \end{pmatrix}, \tag{3.22}$$

where $J^j I^i D^d$ is a monomial with j always equal to 1, i and d are input and output dependent and take on the value 0 or 1. The corresponding transfer function is given by

$$T(J,I,D) = \sum_{j\geq 0}\sum_{i\geq 0}\sum_{d\geq 0} J^j I^i D^d t(j,i,d). \tag{3.23}$$

where j, i and d denote the length, the input weight and the output weight respectively.

Using the technique in [71] and after some manipulations, the recursion formula can be obtained as shown in Appendix A.

3.3.3 Bit Error Rate

The average BER can be upper bounded as [72]

$$\overline{P}_b \leq \frac{1}{K}\sum_{d=d_f}^{\infty} a(d)P(d), \tag{3.24}$$

where d_f represents the free distance, $P(d)$ is the PEP, K is the information length and $a(d)$ is the number of error events with distance d given by

$$a\left(d\right)=\underbrace{\sum_{i=1}^{K}\sum_{d_1=1}^{K}\sum_{d_2=1}^{K}}_{d=i+d_1+d_2}\frac{i}{K}\binom{i}{K}p\left(d_1|i\right)p\left(d_2|i\right), \tag{3.25}$$

with

$$p\left(d_{1/2}|i\right)=\frac{t(K,i,d_{1/2})}{\binom{K}{i}}. \tag{3.26}$$

Using (3.16) in (3.24) yields very loose bounds since many terms on the right hand side of (3.24) contribute to the sum over the entire SNR regime. For this reason, the limit-before-averaging technique [72] on the conditional union upper bound on the BER is reverted to, which results in much tighter bounds and is given by

$$\overline{P}_b\leq\underbrace{\int_0^\infty\cdots\int_0^\infty}_{L-fold}\left[\min\left(\frac{1}{2},\frac{1}{K}\sum_{d=d_f}^{\infty}a(d)P(d|\gamma_{sd}\cdots\gamma_{r_Ld})\right)\right]p(\gamma_{sd})\cdots p(\gamma_{r_Ld})\mathrm{d}\gamma_{sd}\cdots\mathrm{d}\gamma_{r_Ld}. \tag{3.27}$$

Note that the order of summation and integration cannot be interchanged due to the minimization. Hence the L-fold integration is computed numerically.

3.4 Outage Probability

Another performance metric that best describes slowly fading channels is the outage probability denoted by P_{out}. In the proposed scheme, the source broadcasts the entire codeword to the destination with a coding rate R_c, while the cooperating relays receive the source message with a rate $R_1=\frac{R_c}{\alpha}$ where α denotes the cooperation level (amount of time the relays listen to the codeword) and is given by

$$\alpha=\frac{K+f(N-K)}{N}, \tag{3.28}$$

and $0 < \alpha < 1$. Throughout the Chapter, the code rate is given by $R_c = \frac{1}{3}$ (due to the structure of the turbo code used here) without loss of generality.

During the second phase, the decoding relays transmit the parity bits only with a transmission rate $R_2 = \frac{R_c}{1-\alpha}$. In the following, a closed-form expression for the outage probability of the system is derived.

A direct transmission between the source i and destination j is first considered as a baseline. The instantaneous capacity for slowly-fading channels can be expressed as $C(\gamma_{ij}) = \log_2(1+\gamma_{ij})$ [73]. The link is said to be in outage, if the instantaneous capacity falls below a threshold R_c which denotes the code rate and the corresponding outage event is $C(\gamma_{ij}) < R_c$. Hence the outage probability for a Nakagami-m fading can be evaluated as

$$\begin{aligned} P_{out} &= \Pr\{C(\gamma_{ij}) < R_c\} = \int_0^{2^{R_c}-1} p(\gamma_{ij})\mathrm{d}\gamma_{ij} \\ &= 1 - \frac{\Gamma\left(m, \frac{(2^{R_c}-1)m}{\bar{\gamma}_{ij}}\right)}{\Gamma(m)} \\ &= \frac{\varphi\left(m, \frac{(2^{R_c}-1)m}{\bar{\gamma}_{ij}}\right)}{\Gamma(m)}, \end{aligned} \tag{3.29}$$

where $\Pr\{\mathcal{B}\}$ is the probablity of event $\mathcal{B}$, $\varphi(a,x)$[3] and $\Gamma(a,x)$ denote the lower and upper incomplete gamma functions respectively defined in [75, Eqs. (8.350.1)-(8.350.2)] as

$$\varphi(a,x) = \int_0^x e^{-t}t^{a-1}\mathrm{d}t, \tag{3.30}$$

and

$$\Gamma(a,x) = \int_x^\infty e^{-t}t^{a-1}\mathrm{d}t. \tag{3.31}$$

[3]The notation of the lower incomplete gamma function in this thesis is different from the commonly used one. This is done intentionally in order to avoid confusion as γ is already used to express the instantaneous SNR.

3.4.1 Outage Analysis of the proposed scheme

In this scheme, the transmission for the codeword is done over two phases. In the first phase, the source transmits to the destination with a code rate R_c, whereas it transmits to the relays with a code rate $R_1 = R_c/\alpha$, where α denotes the cooperation level.

When a relay r_n does not successfully decode the source message, it is said to be in outage which is equivalent to the event

$$C(\gamma_{sr_n}) = \log_2(1+\gamma_{sr_n}) < R_c/\alpha. \tag{3.32}$$

Otherwise it is not in outage and can translate to the event

$$C(\gamma_{sr_n}) = \log_2(1+\gamma_{sr_n}) > R_c/\alpha. \tag{3.33}$$

In the second phase, the decoding relays forward to the destination. The transmission over the two phases can be seen as time sharing between two independent channels where the second channel (r_n-d) uses a fraction of the total time. Hence, the corresponding outage event involving a relay r_n-d can be given by

$$C(\gamma_{sd}, \gamma_{r_nd}) = \log_2(1+\gamma_{sd}) + \beta(1-\alpha)\log_2(1+\gamma_{r_nd}) < R_c, \tag{3.34}$$

where $\beta = 0$ when there is no retransmission in the second phase and $\beta = 1$ otherwise.

The end-to-end outage probability at the destination given the two transmission phases is

$$\begin{aligned} P_{out} = \Pr\{\gamma_{sd} < 2^{R_c}-1\} \cdot \prod_{j=1}^{L} \Pr\{\gamma_{sr_j} < 2^{R_c/\alpha}-1\} + \sum_{\vartheta=1}^{L} \binom{L}{\vartheta} \Bigg[\prod_{j=\vartheta+1}^{L} \Pr\{\gamma_{sr_j} < 2^{R_c/\alpha}-1\} \\ \times \prod_{j=1}^{\vartheta} \Pr\{\gamma_{sr_j} > 2^{R_c/\alpha}-1\} \Pr\left\{ (1+\gamma_{sd})^{\alpha} \left(1 + \sum_{j=1}^{\vartheta} \gamma_{r_jd}\right)^{1-\alpha} < 2^{R_c} \right\} \Bigg], \end{aligned} \tag{3.35}$$

where the first term of the summation denotes the case where all the relays are in outage and the second term of (3.35) corresponds to all the cases where some or all relays may fully decode the source message (not in outage).

Using (3.29), the expression in (3.35) can be rewritten as

$$\begin{aligned} P_{out} = & \left(\int_0^{2^{R_c}-1} p(\gamma_{sd}) \mathrm{d}\gamma_{sd} \right) \left(\prod_{j=1}^{L} \left[\int_0^{2^{R_c/\alpha}-1} p(\gamma_{sr_j}) \mathrm{d}\gamma_{sr_j} \right] \right) + \sum_{\vartheta=1}^{L} \binom{L}{\vartheta} \\ & \times \left(\prod_{j=\vartheta+1}^{L} \left[\int_0^{2^{R_c/\alpha}-1} p(\gamma_{sr_j}) \mathrm{d}\gamma_{sr_j} \right] \right) \left\{ \left(\prod_{j=1}^{\vartheta} \left[1 - \int_0^{2^{R_c/\alpha}-1} p(\gamma_{sr_j}) \mathrm{d}\gamma_{sr_j} \right] \right) \right. \\ & \left. \times \underbrace{\int \cdots \int}_{\mathcal{A}} p(\gamma_{sd}) \cdot \prod_{j=1}^{\vartheta} p(\gamma_{r_j d}) \mathrm{d}\gamma_{r_j d} \mathrm{d}\gamma_{sd} \right\}, \end{aligned} \tag{3.36}$$

where $\mathcal{A}$ corresponds to the region on integration given by

$$\mathcal{A} \left\{ (\gamma_{sd}, \gamma_{r_j d}) | \gamma_{sd} \geq 0, \gamma_{r_j d} \geq 0, 1 \leq j \leq \vartheta, (1+\gamma_{sd}) \left(1 + \sum_{j=1}^{\vartheta} \gamma_{r_j d} \right)^{1-\alpha} < 2^{R_c} \right\}, \tag{3.37}$$

which is obtained by noting that

$$\log_2(1+\gamma_{sd}) + \log_2 \left(1 + \sum_{j=1}^{\vartheta} \gamma_{r_j d} \right)^{1-\alpha} < R_c, \tag{3.38}$$

where the left term of the inequality represents the instantaneous capacity when cooperation takes place. It is straightforward to see that (3.38) can further be given by

$$(1+\gamma_{sd}) \left(1 + \sum_{j=1}^{\vartheta} \gamma_{r_j d} \right)^{1-\alpha} < 2^{R_c} \tag{3.39}$$

Using (3.37), it is easy to show that

$$\mathcal{A} = \begin{cases} \gamma_{sd} < 2^{R_c} - 1 = a \\ \gamma_{r_j d} < \frac{2^{R_c/(1-\alpha)}}{(1+\gamma_{sd})^{1/(1-\alpha)}} - 1 = b \end{cases} \tag{3.40}$$

After performing some integrations and using the explicit region of integration as shown in (3.40), a more compact form of (3.36) can be given as

$$\begin{aligned} P_{out} = & \left[\frac{\varphi\left(m_{sd}, \frac{m_{sd}}{\bar{\gamma}_{sd}}\left(2^{R_c}-1\right)\right)}{\Gamma(m_{sd})}\right]\left[\prod_{j=1}^{L}\frac{\varphi\left(m_{sr_j}, \frac{m_{sr_j}}{\bar{\gamma}_{sr_j}}\left(2^{R_c/\alpha}-1\right)\right)}{\Gamma(m_{sr_j})}\right] + \sum_{\vartheta=1}^{L}\binom{L}{\vartheta} \\ & \times \left[\prod_{j=\vartheta+1}^{L}\frac{\varphi\left(m_{sr_j}, \frac{m_{sr_j}}{\bar{\gamma}_{sr_j}}\left(2^{R_c/\alpha}-1\right)\right)}{\Gamma(m_{sr_j})}\right]\left\{\left[\prod_{j=1}^{\vartheta}\frac{\Gamma\left(m_{sr_j}, \frac{m_{sr_j}}{\bar{\gamma}_{sr_j}}\left(2^{R_c/\alpha}-1\right)\right)}{\Gamma(m_{sr_j})}\right]\right. \\ & \left. \times \int_0^a \frac{m_{sd}^{m_{sd}}\gamma_{sd}^{m_{sd}-1}}{\Gamma(m_{sd})\bar{\gamma}_{sd}}\exp\left(-\frac{m_{sd}\gamma_{sd}}{\bar{\gamma}_{sd}}\right)\cdot\left[\prod_{j=1}^{\vartheta}\frac{\varphi\left(m_{r_j d}, \frac{m_{r_j d}}{\bar{\gamma}_{r_j d}}\cdot b\right)}{\Gamma(m_{r_j d})}\right]\mathrm{d}\gamma_{sd}\right\}, \end{aligned} \tag{3.41}$$

A closed-form expression for the outage probability in (3.41) can be obtained by solving the following integral

$$I(\mu,\nu,\beta) = \int_0^{2^{R_c}-1}\frac{m_{sd}^{m_{sd}}\gamma_{sd}^{\mu}}{\Gamma(m_{sd})\bar{\gamma}_{sd}}\exp\left(-\nu\gamma_{sd}\right)\varphi\left(m_{r_j d}, \frac{m_{r_j d}}{\bar{\gamma}_{r_j d}}\Big(\frac{2^{R_c\beta}}{(1+\gamma_{sd})^{\beta}}-1\Big)\right)\mathrm{d}\gamma_{sd} \tag{3.42}$$

where $\mu = m_{sd} - 1$, $\nu = \frac{m_{sd}}{\bar{\gamma}_{sd}}$ and $\beta = \frac{1}{1-\alpha}$.

The integral in (3.42) can be evaluated as shown in Appendix B. Hence the closed-form

expression for the outage probability can be derived as

$$
\begin{aligned}
P_{out} = & \left[\frac{\varphi\left(m_{sd}, \frac{m_{sd}}{\bar{\gamma}_{sd}}\left(2^{R_c}-1\right)\right)}{\Gamma(m_{sd})}\right]\left[\prod_{j=1}^{L}\frac{\varphi\left(m_{sr_j}, \frac{m_{sr_j}}{\bar{\gamma}_{sr_j}}\left(2^{R_c/\alpha}-1\right)\right)}{\Gamma(m_{sr_j})}\right] + \sum_{\vartheta=1}^{L}\binom{L}{\vartheta} \\
& \times \left[\prod_{j=\vartheta+1}^{L}\frac{\varphi\left(m_{sr_j}, \frac{m_{sr_j}}{\bar{\gamma}_{sr_j}}\left(2^{R_c/\alpha}-1\right)\right)}{\Gamma(m_{sr_j})}\right]\left\{\left[\prod_{j=1}^{\vartheta}\frac{\Gamma\left(m_{sr_j}, \frac{m_{sr_j}}{\bar{\gamma}_{sr_j}}\left(2^{R_c/\alpha}-1\right)\right)}{\Gamma(m_{sr_j})}\right]\right. \\
& \times \left[\prod_{j=1}^{\vartheta}\frac{m_{sd}^{m_{sd}}}{\Gamma(m_{sd})\bar{\gamma}_{sd}}\left(\left(\frac{m_{sd}}{\bar{\gamma}_{sd}}\right)^{-m_{sd}}\varphi\left(m_{sd}, \frac{m_{sd}}{\bar{\gamma}_{sd}}\left(2^{R_c}-1\right)\right) - \exp\left(\frac{m_{r_jd}}{\bar{\gamma}_{r_jd}}+1\right)\right.\right. \\
& \times \sum_{n=0}^{m_{r_jd}-1}\sum_{m=0}^{n}\frac{(-1)^{n+m}}{n!}\binom{n}{m}\left(\frac{m_{r_jd}}{\bar{\gamma}_{r_jd}}\right)^{n} 2^{\frac{R_c m}{1-\alpha}}\sum_{i=0}^{\infty}\sum_{l=0}^{i}\frac{(-1)^i}{i!}\binom{i}{l}2^{\frac{R_c(i-l)}{1-\alpha}}\left(\frac{m_{sd}}{\bar{\gamma}_{sd}}\right)^{l}\left(\frac{m_{r_jd}}{\bar{\gamma}_{r_jd}}\right)^{i-l} \\
& \left.\left.\left.\times \frac{\left(2^{R_c}-1\right)^{m_{sd}+l}}{m_{sd}+l}{}_2F_1\left(m_{sd}+l, \frac{i-l}{1-\alpha}, m_{sd}+l+1; 1-2^{R_c}\right)\right)\right].
\end{aligned}
\tag{3.43}
$$

3.4.2 Asymptotic behaviour

In order to investigate the asymptotic behaviour of (3.41), all the average SNRs are assumed to be sufficiently large, i.e., $\bar{\gamma}_{sd} = \bar{\gamma}_{sr_j} = \bar{\gamma}_{r_jd} = \bar{\gamma} \to \infty$. This condition will reduce (3.41) to

$$
P_{out} \approx \int_0^a \frac{m_{sd}^{m_{sd}}\gamma_{sd}^{m_{sd}-1}}{\Gamma(m_{sd})\bar{\gamma}}\exp\left(-\frac{m_{sd}\gamma_{sd}}{\bar{\gamma}}\right)\left[\prod_{j=1}^{\vartheta}\frac{\varphi\left(m_{r_jd}, \frac{m_{r_jd}}{\bar{\gamma}}b\right)}{\Gamma(m_{r_jd})}\right]\mathrm{d}\gamma_{sd}. \tag{3.44}
$$

Using $\varphi(a,x) = x^a a^{-1}{}_1F_1(a, 1+a; x)$ given in [75, Eq. (8.351.2)], (3.44) can be rewritten as

$$
\begin{aligned}
P_{out} \approx & \int_0^a \frac{m_{sd}^{m_{sd}}\gamma_{sd}^{m_{sd}-1}}{\Gamma(m_{sd})\bar{\gamma}}\exp\left(-\frac{m_{sd}\gamma_{sd}}{\bar{\gamma}}\right)\left[\prod_{j=1}^{\vartheta}\frac{1}{\Gamma(m_{r_jd})}m_{r_jd}^{m_{r_jd}-1}\bar{\gamma}^{-m_{r_jd}}b^{m_{r_jd}}\right. \\
& \left.\times {}_1F_1\left(m_{r_jd}, 1+m_{r_jd}; -\frac{m_{r_jd}b}{\bar{\gamma}}\right)\right],
\end{aligned}
\tag{3.45}
$$

where ${}_1F_1(a,b;x)$ is the confluent hypergeometric function defined in [75, Eq. (9.211.1)] as

$${}_1F_1(a,b;x) = \frac{\Gamma(b)2^{1-b}e^{\frac{1}{2}x}}{\Gamma(a)\Gamma(b-a)}\int_{-1}^{1}(1-t)^{b-a-1}(1+t)^{a-1}e^{\frac{1}{2}xt}\mathrm{d}t. \tag{3.46}$$

As $\bar{\gamma}\to\infty$, the following approximations $\lim_{x\to\infty}\exp(-1/x)\approx 1$ and ${}_1F_1\left(a,b;0\right)\approx 1$ can be used. After some algebraic manipulations and substitutions as defined in (3.40), the outage probability can be approximated as

$$P_{out}\approx \bar{\gamma}^{-\left(m_{sd}+\sum_{j=1}^{L}m_{r_jd}\right)}\underbrace{\prod_{j=1}^{L}\frac{1}{\Gamma(m_{r_jd})}\int_0^a \frac{m_{sd}^{m_{sd}}\gamma_{sd}^{m_{sd}-1}}{\Gamma(m_{sd})}m_{r_jd}^{m_{r_jd}-1}\left(\frac{2^{R_c/(1-\alpha)}}{(1+\gamma_{sd})^{1/(1-\alpha)}}-1\right)^{m_{r_jd}}\mathrm{d}\gamma_{sd}}_{\Lambda}. \tag{3.47}$$

The expression of Λ in (3.47) can be rearranged as

$$\Lambda = \prod_{j=1}^{L}\frac{m_{sd}^{m_{sd}}m_{r_jd}^{m_{r_jd}-1}2^{R_cm_{r_jd}/(1-\alpha)}}{\Gamma(m_{sd})\Gamma(m_{r_jd})}\int_0^a\frac{\gamma_{sd}^{m_{sd}-1}}{(1+\gamma_{sd})^{m_{r_jd}/(1-\alpha)}}\mathrm{d}\gamma_{sd}. \tag{3.48}$$

Using [75, Eq. (3.194.1)] and substituting $a=2^{R_c}-1$ from (3.40), a closed-form expression of Λ can be expressed as

$$\Lambda = \prod_{j=1}^{L}\frac{m_{sd}^{m_{sd}-1}m_{r_jd}^{m_{r_jd}-1}2^{R_cm_{r_jd}/(1-\alpha)}\left(2^{R_c}-1\right)^{m_{sd}}}{\Gamma(m_{sd})\Gamma(m_{r_jd})}{}_2F_1\left(\frac{m_{r_jd}}{1-\alpha},m_{sd},m_{sd}+1;1-2^{R_c}\right). \tag{3.49}$$

It can be observed that Λ does not depend on $\bar{\gamma}$. Hence, the expression in (3.47) confirms that the achievable diversity order is $m_{sd}+\sum_{j=1}^{L}m_{r_jd}$ which translates to full diversity in the number of relays and fading parameters.

3.5 Numerical Results

In what follows, the numerical results of bit error and outage probabilities of the proposed transmission scheme are presented. In the simulations, an eight-state $(1, 17/13)_{octal}$ turbo code with code rate $R_c = 1/3$ and frame size $K = 128$ was considered. It is assumed, without loss of generality that the s-r channels are identical, as well as the r-d channels for the BER evaluation. In this Chapter, different fading parameters m among the nodes are considered. Simulation results are also presented to validate the analysis derived in this work. Without loss of generality, it is assumed that all the average SNRs are equivalent, $\bar{\gamma}_{sd} = \bar{\gamma}_{sr_1} = \cdots = \bar{\gamma}_{sr_L} = \bar{\gamma}_{r_1 d} = \cdots \bar{\gamma}_{r_L d} = \bar{\gamma}$, all the fading parameters between the source and relays are identical, i.e., $m_{sr_1} = \cdots = m_{sr_L}$ and the fading coefficients are fixed for the duration of an entire frame and vary independently from one frame to another.

Fig. 3.3 provides some comparisons of the proposed scheme to a repetition coded scheme. In the repetition coded scheme, both the destinations and all the relays listen to the entire codeword. The relays that correctly decode the source message are selected to forward the source message by repeating it to the destination. Moreover, the same total power is maintained for both schemes under comparison. It can be noted that our proposed scheme performs better than the repetition coded system in terms of BER over the entire SNR. Furthermore, the similarity in the slope for both systems is an indication that the same diversity order is achieved.

Fig. 3.4 shows the comparison between the simulated BER and the union bounds on the BER of the proposed scheme for a single relay scenario and i.i.d. fading parameters. It can be noted that the simulated BER confirms the analytical results for the three cases presented here, that is, $m = 0.65$, $m = 1$ and $m = 1.5$. Furthermore, the results show that diversity in the number of relays and fading parameters is achieved. It is aso noted that the simulated BER is better than the theoretical ones since the latter represent the upper bounds to the former.

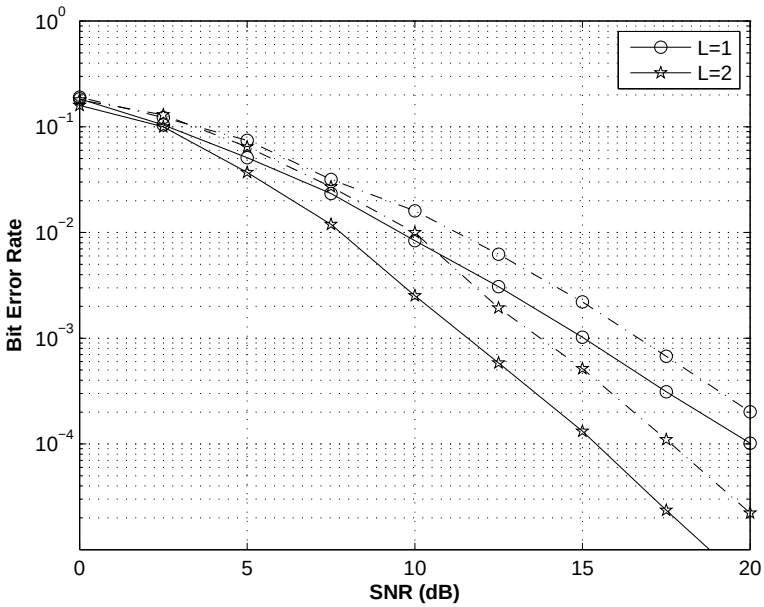

Figure 3.3: BER comparison of simulated repetition codes (dashed) versus proposed scheme (solid) for $L = 1$ and $L = 2$. The Nakagami-m distribution used is similar to Rayleigh distribution, i.e., $m_{ij} = 1$.

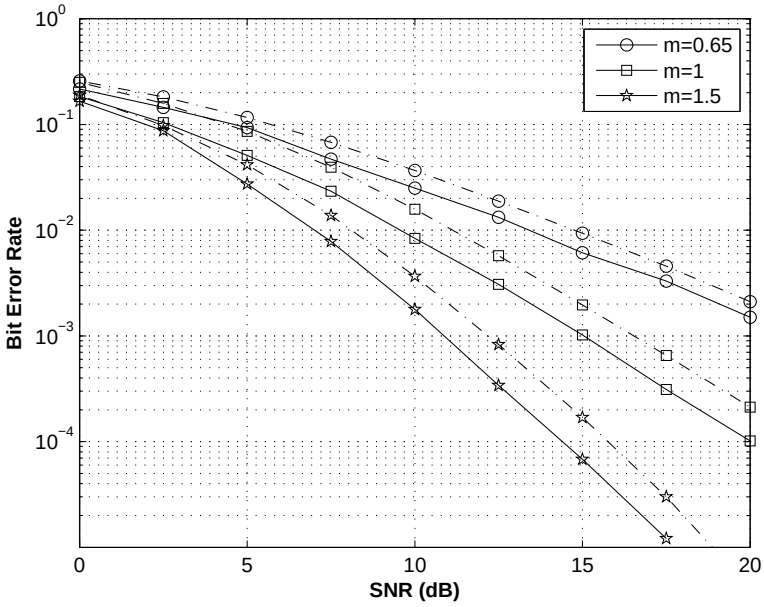

Figure 3.4: BER comparison of simulated (solid) and bounds (dashed) of distributed turbo-coded cooperation over Nakagami-m fading channels. $L = 1$, $m_{sd} = m_{sr} = m_{rd} = m$.

Fig. 3.5 shows the BER performance comparison of the union bounds on the BER and Monte-Carlo simulations for $L = 2$ and different fading parameters as in Fig. 3.4. All the average subchannel SNRs are assumed to be identical. It can be noted that the union bounds on the BER are in agreement with the simulated BER for different fading environments. This validates the analysis presented here. It is aslo noted that full diversity order is achieved and is dependent on the number of cooperating relays and fading indices.

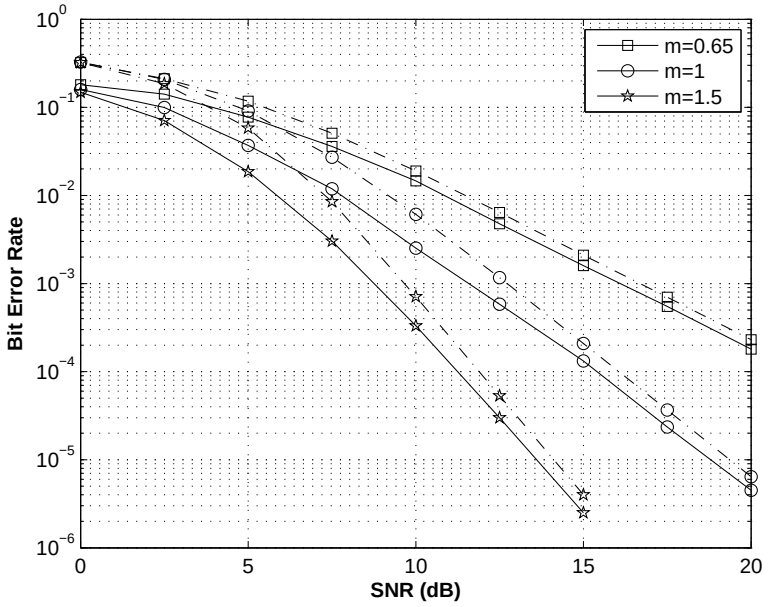

Figure 3.5: BER comparison of simulated (solid) and bounds (dashed) of distributed turbo-coded cooperation over Nakagami-m fading channels. $L = 2$ and $m_{sd} = m_{sr_1} = m_{sr_2} = m_{r_1d} = m_{r_2d} = m$.

In Fig. 3.6, non-identical Nakagami distribution for $L = 3$ is considered and shows the BER perfomance of the proposed scheme. The results show the diversity gain achieved for different fading environments.

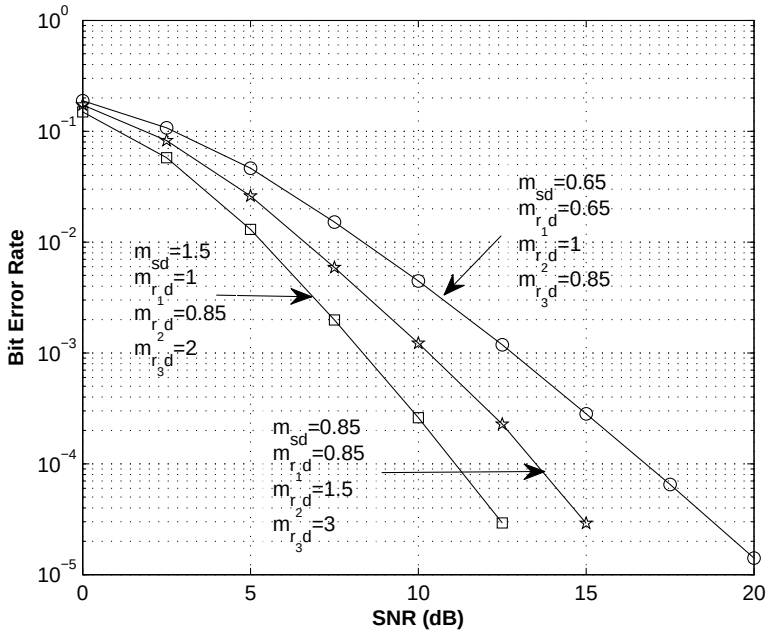

Figure 3.6: BER of distributed Turbo-coded cooperation over Nakagami-m fading channels with $L = 3$ and non-identical and independent Nakagami-m fading coefficients.

Fig. 3.7 shows the outage probability for various numbers of relays $L = \{0, 1, 2, 3\}$ and $m_{sd} = m_{r_1 d} = \cdots = m_{r_L d} = 1$, equivalent to Rayleigh fading channels where $L = 0$ corresponds to the non-cooperative case. A substantial gain is noted as the number of cooperating relays increases. Moreover, it can also be noted that the analytical results are accurate in predicting the outage probability of the proposed scheme since they are in perfect agreement with the simulation results. This is illustrated in Fig. 3.8 where the number of relays $L = 2$ and $m_{sd} = m_{r_j d} \neq m_{sr_j}$ were set. The effects of the fading parameters on the system performance are observed as larger m improves the outage probability. Full diversity in the number of relays and/or corresponding fading parameters from relays to destination and source to destination is achieved, as predicted in the analysis.

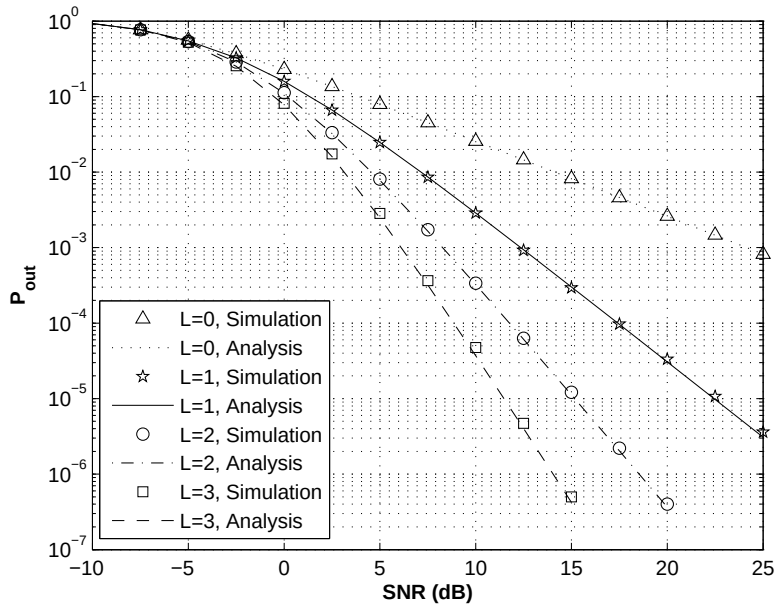

Figure 3.7: Outage probability for cooperative Turbo coded system with different numbers of relays L over Nakagami-m fading channels, $m_{sd} = m_{sr_j} = m_{r_jd} = 1$.

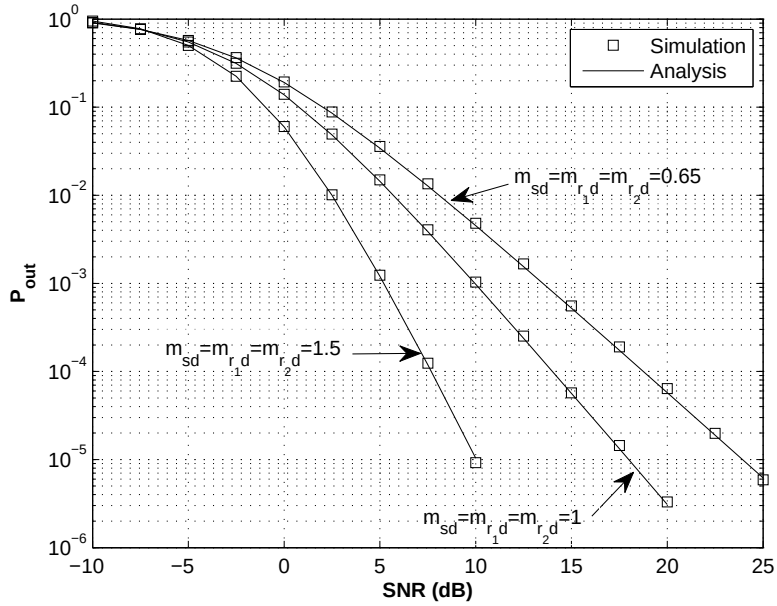

Figure 3.8: Outage probability for cooperative Turbo coded system with different m values and $L = 2$.

Fig. 3.9 presents the outage probability for non-identical relay-destination Nakagami-m fading channels. This scenario is more practical since the links in a cooperative system are

not necessarily similar. Computer simulations are presented and are shown to corroborate the analysis since the they match in all cases.

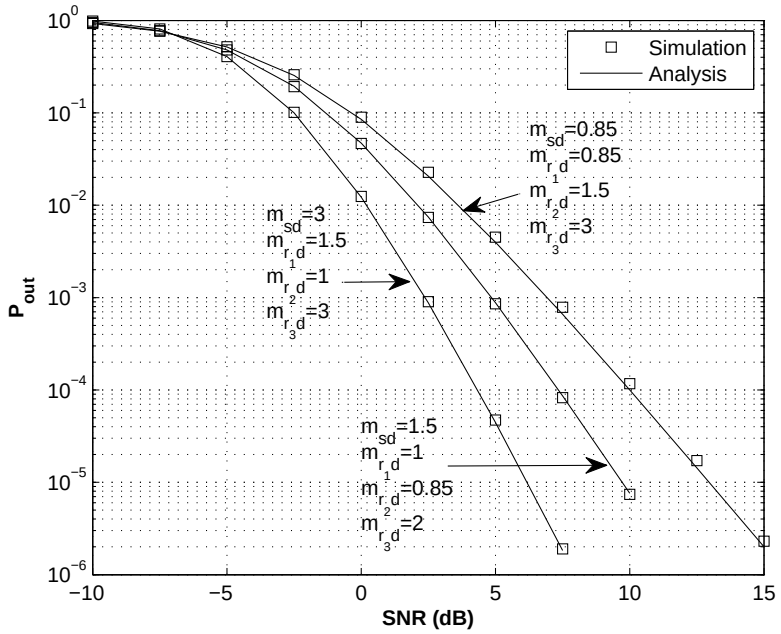

Figure 3.9: Outage probability for cooperative Turbo coded system with non-identical r-d Nakagami fading channels and $L = 3$.

In Fig. 3.10, the effects of the trade-off parameter f on the outage probability are provided through simulations. For this case, it is assumed that all the average SNRs are similar, i.i.d. Nakagami-m channels and $L = 2$. It is noted that, the value of f that minimizes the outage probability is about $f = 0.3$, and this is the case for all fading parameters used in the simulations. Moreover, it is also noted that as $f \to 1$ which has no practical meaning, the outage probability increases. This can be explained as for $f = 1$, the decoding relays dedicate little time to retransmission since they spend all their time in the receiving mode to the source (the entire codeword is received). In this case, the system is similar to a non-cooperative case, hence the performance deteriorates. Fig. 3.11 corroborates Fig. 3.10 which depicts $f = 0.3$ as the optimal value. Moreover, it can be observed in Fig. 3.11 that $f = 1$ is similar to a non-cooperative scenario.

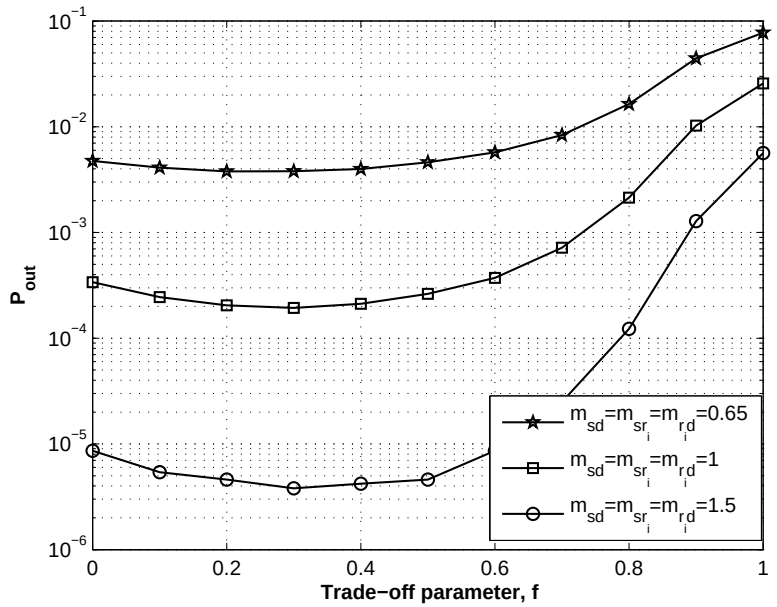

Figure 3.10: Outage probability versus trade-off parameter f with identical Nakagami-m fading channels, $L = 2$. $i = \{1, 2\}$.

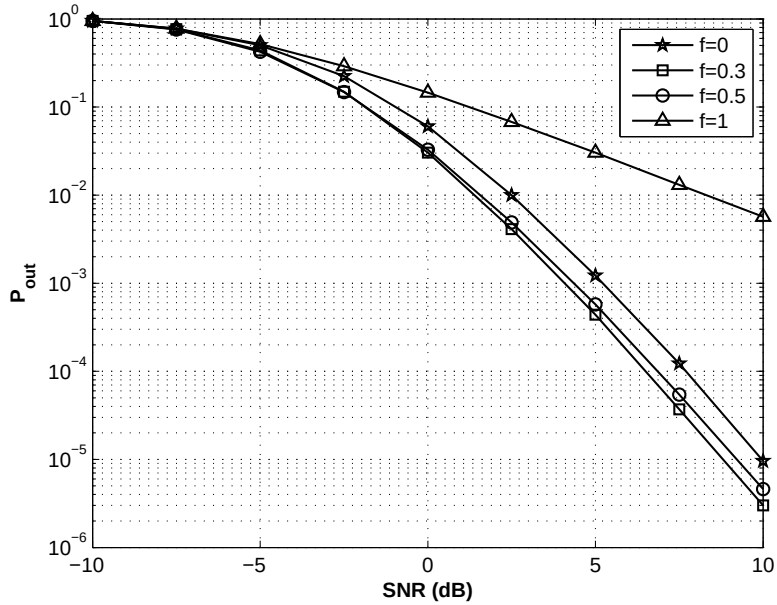

Figure 3.11: Outage probability for various values of f with identical Nakagami-m fading channels $m = 1.5$, $L = 2$.

3.6 Conclusions

In this Chapter, a distributed turbo coded cooperation with multiple relays over Nakagami-m fading channels was considered . To avoid error propagation, an adaptive scheme in which only the decoding relays forward to the destination during the second phase was used. Both the analytical expressions of the bit error and outage probabilities were derived, using the limit-before-average and transfer bounding techniques to provide much tighter bounds for the former. Computer simulations were provided to corroborate the analysis and proved to be in perfect in agreement with the latter. Finally, the proposed scheme showed that full diversity in the number of cooperating relays and/or fading parameters can be achieved for both the bit error and outage probabilities.

Chapter 4

Cross-layer Relay Selection Scheme for Cooperative Networks

This chapter proposes a cross-layer relay selection approach that maximizes the link-layer throughput, namely, relay selection in cooperative ARQ using throughput optimization as a selection criterion. In this approach, the set of reliable relays that participate in the retransmission phase are the ones that provide maximum link-layer throughput and this set is determined at the destination via an exhaustive search. A joint optimization of packet length and constellation size for the proposed scheme is also investigated.

4.1 Introduction

MIMO [6] systems have proved to be an effective way to improve capacity and provide spatial diversity in comparison with SISO systems. However, they cannot be deployed when nodes are limited by their size and hardware constraints. In order to overcome these limitations, a novel approach termed *cooperative communications* [9]- [13] has been proposed as a viable solution for the high-data rate coverage which will be required in future wireless systems.

Cooperative communications allows for a single-antenna node to assist the source node by relaying its message to the destination node, in addition to the direct signal from the source to the destination, hence creating a virtual antenna array. Two main cooperative diversity strategies have been extensively studied: AF and DF. In the AF stragegy, the relay node amplifies the signal received from the source node in the first time slot and forwards it to the destination node in the second time slot. No form of demodulation or decoding is required for this strategy. In the DF method, the relay first decodes the source signal prior to re-encoding and forwarding to the destination in the next time slot.

To avoid error propagation at the relay node that can be detrimental to DF cooperative systems, error detection schemes such as CRC codes are commonly used. Various works have also suggested ARQ protocol at the data link layer where CRC codes are used for detection prior to requesting retransmission. In practice, the maximum number of retransmissions is limited to a pre-defined value in order to avoid long delays. This variant of ARQ is called *truncated* ARQ.

A cross-layer design of cooperative diversity at the physical layer and truncated ARQ at the data-link layer has been investigated in [20] and [22], using the throughput as the performance metric. In [20], the source and the reliable relay nodes use a suitable orthogonal space-time block code (STBC) in the retransmission phase. A selective cooperation relaying is used for retransmission in [21]. Liu *et al.* [22] proposed a combination of adaptive modulation and coding (AMC) at the physical layer and truncated ARQ at the link layer. However, the selection of reliable relays is based on the minimization of the error rate, namely, the capacity improvement at the physical layer. Recently, capacity optimization at the link-layer through antenna selection has been investigated. In [78]- [79], a cross-layer transmit antenna selection (TAS) that maximizes the link-layer throughput of MIMO systems has been proposed. The criterion for antenna selection depends on the antenna subsets that see better channel conditions.

Motivated by these observations, a cross-layer relay selection approach that maximizes the link-layer throughput is proposed. In this approach, the set of reliable relays that participate in the retransmission phase are the ones that provide optimal link-layer throughput and this set is determined at the destination via an exhaustive search. To the author's knowledge, no work has been investigated on a relay selection in cooperative ARQ using throughput optimization as a selection criterion. This is a void it is hoped to fill. A joint optimization of packet length and constellation size for the proposed scheme is also investigated. The results show that the proposed approach (CROSS-layer) which assigns transmission to relays that see better channel conditions outperforms the PHY-layer approach used for comparison, in terms of throughput performance. Moreover, the CROSS-layer approach is more attractive since it incurs less bandwidth penalty than the PHY-layer approach does. This can be explained by noting that in CROSS-layer not all the reliable relays are used during every retransmission whereas in PHY-layer all the reliable relays always participate in the retransmission.

4.2 Proposed Scheme

4.2.1 System Model

Consider a cooperative scenario with a source node (S), a destination node (D) and L relay nodes (R). At the link layer, a truncated ARQ is employed for retransmission requests at the destination. It is assumed that all transmissions are organized as packets of fixed length K. Fig. 4.1 presents the block diagram of a communication channel including the link layer for the proposed system.

The system works as follows. The source transmits a packet to the destination and L relay nodes in the first time slot. Prior to broadcasting, CRC bits are appended to the source packets for error detection at the receiving end. The destination and relay nodes check for errors. The transmission in the second time slot is dependent on the ARQ status at the destination. Two cases are possible:

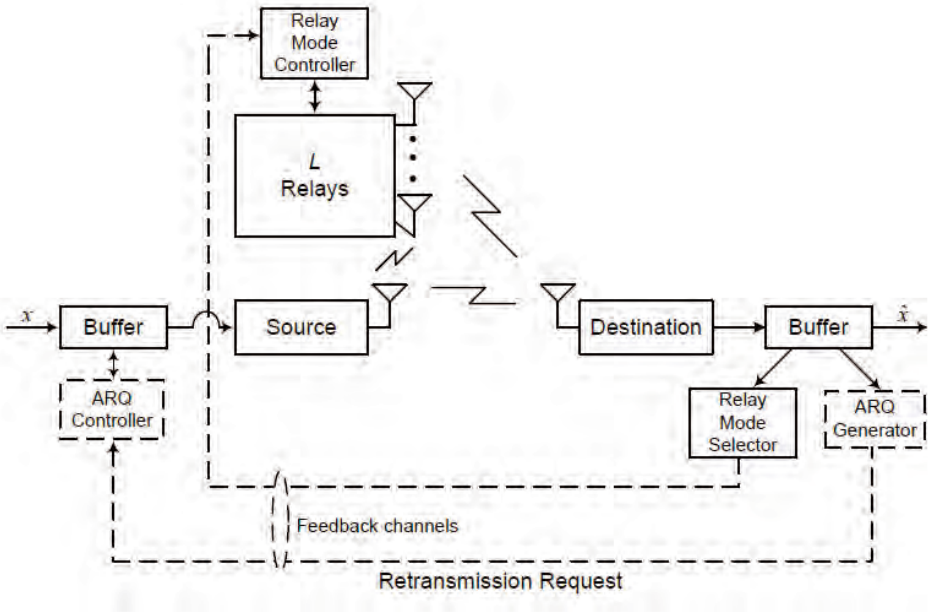

Figure 4.1: Block diagram of the communication system model including the link layer.

1. If the destination successfully decodes the source packet, it then notifies the source by sending a ACK through a low-rate and error-free feedback channel. In this case, the relays need not transmit in the second time slot and the source transmits a new packet.

2. If errors are detected at the destination, it sends a NACK to the source with a request for retransmission. In this Chapter, the source and the relays that have successfully decoded the source packet will send packets in the retransmission phase.

When a retransmission is requested by the destination, the source and a combination set of reliable relays operate during that phase. The selection of the relays among the reliable relays per transmission is performed at the destination through an exhaustive search. The set of reliable relays among all possible combinations that yields maximum throughput is selected by the destination and a notification is sent through a feedback channel. This feedback channel is assumed to be an error-free and low-rate channel. In practice, errors can occur in the channel which will result in performance degradation of the system. The

optimal subset, denoted by Ξ, is chosen from the set $\mathcal{S}$ which is given by

$$\mathcal{S} = \left\{ \binom{N_r}{i}, i = 1, \cdots, N_r \right\}, \tag{4.1}$$

where N_r represents the number of reliable relays. It should be emphasized that N_r changes per packet transmission according to the channel conditions.

The retransmission phase is terminated when the destination correctly decodes the source message or when the number of retransmissions reaches its maximum N_{max}. After the retransmission phase, the destination employs an MRC to optimally combine the signals from the source and the relays emanating from the relay subset.

4.2.2 Channel Model

It is considered that the relay nodes operate in half duplex mode, i.e., they cannot transmit and receive simultaneously. All nodes are equipped with single antenna. It is assumed that the channels are modelled as quasi-static and all are subject to flat Rayleigh fading. That is, the fading coefficients are constant for the entire duration of a transmission packet, but vary independently from one packet to another. It is also assumed that all receivers perfectly know the channel statistics of the transmitter-to-receiver link, namely the relays know their respective source-to-relay $S - R$ channel statistics and similarly the destination knows the source-to-destination $S - D$ and relay-to-destination $R - D$ channel statistics. To estimate the optimal subset of relays that maximizes the link-layer throughput, the CSI of the reliable relays-to-destination will be used. The channel coefficients of the $S-D$, $S - R$ and $R - D$ links denoted as h_{sd}, h_{sr} and h_{rd} respectively, are modelled as $\mathcal{CN}(0, 1)$.

The received signals y_{sd} at the destination and y_{sr_m} at the relays in the first time slot are given as

$$y_{sd} = h_{sd}x + n_{sd}, \tag{4.2}$$

$$y_{sr_m} = h_{sr_m}x + n_{sr_m}, \tag{4.3}$$

and y_{r_id} at the destination in the second time slot as

$$y_{r_id} = h_{r_id}\hat{x} + n_{r_id}, \tag{4.4}$$

where $\hat{x}$ is estimate of the transmitted signal x, i represents the i^{th} relay that could be used per retransmission and is defined in (4.1), $1 \leq m \leq L$, n_{sd}, n_{sr_m} and n_{r_id} are AWGN which are modelled as independent identically distributed $\mathcal{CN}(0, N_0)$ random variables.

4.3 Throughput Performance

In the proposed scheme, the number of relay nodes that can potentially participate in forwarding the source message or that are involved in the retransmission is not fixed. This number depends on the relays that correctly decode the source message (pass CRC test). Using (4.1) in the throughput expression given below, the set of relays that yield optimal throughput can be determined through an exhaustive search. Unlike most optimization problems, the objective function which is given by the throughput expression is maximized and obtained through an objective search. Hence, the throughput and its corresponding expressions are given by [20]

$$\eta(i) = b\left(\frac{K-C}{K}\right)\left(\frac{\Pr\{P_s(i)\}}{\mathbb{E}\langle Tr_{packet}(i)\rangle}\right), \tag{4.5}$$

where $\Pr\{P_s(i)\}$ and $\mathbb{E}\langle Tr_{packet}(i)\rangle$ denote the probability of successfully transmitted packets and average number of transmissions per packet, respectively, with $Tr_{packet}(i)$ representing the number of transmissions per packet when the subset of reliable relays corresponding to i is used. K denotes the packet length, b is the number of bits per symbol and C is the number of CRC bits. The total probability of packets successfully transmitted, $\Pr\{P_s(i)\}$,

when the subset of reliable relays corresponding to i is used, is given by

$$\begin{aligned}\Pr\{P_s(i)\} &= \Pr\{P_{s,0}\} + \Pr\{P_{s,j}(i)\} \\ &= \Pr\{P_{s,0}\} + \sum_{j=1}^{L}\Big(1 - PER_{sd}\big(PER_{Retr,j}(i)\big)^{N_{max}}\Big)\cdot \Pr\big(v=j\big), \end{aligned} \quad (4.6)$$

where $PER_{Retr,j}(i)$ denotes the average packet-error rate (PER) of the j^{th}relay retransmission, and L represents the total number of relays. In addition, $\Pr\{P_{s,0}\}$ is the probability of packets successfully transmitted when $N_r = 0$ and is given by

$$\Pr\{P_{s,0}\} = \big(1 - PER_{sd}(PER_{Retr,0})^{N_{max}}\big)\cdot \Pr\big(v=0\big). \quad (4.7)$$

Furthermore, the PER of the uncoded $S-D$ link is given by $PER_{sd} = 1-(1-SER_{sd})^{K/b}$ where SER_{sd} is the SER of an uncoded SISO system for M-ary Quadrature Amplitude Modulation (M-QAM) under the assumption that CSI is known at the receiver and the channel gain is Rayleigh distributed, and its closed-form expression is given by [57]

$$\begin{aligned} SER_{sd} = 2\left(1-\frac{1}{\sqrt{2^b}}\right)\left(1-\sqrt{\frac{g_{QAM}\bar{\gamma}_{sd}}{1+g_{QAM}\bar{\gamma}_{sd}}}\right) + \left(1-\frac{1}{\sqrt{2^b}}\right)^2\left[\frac{4}{\pi}\sqrt{\frac{g_{QAM}\bar{\gamma}_{sd}}{1+g_{QAM}\bar{\gamma}_{sd}}}\right. \\ \left.\times \tan^{-1}\left(\sqrt{\frac{1+g_{QAM}\bar{\gamma}_{sd}}{g_{QAM}\bar{\gamma}_{sd}}}\right) - 1\right], \end{aligned} \quad (4.8)$$

where $g_{QAM} = \frac{3}{2(2^b-1)}$.

For the particular case $j = 0$, where no single relay node correctly decodes the source packet, $PER_{Retr,0} = 1-(1-SER_{Retr,0})^{K/b}$ which yields the relationship between the packet error rate and symbol error rate for an uncoded system and $SER_{Retr,0} = SER_{sd}$.

In (4.6), $\Pr\big(v=j\big)$ is the probability that there are j reliable relays. Since all variances

are assumed to be equal, it can be given by

$$\Pr\big(v=j\big)=\binom{L}{j}\left(1-PER_{sr}\right)^{j}\left(PER_{sr}\right)^{L-j}, \tag{4.9}$$

where $j=0,...,L$, and $PER_{sr}=1-\left(1-SER_{sr}\right)^{K/b}$. The SER of each uncoded $S-R$ communication channel is similar to (4.8) with $\bar{\gamma}_{sd}$ replaced by $\bar{\gamma}_{sr}$.

In (4.5), the average number of transmissions per packet when the subset of reliable relays corresponding to i is used, denoted $\mathbb{E}\langle Tr_{packet}(i)\rangle$ is given by

$$\mathbb{E}\langle Tr_{packet}(i)\rangle=\mathrm{E}\langle Tr_{packet,0}\rangle+\sum_{j=1}^{L}\mathbb{E}\langle Tr_{packet,j}(i)\rangle\cdot\Pr(v=j). \tag{4.10}$$

In (4.10), $\mathbb{E}\langle Tr_{packet,0}\rangle$ is the average number of transmissions per packet when $N_r=0$, given by

$$\begin{aligned}\mathbb{E}\langle Tr_{packet,0}\rangle=1-PER_{sd}+PER_{sd}\Bigg[&\sum_{i=2}^{N_{max}+1}i\cdot\Big(PER_{Retr,0}\Big)^{i-2}\left(1-PER_{Retr,0}\right)\\&+\left(1+N_{max}\right)\cdot\Big(PER_{Retr,0}\Big)^{N_{max}-1}\Bigg],\end{aligned} \tag{4.11}$$

and

$$\begin{aligned}\mathbb{E}\langle Tr_{packet,j}(i)\rangle=1-PER_{sd}+PER_{sd}\Bigg[&\sum_{i=2}^{N_{max}+1}i\cdot\Big(PER_{Retr,j}(i)\Big)^{i-2}\left(1-PER_{Retr,j}(i)\right)\\&+\left(1+N_{max}\right)\cdot\Big(PER_{Retr,j}(i)\Big)^{N_{max}-1}\Bigg],\end{aligned} \tag{4.12}$$

with $PER_{Retr,j}(i)$ representing the average PER of the j^{th}-relay retransmission when the

subset of reliable relays corresponding to i is used given by

$$PER_{Retr,j}(i) = 1 - \left(1 - SER_{Retr,j}(i)\right)^{\frac{K}{b}}. \tag{4.13}$$

The above equations (4.11) and (4.12) differ by the PER expression in which the former represents a direct transmission scenario whereas the latter represents a cooperative scenario.

During the retransmission phase, only the relays that have successfully decoded the source packet are able to forward to the destination. The SER of retransmission is similar to [57] where a closed-form expression of the SER for M-QAM over L i.i.d. Rayleigh fading channels is proposed. After susbstituting L by $j+1$, the SER of the retransmission for the system under study is given by

$$\begin{aligned} SER_{Retr,j}(i) = {} & 4\left(1 - \frac{1}{\sqrt{2^b}}\right)\left(\frac{1-\mu_c}{2}\right)^{j+1} \sum_{l=0}^{j} \binom{j+l}{l} \left(\frac{1+\mu_c}{2}\right)^{l} - 4\left(1 - \frac{1}{\sqrt{2^b}}\right)^2 \\ & \times \left(\sum_{l=0}^{j} \frac{\binom{2l}{l}}{\left[4(1+g_{QAM}\bar{\gamma}_{Retr,j})\right]^l} - \sin\left(\tan^{-1}\mu_c\right) \sum_{l=1}^{j}\sum_{i=1}^{l} \frac{\binom{2l}{l}/\binom{2(l-i)}{l-i}}{\left(1+g_{QAM}\bar{\gamma}_{Retr,j}\right)^l} \right. \\ & \left. \times \cos\left(\tan^{-1}\mu_c\right) \right), \end{aligned} \tag{4.14}$$

where $j+1$ represents the $R-D$ links (from the reliable relays) and the $S-D$ link, $\mu_c = \sqrt{\frac{g_{QAM}\bar{\gamma}_{Retr,j}}{1+g_{QAM}\bar{\gamma}_{Retr,j}}}$, with $\bar{\gamma}_{Retr}$ denoting the average SNR of the retransmission given by $\bar{\gamma}_{Retr,j} = \frac{\bar{\gamma}_{sd}}{j+1}$.

After substituting the corresponding terms of (4.6)$-$ (4.10) in (4.5), the overall throughput of the system is obtained. This throughput expression is used at the destination to determine the optimal susbet of relays. That is, the subset that maximizes the link-layer throughput. The destination will then notify the reliable nodes on the selected subset through a low-rate and error-free feedback channel.

A throughput improvement can also be achieved through the optimization of packet parameters such as: packet length K and constellation size b. Due to the highly non-linear nature of the throughput as shown in (4.5), obtaining optimal packet length $K^\star$ and $b^\star$ numerically is a very difficult task. The Hooke and Jeeves method presented in [80] is used in this Chapter to determine $K^\star$ and $b^\star$ for the proposed scheme. This method is used to find the minimum or maximum of a nonlinear, multivariable and unconstrained function. It sequentially performs two types of search[1] – exploratory and pattern – and no derivatives are required. The exploratory move is first used to get information about the objective function in the neighbourhood of the current base point. In the case of a successful move, the exploratory moves are followed by the pattern search. The latter search aims to determine the best search direction by speeding up the search using the information already acquired about the objection function.

The proposed CROSS-layer scheme involves an exhaustive search over all possible relay combinations or subsets of $\left\{\binom{N_r}{j}, j = 1, 2, \cdots N_r\right\}$. The complexity corresponding to the proposed scheme is mainly due to the exhaustive search and is given by $O(2^{N_r})$ obtained through the summation of all possible relay combinations given by $\sum_{j=0}^{N_r}\binom{N_r}{j} = 2^{N_r}$.

4.4 Numerical Results

In this section, the throughput performance of the CROSS-layer scheme with optimized and non-optimized packet length and constellation size is examined. The throughput performance of the CROSS-layer (CL) to a PHY-layer (PL) approach is also compared. The optimization of the packet length and constellation size is also investigated in order to further enhance the system throughput.

Unless otherwise specified, the packet length $K = 100$, the modulation size $b = 4$, the maximum number of retransmissions $N_{max} = 3$, a 16-bit CRC is used for error detection,

[1] A search is a made of a sequence of moves. Furthermore a base point is selected prior to starting the search.

and the total number of available relays $L = 4$ are used in this Chapter.

Table 4.1 displays the optimal packet length, modulation size and throughput values corresponding to various uplink SNRs ranging from 0–20dB. $K_i^\star$, $b_i^\star$ and $\eta_i^\star$ where $i \in \{PL, CL\}$, represent the optimal packet length, modulation level and throughput for both PL and CL respectively. The CROSS-layer approach is discussed here, as the results obtained for this scenario can be applied to PHY-layer. It is noted that the values for the modulation level obtained are continuous. In practice, these values should be discrete. For $\bar{\gamma}_{sd} = 12$dB, $K_{CL}^\star = 53$ as shown in the table and its corresponding $b_{CL}^\star = 2.28$ and $\eta_{CL}^\star = 0.937$. Using $b_{CL} = 2$ and $b_{CL} = 3$ with the same value of $K_{CL}^\star$, the throughput values are $\eta_{CL}^\star = 0.9378$ and $\eta_{CL}^\star = 0.9373$ respectively. The value of b_{CL} is chosen to $b_{CL} = 2$, since it yields greater throughput than the one corresponding to other assumed value of b_{CL}. This can be done over the entire SNR regime.

Table 4.1: Optimal $K^\star$ and $b^\star$ for CROSS-layer and PHY-layer, $\bar{\gamma}_{sr} = 20$dB.

$\bar{\gamma}_{sd}$(dB)	0	4	8	12	16	20
$K_{CL}^\star$	53	54	54	53	53	54
$b_{CL}^\star$	0.42	0.87	1.52	2.28	3.04	3.76
$\eta_{CL}^\star$	0.40	0.54	0.67	0.93	1.27	1.70
$K_{PL}^\star$	50	57	57	57	56	59
$b_{PL}^\star$	0.51	1	1.64	2.15	2.70	3.20
$\eta_{PL}^\star$	0.11	0.25	0.46	0.77	1.17	1.55

Fig. 4.2 shows a plot of the overall throughput versus packet length K and constellation size b with $\bar{\gamma}_{sd} = \bar{\gamma}_{sr_i} = 20$dB. This case corresponds to a case where one relay maximizes the link-layer throughput, namely, when a single relay participates in the retransmission where it is observed that the throughput plane is smooth[2]. This observation was also made in [20] and is presented here to show that they both present the same characteristics, hence the

[2]This is merely to show the smoothness of the throughput plane and does not necessarily imply that a single relay is always used in the retrasnmission phase. The smoothness of the throughput plane was also observed when more than one relay was used in the retransmission phase and various SNRs values $\bar{\gamma}_{sd}$ and $\bar{\gamma}_{sr}$

same method could be used to determine the optimal K and b for the proposed scheme. As previously mentioned, obtaining optimal K and b analytically is intractable due to the nature of the throughput expression. As mentioned previously, the method of Hooke and Jeeves [80] is used here to determine the optimal values of K and b based on the observations of the throughput plane.

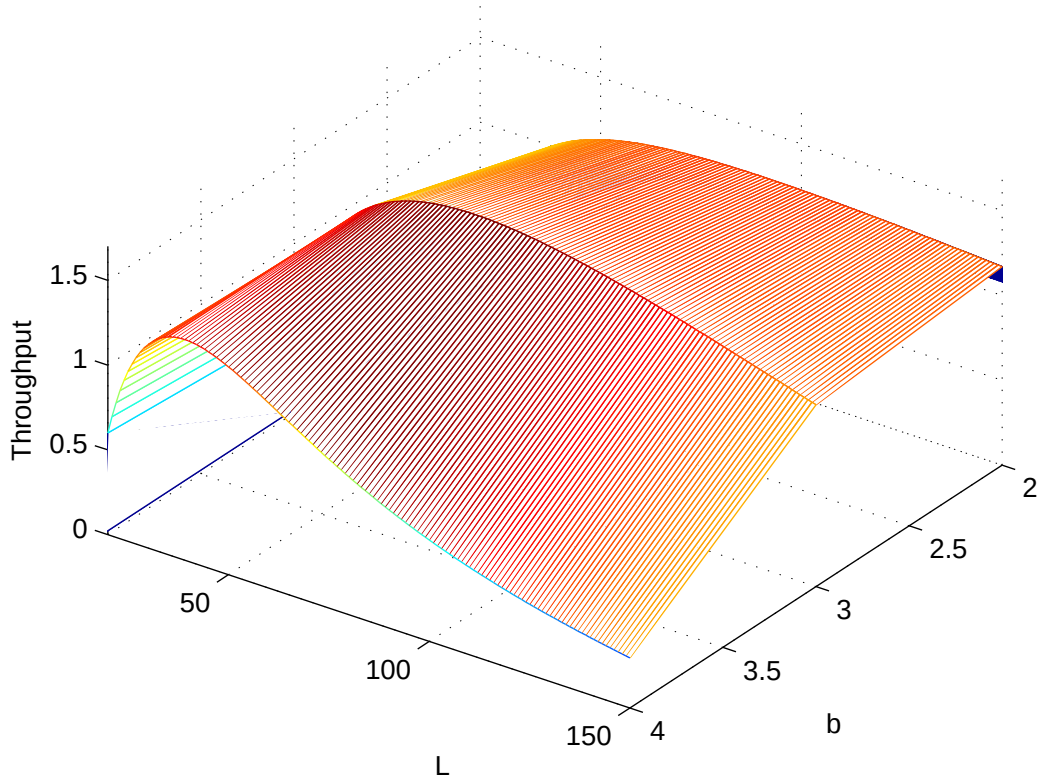

Figure 4.2: Throughput plane of relay selection scenario versus K and b, $\bar{\gamma}_{sd} = 20$dB.

In Fig. 4.3, the throughput versus SNR performance with non-optimized K and b for both the CROSS-layer approach and PHY-layer scenario is presented. It is noted that the performance of the CROSS-layer outperforms the PHY-layer from low to high SNRs for $(K, b)= \{(100, 4); (80, 3)\}$. From low to moderate SNRs, the throughput gains are substantial for $(K, b)= \{(100, 4); (80, 3)\}$ values given previously. At high SNRs, the throughput gain decreases considerably. This can be explained intuitively by noting that at high SNRs, the

optimal subset of reliable relays for the CROSS-layer approach is most of the time equal to the number of relays for PHY-layer (Fig. 4.5 clearly illustrates the intuition here).

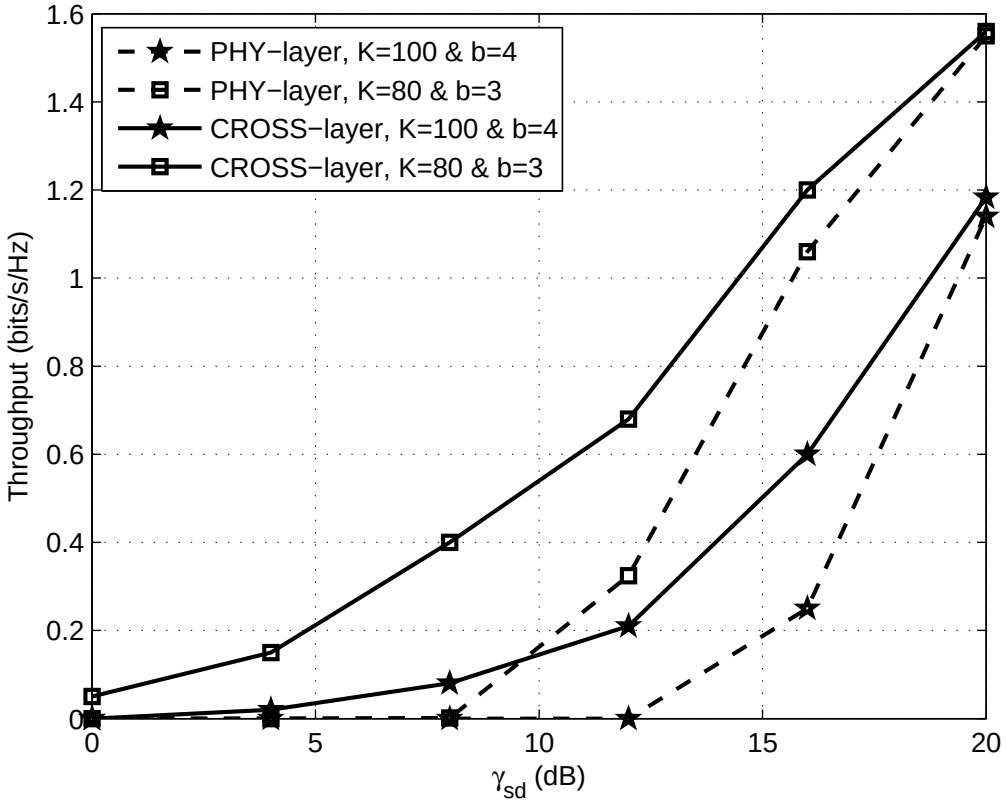

Figure 4.3: Throughput with fixed K and b for the best relays combination, $\bar{\gamma}_{sr} = 20$dB.

Fig. 4.4 shows a throughput comparison between the CROSS-layer design and the PHY-layer approach. For a fair comparison, the same number of decoding relays are used. In the PHY-layer, all the decoding/reliable relays participate in the retransmission whereas in the CROSS-layer this number varies depending on the relay selection criterion. It is noted that the CROSS-layer approach with $K^\star$ and $b^\star$ outperforms the PHY-layer with optimized K and b over the entire SNR regime. This implies that, relay selection performed at the link-layer provides system throughput improvement. Furthermore, the proposed CROSS-layer approach yields optimal throughput performance since it outperforms the PHY-layer throughput with optimized K and b.

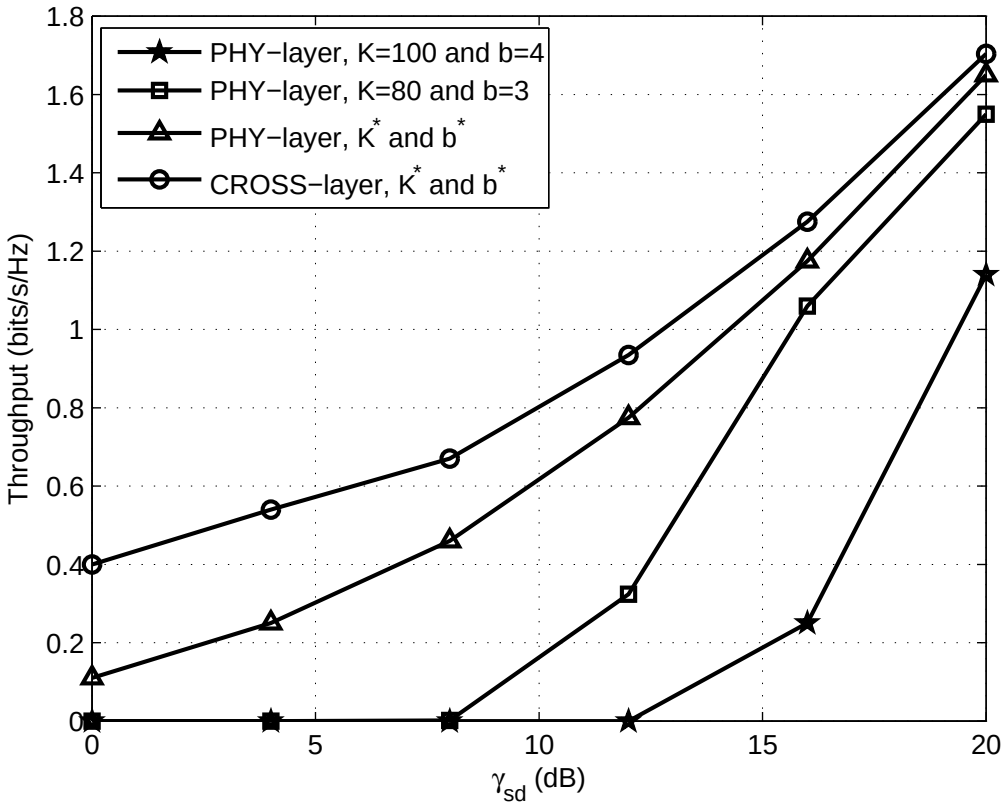

Figure 4.4: Optimal and sub-optimal throughput for the best relays combination (CROSS-layer), $\bar{\gamma}_{sr} = 20$dB.

Fig. 4.5 shows the percentage of relay usage of both the CROSS-layer and PHY-layer with $N_r = 4$. The usage of the PHY-layer is trivial as the same number of reliable relays which in this case is four, always forward during the retransmission phase. However, the number of transmitting reliable relays changes for the CROSS-layer based on the maximization of the link-layer throughput. At 8dB, two, three and four relays out four reliable relays maximize the link-layer throughput about 35%, 25% and 40% of the time, respectively. It can also be noted that the CROSS-layer approach is more bandwidth efficient than the PHY-layer one, since not all the reliable relays are used at all times. Also there are instances where one relay is used for retransmission.

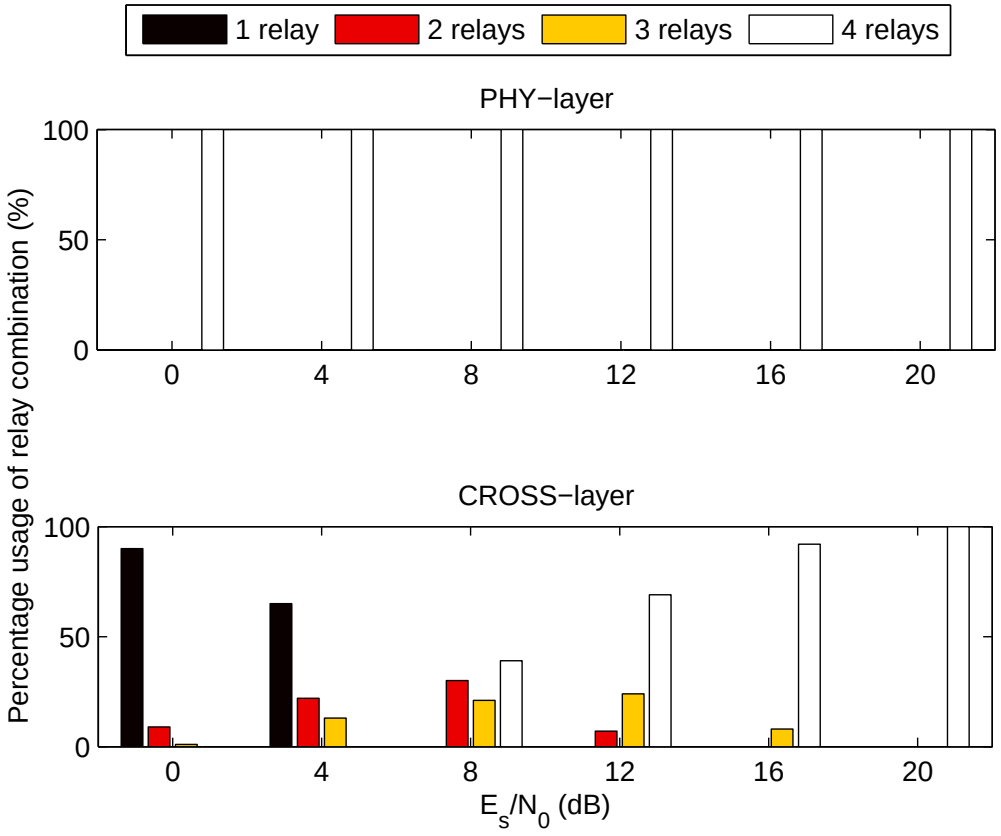

Figure 4.5: Usage rate of relay combination, reliable relay v of L relay candidates.

4.5 Conclusion

In this paper, a CROSS-layer relay selection based on maximization of link-layer throughput, namely the relay selection combination, based on the reliable relays that maximize the overall throughput at the link layer is proposed . This can be obtained through an exhaustive search. Furthermore, it was shown that the CROSS-layer approach provides throughput gain over the PHY-layer which is based on the minimization of the error probabilities or maximization of the system capacity. Moreover, the CROSS-layer approach utilizes the channel resources more efficiently than the PHY-layer, since not all reliable relays are always used in the retransmission. Hence it incurs less bandwidth penalty. Also joint optimization of packet length and modulation size (K and b) is performed for both PHY-layer and CROSS-layer to

further improve the throughput performance.

Chapter 5

Cross-layer Throughput Maximization via Power Optimization in Cooperative Networks

In this chapter, a joint optimization and best relay selection scheme in a cooperative diversity combined with truncated ARQ in order to maximize the system throughput is proposed. In the cooperative diversity system, a single relay is chosen among L relays to cooperate with the source through an uncoded DF protocol if requested. In the proposed scheme, it is shown that maximizing the throughput is equivalent to minimizing the SER of the retransmission. An asymptotic SER for the best DF relay selection with tight bounds at high SNR is derived. Furthermore, under a general optimization problem, the optimal power at the source and the best relay for different modulation schemes is obtained. This optimal power distribution is not necessarily the equal power distribution. Results show that power optimization for the best relay selection yields maximum throughput in comparison to the non-optimized power distribution, for various constellation sizes.

5.1 Introduction

Recently, various works have been undertaken in the area of cooperative communications to improve the throughput at higher layers by using various approaches [20], [21] which have been discussed in the previous chapter. However, the scheme in [20] incurs a bandwidth loss due to the number of orthogonal channels it requires per retransmission. Allowing for a single relay out of L potential relays to retransmit, will improve the bandwidth efficiency of the system. In [81]- [83], it is shown that the proposed schemes achieve the same diversity-multiplexing tradeoff as achieved by a system with L relay nodes. Furthermore, Ikki *et al.* [82], [83] proved that this scheme achieves the same diversity order as regular multi-relay cooperative-diversity systems. In [83], the authors derived closed-form expressions for the outage probability and average channel capacity of the best relay adaptive DF over i.n.i.d. Rayleigh fading channels. In [84], closed-form expressions of the AF and DF N^{th} best relay selection are derived for both i.n.i.d. and i.i.d. Rayleigh fading channels. The authors in [84] also derived asymptotic bounds for the SER of the AF N^{th} best relay selection, but no bounds for the DF. In [85], the authors derived an asymptotic bound of the outage probability for the N^{th} best relay selection for DF cooperative networks. The selection of the best relay can be based on various criteria: highest relay-to-destination instantaneous SNR [82] or threshold-based [86]. From a cross-layer standpoint, an incremental best relay cooperative diversity was proposed in [87], where only the best relay node participates in the retransmission phase. In this scheme, the user cooperation takes place upon NACK from the destination. Many works have been proposed using incremental relaying protocol. In [88], the authors considered a cooperative Type II hybrid ARQ (CHARQ) where the relay node only resends the source packet in the retransmission phase using AMC.

Motivated by these observations, a system that employs the best relay selection of [20] in the retransmission phase is proposed and the throughput maximization of the proposed scheme via power optimization is investigated. It is shown that maximizing the throughput

performance is equivalent to minimizing the SER. In what follows, the asymptotic bounds of the SER for the best relay in DF cooperative networks in order to evaluate the optimal power allocation are derived. The results show that optimal power allocation yields throughput performance superior to the non-optimized assigned power values.

5.2 System and Transmission Models

In the proposed scheme, a source node (S) transmits information bits to the destination node (D) while the neighbouring users remain idle since they operate in half-duplex mode – they cannot transmit and receive simultaneously. Some CRC bits are appended to the message at the source prior to transmitting to the destination. If the destination successfully decodes the message, then it sends an ACK through a highly-protected feedback channel. In this case, the source sends a new packet. Otherwise, retransmission is initiated upon reception of a NACK and the adjacent users turn their receivers on to act as relay nodes (R). The retransmission phase is divided into two time slots. In the first time slot of the retransmission phase, the source transmits to the relays and destination. In the second time slot of the retransmission phase, the relay with the highest $R-D$ instantaneous SNR selected among the reliabe relays, forward the source packet to the destination. The destination employs an MRC to combine the packets before the decoding process. The retransmission phase is repeated until the destination correctly decodes the source message or the number of retransmissions reaches its maximum, N_{max}. This scenario is depicted in Fig. 5.1, where the maximum number of retransmissions N_{max} is set to 1 for the sake of brevity.

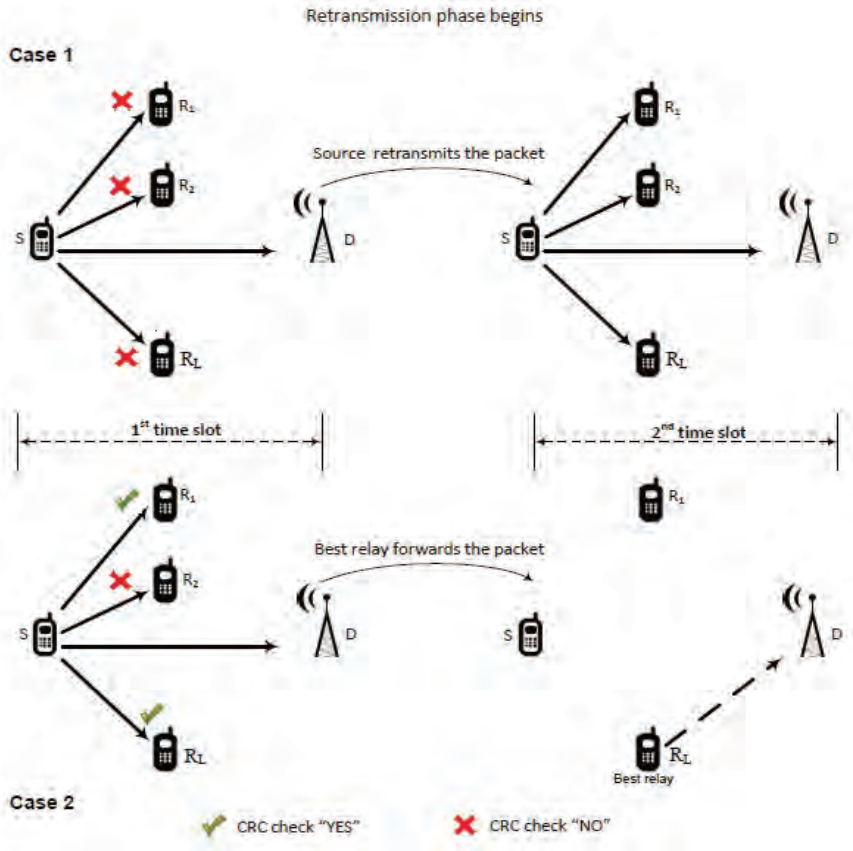

Figure 5.1: Cooperative scenario with best relay selection and truncated ARQ during the retransmission phase.

The channels are modelled as quasi-static fading, i.e., the fading coefficients are fixed for the entire duration of a transmission packet, but vary independently from one packet to another. The channels are subject to flat Rayleigh fading and uniform pathloss with a pathloss exponent ε. We assume perfect CSI at the receivers and perfect synchronization. The channel coefficients of the $S-D$, $S-R$ and the best $R-D$ links are denoted by h_{sd}, h_{sr_m} and h_{r^*d} respectively. All nodes are equipped with single transmit and receive antennas.

The received signals y_{sd} at the destination and y_{sr_m} at the relays in the first time slot are given by

$$y_{sd} = h_{sd}s + n_{sd}, \tag{5.1}$$

$$y_{sr_m} = h_{sr_m}s + n_{sr_m}, \tag{5.2}$$

and y_{r^*d} in the second time slot as

$$y_{r^*d} = h_{r^*d}\hat{s} + n_{r^*d}, \tag{5.3}$$

where s is the transmitted signal from the source, $\hat{s}$ is the estimate of the transmitted signal s at the best relay, r^* represents the best relay, $1 \leq m \leq L$, n_{sd}, n_{sr_m} and n_{r^*d} are AWGN and modelled as independent and identically distributed $\mathcal{CN}(0, N_0)$ RV.

5.3 Throughput Maximization

5.3.1 Throughput

Throughout this Chapter, the following notation is used: the PER, PER_{ij} to denote the average PER on the ij link, PER_r is the average PER of the retransmission from relay to destination, where in general $PER = 1 - (1 - SER)^{K/b}$ with K and b represent the packet length and the number of bits per symbol, respectively. SER_{ij} represents the average SER on the ij link, and SER_r is the average SER of the retransmission from relay to destination, $\bar{\gamma}_{ij}$ is the average SNR of the ij link.

The throughput expression and its corresponding terms are given by [20]

$$\eta = b\left(\frac{K-C}{K}\right)\left(\frac{\Pr\{P_s\}}{\mathbb{E}\langle Tr_{packet}\rangle}\right), \tag{5.4}$$

where $\Pr\{P_s\}$ and $\mathbb{E}\langle Tr_{packet}\rangle$ denote the probability of successfully transmitted packets and average number of transmissions per packet, respectively, with Tr_{packet} representing the number of transmissions per packet and $\mathbb{E}\langle\bullet\rangle$ the statistical average operator. C is the number of CRC bits.

The total probability of packets successfully transmitted, $\Pr\{P_s\}$ is given by

$$\Pr\{P_s\} = \sum_{j=0}^{L} \left(1 - PER_{sd}\big(PER_r(j)\big)^{N_{max}}\right) \cdot \Pr(j), \tag{5.5}$$

where L represents the total number of relays and $PER_r(j)$ denotes the average PER of the j^{th} relay retransmission, $\Pr(j)$ is the probability of having j reliable relays and N_{max} is the maximum number of retransmissions. In (5.4), the average number of transmissions per packet is given by

$$\begin{aligned}\mathbb{E}\langle Tr_{packet}\rangle = \sum_{j=0}^{L} \Bigg(1 - PER_{sd} + PER_{sd}\Bigg[\sum_{i=2}^{N_{max}+1} i\Big(PER_r(j)\Big)^{i-2}\Big(1 - PER_r(j)\Big) \\ + (1 + N_{max}) \cdot \Big(PER_r(j)\Big)^{N_{max}-1}\Bigg]\Bigg) \cdot \Pr(j),\end{aligned} \tag{5.6}$$

where $\Pr(j)$ is the probability of j reliable relays and can be expressed as

$$\Pr(j) = \binom{L}{j} (1 - PER_{sr})^j \, (PER_{sr})^{L-j}. \tag{5.7}$$

It is noted that (5.6) is a function of SER_{sd} (since the SER is a function of PER) which can be given by [57, Eq. (8.107)]

$$\begin{aligned}SER_{sd} = 2\left(1 - \frac{1}{\sqrt{M}}\right)\left(1 - \sqrt{\frac{g_{QAM}\bar{\gamma}_{sd}}{1 + g_{QAM}\bar{\gamma}_{sd}}}\right) + \left(1 - \frac{1}{\sqrt{M}}\right)^2 \Bigg[\frac{4}{\pi}\sqrt{\frac{g_{QAM}\bar{\gamma}_{sd}}{1 + g_{QAM}\bar{\gamma}_{sd}}} \\ \times \tan^{-1}\left(\sqrt{\frac{1 + g_{QAM}\bar{\gamma}_{sd}}{g_{QAM}\bar{\gamma}_{sd}}}\right) - 1\Bigg],\end{aligned} \tag{5.8}$$

where $g_{QAM} = 1.5/(M-1)$ and M is the modulation order. It should be mentioned that (5.8) represents the SER of the M-QAM.

In [84], a closed-form expression for the average SER of the N^{th} best relay selection with DF in Rayleigh fading channels is derived. By substituting $N = 1$, the SER of the best relay

selection can be obtained and given by

$$SER_r\left(j\right) = A \cdot P_{e,sr}^{j}(e)\left[1-\sqrt{\frac{b\bar{\gamma}_{sd}}{1+b\bar{\gamma}_{sd}}}\right] + A \cdot j \sum_{k=0}^{j-1}(-1)^k \binom{j-1}{k} \frac{\left(1-P_{e,sr}(e)\right)^{k+1}}{k+1} \times \left(1-\frac{\frac{\bar{\gamma}}{k+1}}{\frac{\bar{\gamma}}{k+1}-\bar{\gamma}_{sd}}\sqrt{\frac{\frac{b\bar{\gamma}}{k+1}}{1+\frac{b\bar{\gamma}}{k+1}}} + \frac{\bar{\gamma}_{sd}}{\frac{\bar{\gamma}}{k+1}-\bar{\gamma}_{sd}}\sqrt{\frac{b\bar{\gamma}_{sd}}{1+b\bar{\gamma}_{sd}}}\right), \tag{5.9}$$

where j denotes the number of reliable relays, $A = \frac{M-1}{M}$, $B = \frac{3}{M^2-1}$ and $P_{e,sr}(e)$ is the probability that an error occurs in the $S-R$ link and is given by [57, Eq. (8.103)]

$$P_{e,sr}(e) = A\left(1-\sqrt{\frac{B\bar{\gamma}_{sr}}{1+B\bar{\gamma}_{sr}}}\right), \tag{5.10}$$

A and B are constants dependent on the modulation used.

Substituting (5.5) and (5.6) in (5.4), the overall throughput of the scheme is obtained. The throughput is maximized by determining the optimal power allocated between the source node and the relay node. This is an optimization for the PER of the retransmission depends on the allocated power at the source and relay. Figs. 5.2, 5.3 and 5.4 show the behavior of the throughput as a function of SER_r for 4-QAM, 16-QAM and 64-QAM respectively, when $L = 4$. In all three cases, it can be seen that the throughput improves over the entire SNR regime as SER_r decreases. This has been tested for other constellation sizes and number of relays, and the same observation on the behavior of the throughput versus SNR as the SER_r decreases has been found. Hence minimizing the SER of the retransmission will result in maximizing the throughput based on the aforementioned observations.

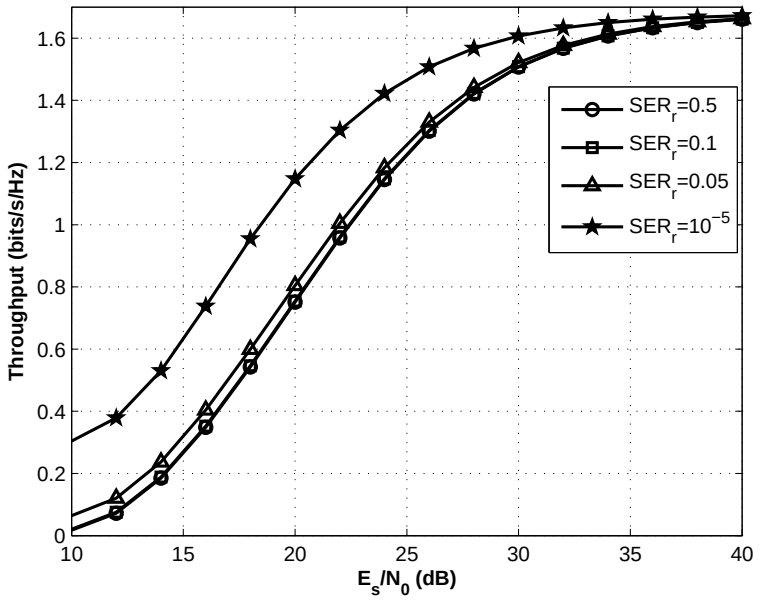

Figure 5.2: Throughput as the SER of the retransmission varies. $L = 4$, modulation set to 4-QAM, and $\bar{\gamma}_{sr} = \bar{\gamma}_{rd} = \bar{\gamma}_{sd}$.

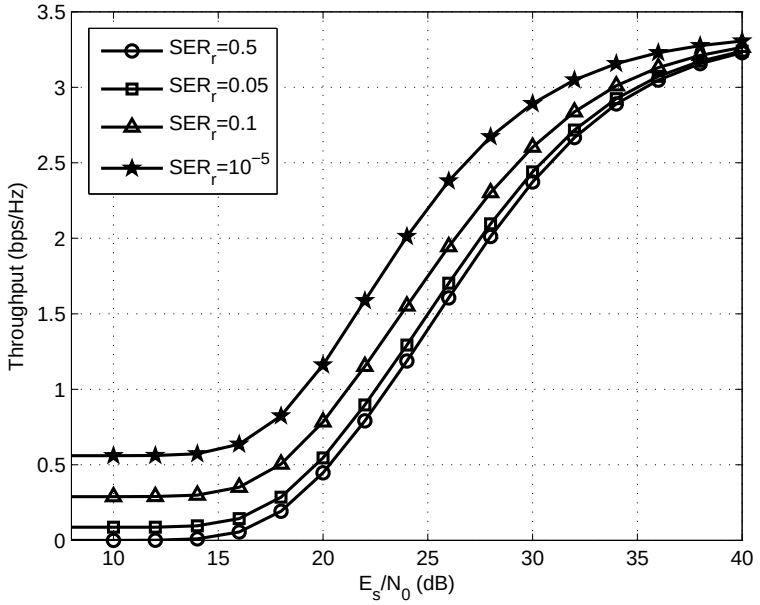

Figure 5.3: Throughput as the SER of the retransmission varies. $L = 4$, modulation set to 16-QAM, and $\bar{\gamma}_{sr} = \bar{\gamma}_{rd} = \bar{\gamma}_{sd}$.

Since the closed-form expression of the exact SER in (5.9) is difficult to analyze, the

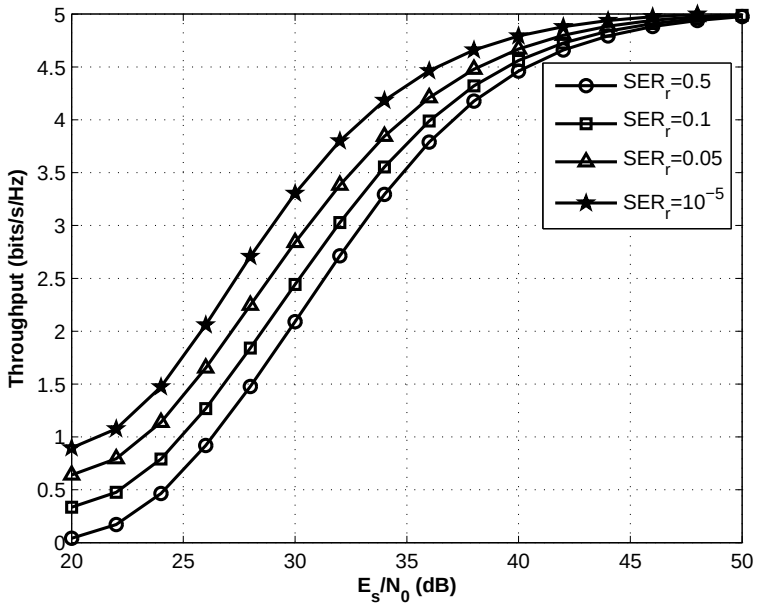

Figure 5.4: Throughput as the SER of the retransmission varies. $L = 4$, modulation set to 64-QAM, and $\bar{\gamma}_{sr} = \bar{\gamma}_{rd} = \bar{\gamma}_{sd}$.

asymptotic bounds for the SER of the retransmission is derived. In what follows, the asymptotic SER analysis of the best relay selection for DF over Rayleigh fading channels is presented.

5.3.2 Asymptotic bounds

First, the asymptotic bounds for the SER of the best relay selection for DF taking into account the effects of pathloss are derived. In [84], the authors proposed an analysis of the exact SER and the PDF of the DF strategy for the N^{th} best relay selection over Rayleigh fading channels, but no bounds on the PDF or SER of the proposed scheme are provided. Wang *et al.* [89] proposed a simple and unifying method for evaluating the average error rate performance of uncoded transmissions over a large range of fading channels for various modulation schemes. They argued that if the PDF can be approximated using the polynomial $f(x) = \beta x^t + O(x^t)$ where β is a constant, t represents the smoothness order, x is a RV, then asymptotic bounds on average error rate can be obtained. The PDF of the $S - R - D$ link

for the DF best relay selection given by [84] can be written as

$$f_{\gamma_\chi}(x) = P_{e,sr}^{L}(e)\delta(x) + \frac{L}{\bar{\gamma}_{rd}} \sum_{k=0}^{L-1} (-1)^k \binom{L-1}{k} \big(1 - P_{e,sr}(e)\big)^{k+1} \exp\left(\frac{-x(k+1)}{\bar{\gamma}_{rd}}\right), \quad (5.11)$$

The first term in (5.11), $P_{e,sr}^{L}(e)\delta(x)$, can be left out of the expression since, it is negligible compared to the second term (at least one order of a magnitude smaller).

In [89], the authors showed that the average error rate can be obtained using an approximated PDF in the form of a single polynomial term. Following the approach in [89], (5.11) can be written in the form a single polynomial term $f_{\gamma_\chi}(x) = a_b x^{t_b} + O(x)$ and $f_{\gamma_{sd}}(x) = a_{sd} x^{t_{sd}} + O(x)$, where t_b and t_{sd} are positive integers, a_b and a_{sd} are constants, and $O(x)$ is a polynomial function of x of higher order, For γ_{sd}, [89] gives the values of a_{sd} and t_{sd} as $a_{sd} = 1/\bar{\gamma}_{sd}$ and $t_{sd} = 0$, respectively. Using series expansion and after some manipulations, the PDF of $f_{\gamma_\chi}(x)$ in (5.11) at high SNR, can be approximated as

$$\begin{aligned} f_{\gamma_\chi}(x) &\approx L \left(\frac{1}{\bar{\gamma}_{rd}}\right)^{L} \big(x + P_{e,sr}(e)\bar{\gamma}_{rd}\big)^{L-1} \\ &\approx L \left(\frac{1}{\gamma_{rd}}\right)^{L} \sum_{k=0}^{L-1} \binom{L-1}{k} x^{L-1-k} \big(P_{e,sr}(e)\bar{\gamma}_{rd}\big)^{k}. \end{aligned} \quad (5.12)$$

The cumulative density function (CDF) can be obtained by taking the anti-derivative of (3.15) and given by

$$F_{\gamma_\chi}(x) = \sum_{k=0}^{L} \binom{L}{k} \left(\frac{1}{\gamma_{rd}}\right)^{L-k} P_{e,sr}^{k}(e) x^{L-k}. \quad (5.13)$$

From (5.13), $a_b^k = \binom{L}{k} \left(\frac{1}{\bar{\gamma}_{rd}}\right)^{L-k} P_{e,sr}^{k}(e)$ and $t_b^k = L - k$ with $k = 0, \cdots, K$ can be obtained.

Hence, the PDF of the indirect link ($S \to R \to D$) is given by

$$f_{\chi}^{DF}(x) = \frac{1}{\bar{\gamma}_{sd}} \sum_{k=0}^{L} \frac{1}{\bar{\gamma}_{rd}^{L}} \binom{L}{k} x^{L-k} \big(P_{e,sr}(e)\bar{\gamma}_{rd}\big)^{k}, \quad (5.14)$$

where $P_{e,sr}(e)$ can be approximated (see proof in Appendix C)

$$P_{e,sr}(e) \approx \frac{A}{2B\bar{\gamma}_{sr}}, \tag{5.15}$$

where A and B were defined in (5.10).

The approximation of $P_{e,sr}(e)$ is necessary to evaluate SER_r. Therefore, the optimization problem using this simple form of SER_r can easily be solved. It is worth mentioning that the diversity order can also be obtained from the approximated SER_r.

The average SER of the retransmission denoted SER_r can be obtained using

$$SER_r = A \int_0^{\infty} \text{erfc}(\sqrt{Bx}) f_{\chi}^{DF}(x) dx, \tag{5.16}$$

where the complementary error function is given by [90, Eqs. (13.2.1.1.1)-(13.2.1.1.4)] $\text{erfc}(x) = 2/\sqrt{\pi} \int_x^{\infty} e^{-t^2} \mathrm{d}t$. After substituting (5.14) (i and k are interchanged in (5.16)) and performing some manipulations, the following expression is obtained

$$SER_r = \frac{A}{\bar{\gamma}_{sd}} \sum_{i=0}^{L} \frac{1}{\bar{\gamma}_{rd}^{L-i}} \binom{L}{i} \left(P_{e,sr}(e)\right)^i \int_0^{\infty} \text{erfc}\left(\sqrt{Bx}\right) x^{L-i} \mathrm{d}x. \tag{5.17}$$

The integral expression in (5.17) can easily be evaluated, hence the asymptotic bounds for the SER can be given by

$$SER_r \approx \left(\frac{1}{\bar{\gamma}_{sd}}\right) \sum_{i=0}^{L} g(i-1) \left(\frac{1}{\bar{\gamma}_{sr}}\right)^i \left(\frac{1}{\bar{\gamma}_{rd}}\right)^{L-i}, \tag{5.18}$$

where $\bar{\gamma}_{sr} = \mathbb{E}\langle \|h_{sr}\|^2 \rangle \frac{P_s}{N_0}$, $\bar{\gamma}_{sd} = \mathbb{E}\langle \|h_{sd}\|^2 \rangle \frac{P_s}{N_0}$, $\bar{\gamma}_{rd} = \mathbb{E}\langle \|h_{rd}\|^2 \rangle \frac{P - P_s}{N_0}$ with N_0 denoting the noise power spectral density and $g(i-1)$ is given by

$$g(i-1) = \binom{L}{i} \frac{A^{i+1} \cdot B^{-L-1} \Gamma\big((L-i+1)+0.5\big)}{2\sqrt{\pi}(L-i+1)}. \tag{5.19}$$

It is noted that at high SNR and for L relays, a diversity order of $L+1$ is achieved for the best relay selection. In the following section, the optimum asymptotic power by using the asymptotic SER in (5.18) is derived. Hence, the need to formulate the optimization problem where the objective function is given by (5.18).

5.3.3 Power optimization and relay selection

The optimal power allocation between the source and the relay is combined with the uncoded DF best relay selection to minimize the SER. With this in mind, questions on the selection criterion arise since power optimization is involved. It is noted that the selection of the aforementioned system is somewhat different from the conventional relay selection where no optimization is considered. In the case of [83], i.e., relay selection only, the selection criterion depends on the instantaneous SNR between the relay and the destination. In that work, the relay selected from a set of reliable relays –relays that can correctly decode the source message –which can achieve the highest SNR at the destination node is branded the *best relay* and is selected to forward the source message to the destination. In the proposed system, power optimization is integrated with relay selection. Hence both factors should be taken into consideration.

In a multi-relay network, the DF best relay selection with optimal power allocated between the source and the relay operates as follows. The output SNR at the destination for each possible relay node is computed, and the destination selects the relay with the highest output SNR. The destination also computes the optimal power distribution between the source and the selected relay. The relay nodes taken into account here are the ones that belong to the decoding set $\mathcal{D}(s)$. Then after selecting the relay and determining the optimum power distribution between the source and the selected relay, the destination notifies through a low-rate, error-free feedback channel, the source and the selected relay of their allocated powers. Without loss of generality, this can also be applied to a system where two or more relays are selected for retransmission. In general, when no selection is performed,

the destination will still be able to compute the power distribution and inform the source and the forwarding relays on their respective power levels through a feedback channel.

In order to find the optimal power, a model [91] that takes into account the effects of the pathloss in the SER performance is considered. In this model, $\mathbb{E}\langle\|h_{sd}\|^2\rangle = 1$, $\mathbb{E}\langle\|h_{sr}\|^2\rangle = (d_{sd}/d_{sr})^{\varepsilon}$ and $\mathbb{E}\langle\|h_{rd}\|^2\rangle = (d_{sd}/d_{rd})^{\varepsilon}$ where ε is the pathloss exponent, d_{sd}, d_{sr} and d_{rd} represent the $S-D$, $S-R$ and $R-D$ distances, respectively. For simplicity, it is assumed that the $S-D$ distance is normalized to one and all the relays are located on the same axis or line (line topology). In what follows, the power is optimized in order to minimize the SER in (5.18). After rearranging (5.18) and expressing it as a function of P_s and d_{sr}, the following SER expression at high SNR is obtained,

$$SER_r \approx \left(\frac{N_0}{P_s}\right) \sum_{i=0}^{L} g(i-1) \left(\frac{d_{sr}^{-\alpha} N_0}{P_s}\right)^{i} \left(\frac{(1-d_{sr})^{-\alpha} N_0}{P_r}\right)^{L-i}, \tag{5.20}$$

and the optimization problem can be formulated as follows:

$$\begin{aligned} &\underset{P_s, d_{sr}}{\text{minimize}} \quad \underset{\bar{\gamma}\to\infty}{SER_r} \\ &\text{subject to} \quad \begin{cases} 0 < P_s < P \\ 0 < d_{sr} < 1 \end{cases} \end{aligned} \tag{5.21}$$

P_s is the transmit power at the source and P_r is the transmit power at the relay given by $P_r = P - P_s$ with P denoting the total transmit power. The objective function in (5.21) represents the high-SNR or asymptotic SER given in (5.20).

For the aforementioned power optimization problem, the total power is assumed as P. The transmit power allocated at the source is $P_s = \rho P$ and $P_r = (1-\rho)P$ by the potential selected relay, where $0 \leq \rho < 1$. The output SNR at the destination corresponding to each

relay is given by

$$\begin{aligned}\gamma_{out} &= \gamma_{sd} + \max_{i\in\mathcal{D}(s)}\{\gamma_{r_i d}\} \\ &= \rho\|h_{sd}\|^2\frac{P}{N_0} + \max_{i\in\mathcal{D}(s)}\left\{(1-\rho)\|h_{r_i d}\|^2\frac{P}{N_0}\right\}.\end{aligned} \tag{5.22}$$

Note that the optimization problem in (5.21) is convex since the Hessian matrix [92] of the objective function is positive definite given $0 < P_s < P$ and $0 < d_{sr} < 1$ (see proof in Appendix D). This implies that the local minimum is identical to the global minimum (which can be obtained by taking the derivative of the objective function in (5.21)). Since finding a closed-form expression for the optimal power is not easy, numerical techniques such as the Bisection method and Newton's method to find the optimal power allocation are resorted to. For $L = 2$ relays and 64-QAM, the optimal power at the source $P_s^\star = 0.6944P$ and the optimal power at the relay $P_r^\star = 0.3056P$.

5.4 Numerical Results

In this section, the numerical results of the asymptotic SER as well as the exact SER versus E_s/N_0, where E_s is the transmitted energy of the signal per symbol are shown. A packet length $K = 100$, a 16-bit CRC for error detection, (i.e., $C = 16$) and the maximum number of retransmissions $N_{max} = 3$ are used without loss of generality. The various modulation schemes used in this Chapter are $4-$QAM, $16-$QAM and $64-$QAM. Finally, a pathloss exponent of $\varepsilon = 3$[1] is assumed without loss of generality.

In the sequel, the simulated SER and the asymptotic SER of the best relay selection of DF for $4-$QAM, $16-$QAM and $64-$QAM and different number of available relays are compared. The cases in which all the relays are located closer to the source, closer to the destination and at equidistance from the source and destination are considered. Fig. 5.5

[1]The pathloss coefficient depends on the propagation environments. In practice, the propagation that mimics a two-ray or free-space model typically has a pathloss coefficient between 2 and 4.

shows the simulated and asymptotic SER of the best relay selection when $L = 3$ and the the available relays are located closer to the destination. In Fig. 5.6, the available relays $L = 5$ are all located closer to the destination, hence more power is allocated to the source than the best relay. In Figs. 5.7 and 5.8 the relays are equidistant from the source and destination. It is noted that for all three modulation schemes, at high SNRs, the simulated and asymptotic SER are in excellent agreement. It is also noted that all curves have the same slope, indicating the same diversity order (i.e., a diversity of order $L + 1$ is attained).

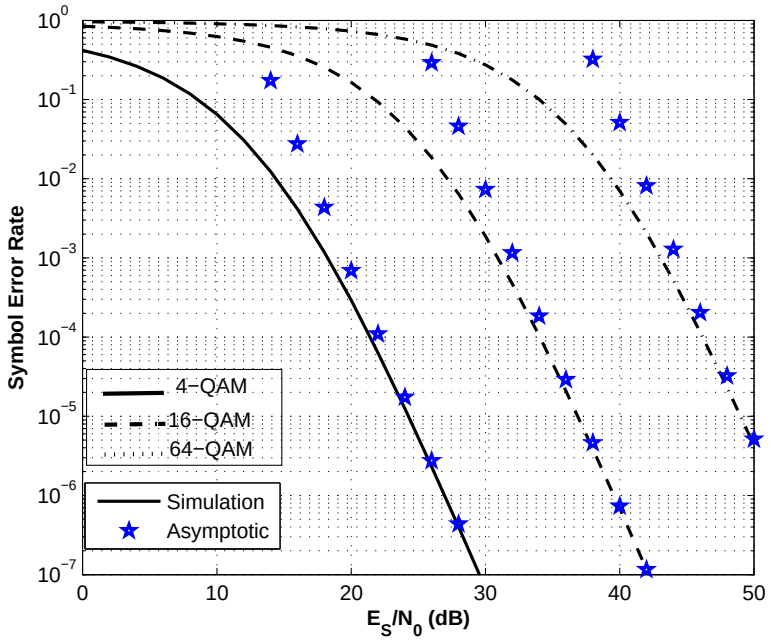

Figure 5.5: Simulated SER and Asymptotic SER versus SNR for the best relay selection in DF cooperative diversity. $L = 3$ and $P_s = 0.25$ & $P_r = 0.75$.

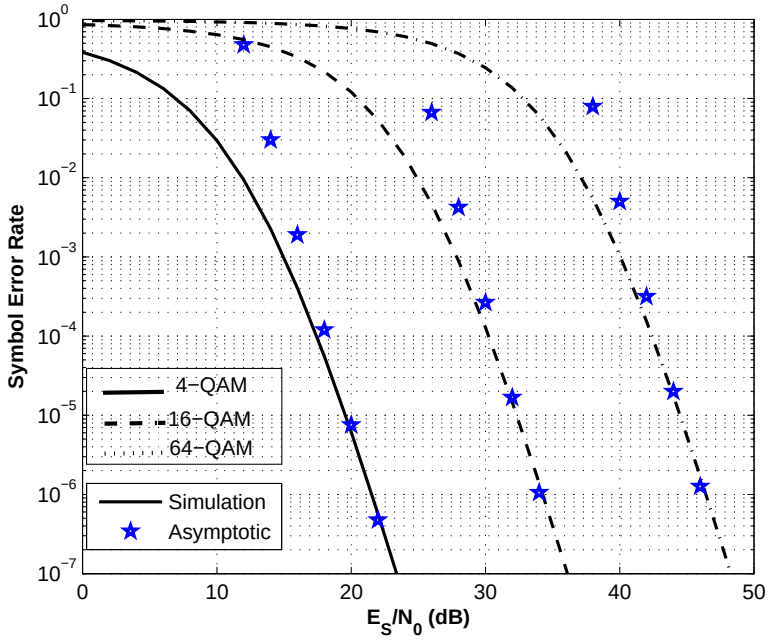

Figure 5.6: Simulated SER and Asymptotic SER versus SNR for the best relay selection in DF cooperative diversity. $L = 5$ and $P_s = 0.75$ & $P_r = 0.25$.

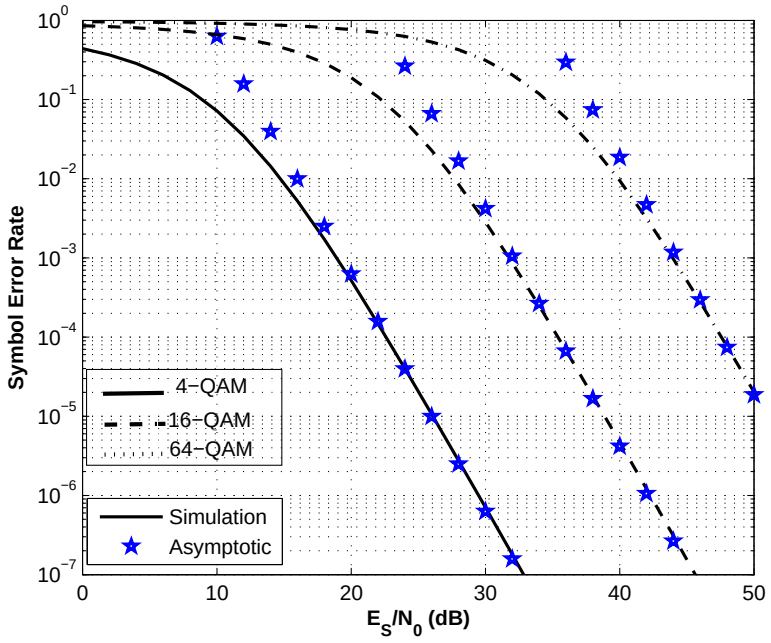

Figure 5.7: Simulated SER and Asymptotic SER versus SNR for the best relay selection in DF cooperative diversity. $L = 2$ and $P_s = P_r = 0.5$.

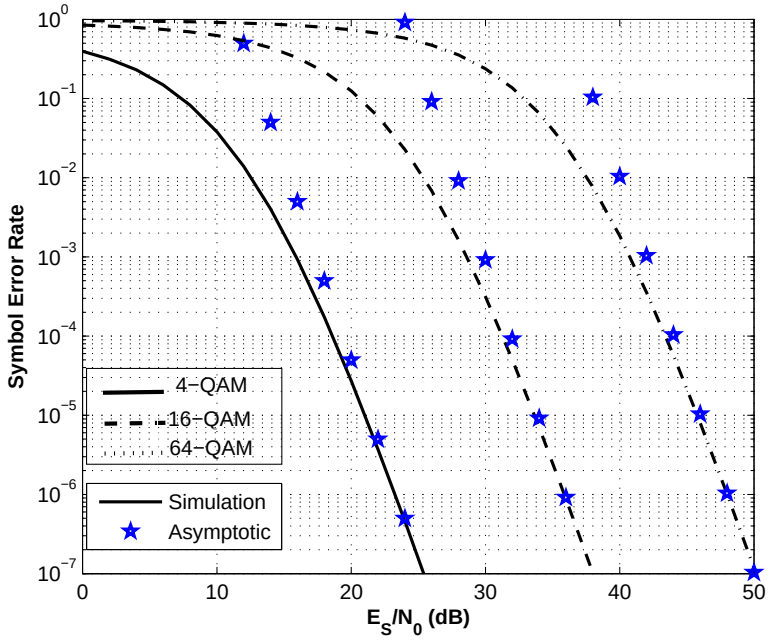

Figure 5.8: Simulated SER and Asymptotic SER versus SNR for the best relay selection in DF cooperative diversity. $L = 4$ and $P_s = P_r = 0.5$.

In Figs. 5.9 and 5.10, the SER performance versus SNR for different power allocations taking into account the effects of pathloss for $L = 4$ and $L = 6$ relays, respectively are shown. It is noted that the SER with equal power distribution is not the optimal one. This implies that equal power distribution does not always yield optimum SER or BER. Similarly in both figures, the SER for power allocations (P_s, P_r)=$(0.20, 0.80)$ on one hand, and (P_s, P_r)=$(0.40, 0.60)$ on the other hand are presented. It is also noted that, regardless of the power distribution used, neither yields the minimum SER. As seen from these results, the optimal transmit power outperforms the equal power allocation by about 1.5dB at 10^{-5} for $L = 4$ and by about 2dB at 10^{-5} for $L = 6$.

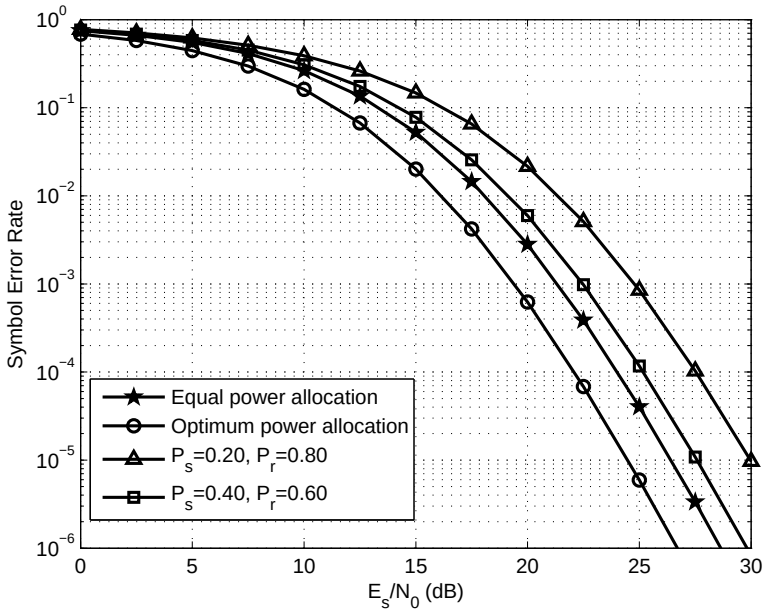

Figure 5.9: SER performance versus SNR for the best relay selection for with optimal power allocation. $L = 4$ and $M = 16$.

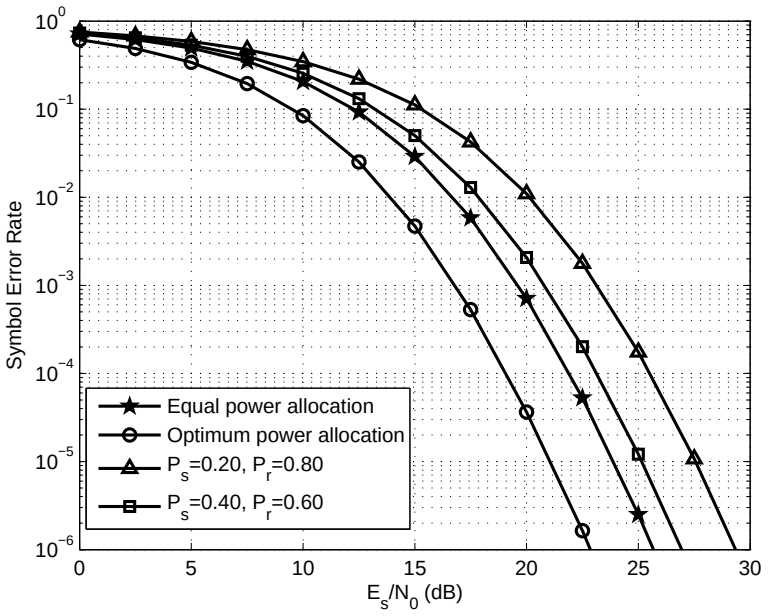

Figure 5.10: SER performance for the best relay selection for with optimal power allocation. $L = 6$ and $M = 16$.

Figs. 5.11 and 5.12 plot the throughput of the system for different power allocations versus SNR. It is noted that the throughput obtained with optimal allocation is superior, from moderate to high SNR, in both cases. Some important observations are made. Firstly, at low SNR regime, the throughput values with different power distribution are identical and almost equal to zero. This is due to the fact that when the system operates at such SNRs, the decoding set $\mathcal{D}(s)$ is empty (i.e., poor $S - R$ links). Hence, cooperation does not take place and the throughput is minimal. Secondly, it can be seen that the throughput gain increases as the SNR increases at moderate SNRs. In this SNR regime, cooperation often takes place since the $S - D$ link quality varies and hence, the size of the decoding set increases. This SNR range is more relevant to this work as it shows the advantage of the power optimization and relay selection on the overall throughput. Lastly, at high SNR regime, even though the number of relays that successfully decode the source's packet is large, relay selection and power optimization do not help in this SNR regime. This can be explained by the fact that the $S - D$ link is reliable and hence there is no need for retransmission.

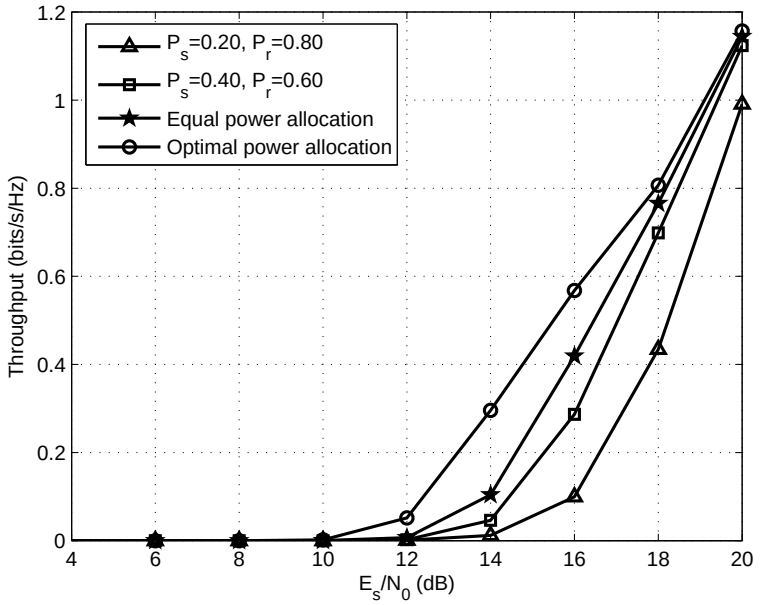

Figure 5.11: Throughput performance for DF with truncated ARQ. $L = 4$, $M = 16$, and $\bar{\gamma}_{sd} = \bar{\gamma}_{sr} = \bar{\gamma}_{rd}$.

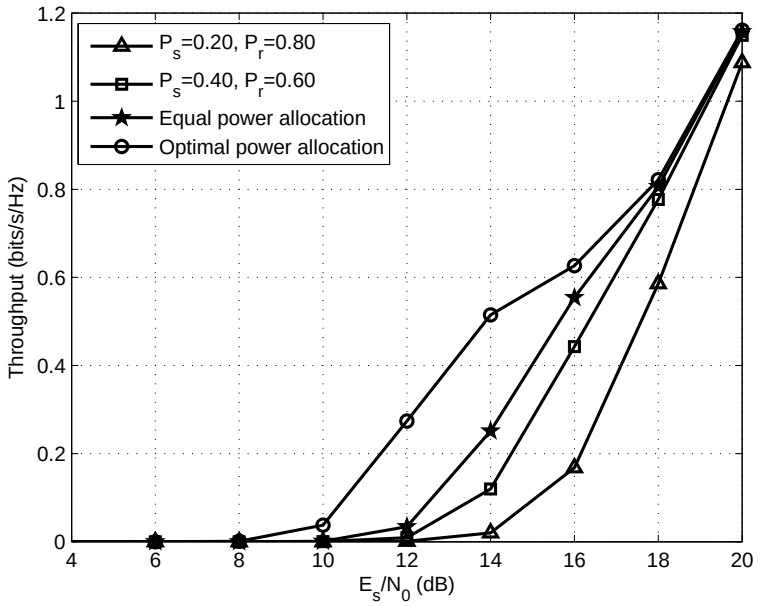

Figure 5.12: Throughput performance for DF with truncated ARQ. $L = 6$, $M = 16$, and $\bar{\gamma}_{sd} = \bar{\gamma}_{sr} = \bar{\gamma}_{rd}$.

Figs. 5.13 and 5.14 show the throughput versus the number of relays with $P_s = 0.2$, $P_s = 0.5$, and optimal power distribution for 16-QAM and 64-QAM respectively. It can be

observed that the throughput improves with the number of relays for any allocated power and constellation size.

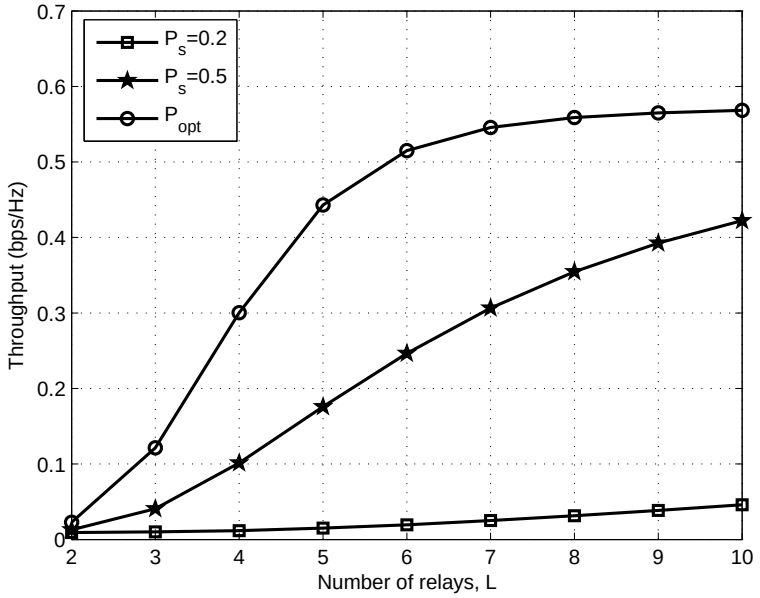

Figure 5.13: Throughput gain for optimal and equal power distributions, 16-QAM.

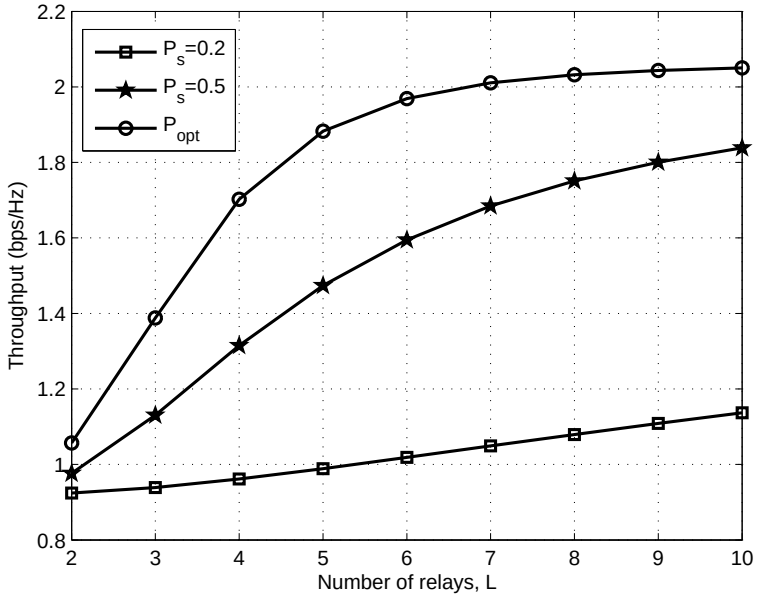

Figure 5.14: Throughput comparison of optimal and equal power distribution versus number of relays for 64-QAM.

Table 5.1 shows the different optimal power allocated between the source and the relay P_s and P_{r^*} for $b = 6$ and $L = 2$, $L = 4$ and $L = 6$. It is noted that these values depend on the number of relays ready to assist the source, even though only one relay (the *best* one) will be employed for retransmission. It is further noted that in terms of power allocation at the source and *best* relay node, equal power allocation is not the optimal solution for SER. More power is allocated to the source node than the relay when the $R - D$ link is reliable. To illustrate this, scenarios $L = 2$ and $L = 6$ should be compared. The best $R - D$ link for $L = 6$ is likely to be better than the one for $L = 2$. Hence, the power allocated at the source for $L = 6$ is greater than the one for $L = 2$. However, allocating more power to the source does not necessarily mean that the system will revert to a non-cooperative mode.

Table 5.1: Optimal values of P_s and $P_{r^\star}$ with different number of relays L and $b = 6$, and normalized power, $P = 1$.

L	2	4	6	8
P_s	0.6944	0.7037	0.7251	0.7433
$P_{r^\star}$	0.3056	0.2953	0.2749	0.2567

5.5 Conclusion

A joint optimization and relay selection strategy in combination with truncated ARQ is proposed. This cross-layer design aims at maximizing the system throughput and saving channel resources. For throughput maximization, the allocated power at the source is used as the optimization variable. In order to find the optimal power allocation, the asymptotic SER of the system under study is first derived. The derived asymptotic SER is shown to be in perfect agreement with the simulated SER at high SNRs. It has also been shown that the optimal power allocation, obtained under a general optimization problem, yields a throughput performance that is superior to non-optimized power values from moderate to high SNRs.

Chapter 6

Power Assignment in Multi-relay Adaptive DF Cooperative Networks

A power assignment scheme in multi-relay adaptive DF cooperative-diversity networks over non-identical Rayleigh fading channels, that integrates ARQ at the link layer is investigated. The aim of this chapter is to maximize the system throughput via power optimization and it is shown that this can be done by minimizing the SER of the retransmission. Finally, closed-form expressions for the exact SER of the multi-relay adaptive DF as well as the asymptotic error bounds are derived.

6.1 Introduction

In Chapter 5, a cooperative diversity scenario where all the relays experienced identical fading was dealt with. Furthermore, only the best relay was selected out of a pool of L relays to forward the source packets in the retransmission phase. In this chapter, the case where all the reliable relays forward during the retransmission phase and not necessarily at the same location is considered. It can be seen that the power among the reliable relays is not equally distributed and depends on the relay location as well as the modulation

scheme in use. Some work has been conducted on both single and multi-relay adaptive DF cooperative diversity. The authors in [17] proposed a scheme where the relay retransmits to the destination provided that it has correctly decoded the source signal. For a multi-relay scenario, Ikki *et al.* [58] presented a performance analysis framework (bit error probability, outage probability and average channel capacity) using BPSK of multi-branch adaptive DF over Nakagami-m fading channels. In [59], Lee *et al.* examined the SER of the single and multi-relay adaptive DF over Nakagami-m fading channels. They numerically evaluated the exact SER of the system using the Gaussian Q-function, but no closed-form expression was obtained.

Data throughput is one of the most important performance metrics in wireless communications and is commonly used in cross-layer designs. In [87], the authors proposed an incremental best relay cooperative diversity, where only the best relay retransmits the source packet to the destination during the retransmission phase. The authors in [52] investigated a single-relay cooperative system in which they proposed a new analytical methology for evaluating the outage probability of cooperative DF ARQ. Furthermore, they developed the optimum power allocation based on the outage probability for the proposed scheme. Boujemaa [93] analyzed the delay experienced by the packets for a cooperative truncated hybrid ARQ with opportunistic relaying over block Nakagami-m fading channels. The delay analysis applies to any number of relays for both DF and AF.

A scheme that combines truncated ARQ and multi-relay adaptive DF strategy over non-identical fading channels is proposed. The relay nodes are situated at different locations relative to the source, hence the power allocated to each reliable relay is dissimilar. The throughput maximization via power optimization is also investigated. Moreover, it is shown that maximizing the throughput is equivalent to minimizing the SER of the retransmission. Given this, a closed-form expression for the SER of multi-relay adapative DF over non-identical Rayleigh fading channels using the MGF-based approach is derived. Moreover, an asymptotic SER for the retransmission phase is also obtained.

6.2 System and channel Models

In this scheme, a source node (S) transmits information bits to the destination node (D) while the users that appear to be in the vicinity remain idle due to the half-duplexity mode (receivers are turned off). Before transmitting to the destination, the source appends some CRC bits to its message for error detection. After receiving the source message, the destination checks for errors. If the destination correctly decodes the source message, then it sends an ACK to the source, through a low-rate and error-free feedback channel which is assumed to be perfect and the source transmits a new packet. Otherwise, it sends a NACK requesting retransmission. In this case, neighbouring users will switch to the relay mode (R). The retransmission phase is divided into two time slots. In the first time slot of the retransmission phase, the source transmits to the relays and destination. In the second time slot, the relays that have correctly decoded the source message resend the packet to the destination. Both time-slot packets (i.e., packets from the source and packets from the reliable relays) are optimally combined at the destination using a MRC. This is done until the destination correctly decodes the source message or the number of retransmissions reaches its maximum, N_{max}. It is assumed that the system is perfectly synchronized. All nodes are equipped with single transmit and receive antennas. The channels are modelled as quasi-static fading, i.e., the fading coefficients are fixed for the entire duration of a packet transmission, but vary independently from one packet to another. The channels are subject to flat Rayleigh fading. We assume perfect CSI at the receivers only, i.e., the relay and the destination nodes. The channel coefficients of the $S-D$, $S-R$ and $R-D$ links are denoted by h_{sd}, h_{sr_L} and h_{r_id} respectively, where $i \in \mathcal{D}$ and $1 \leq i \leq L$, with $\mathcal{D}$ denoting the decoding set and L the total number of relays.

The received signals y_{sd} at the destination and y_{sr_L} at the relays in the first time slot of

the retransmission phase are given by

$$y_{sd} = \sqrt{P_0} h_{sd} s + n_{sd}, \tag{6.1}$$

$$y_{sr_L} = \sqrt{P_0} h_{sr_L} s + n_{sr_L}, \tag{6.2}$$

and the $y_{r_i d}$ at the destination in the second time slot as

$$y_{r_i d} = \sqrt{P_i} h_{r_i d} \hat{s} + n_{r_i d}, \tag{6.3}$$

where s is the transmitted signal at the source, $\hat{s}$ is the esimated signal at the relay (decode-and-forward strategy is used here), r_i represents the decoding relays, the additive noise n_{sd}, n_{sr_L} and $n_{r_i d}$ are Gaussian random variables with zero-mean and variance N_0.

6.3 Throughput Performance

6.3.1 Throughput

The throughput expression can be given by [20],

$$\eta = b\left(\frac{K-C}{K}\right)\left(\frac{\Pr\{P_s\}}{\mathbb{E}\langle Tr_{packet}\rangle}\right), \tag{6.4}$$

where $\Pr\{P_s\}$ and $\mathbb{E}\langle Tr_{packet}\rangle$ denote the packet successful probability and average number of transmissions per packet, respectively, with Tr_{packet} representing the number of transmissions per packet. C is the number of CRC bits.

The total probability of packets successfully transmitted, $\Pr\{P_s\}$ is given by

$$\Pr\{P_s\} = \sum_{j=0}^{L} \left(1 - PER_{sd}(PER_{Retr}(j))^{N_{max}}\right) \Pr(j), \tag{6.5}$$

where $PER_{Retr}(j)$ denotes the average PER of the j^{th} relay retransmission. In (6.4), the average number of transmissions per packet is given by

$$\mathbb{E}\left\langle Tr_{packet}\right\rangle = \sum_{j=0}^{L}\left(1 - PER_{sd} + PER_{sd}\left[\sum_{i=2}^{N_{max}+1} i\Big(PER_{Retr}(j)\Big)^{i-2}\Big(1 - PER_{Retr}(j)\Big) + (1+N_{max})\cdot\Big(PER_{Retr}(j)\Big)^{N_{max}-1}\right]\right)\Pr\left(j\right), \tag{6.6}$$

where $\Pr\left(j\right)$ is the probability of j reliable relays and can be expressed as

$$\Pr\left(0\right) = PER_{sr_1}\cdot PER_{sr_2}\cdots PER_{sr_L} \tag{6.7}$$

$$\begin{aligned}\Pr\left(1\right) = {} & (1 - PER_{sr_1})\cdot PER_{sr_2}\cdots PER_{sr_L} + PER_{sr_1}\left(1 - PER_{sr_2}\right)\cdots PER_{sr_L} \\ & + PER_{sr_1}\cdot PER_{sr_2}\cdots(1 - PER_{sr_L})\end{aligned} \tag{6.8}$$

$$\begin{aligned}\Pr\left(2\right) = {} & (1 - PER_{sr_1})\cdot(1 - PER_{sr_2})\cdots PER_{sr_L} + (1 - PER_{sr_1})\,PER_{sr_2}\cdots(1 - PER_{sr_L}) \\ & + PER_{sr_1}\cdot(1 - PER_{sr_2})\cdots(1 - PER_{sr_L})\end{aligned} \tag{6.9}$$

$$\vdots$$

$$\Pr\left(L\right) = (1 - PER_{sr_1})\cdot(1 - PER_{sr_2})\cdots(1 - PER_{sr_L}) \tag{6.10}$$

It can be noted that (6.6) and (6.7)-(6.10) are a function of SER_{sd} and SER_{sr_i} respectively, denoting the SER of the $S - D$ and $S - R_i$ links prior to retransmission. SER_{sd} is

given by [57]

$$SER_{sd} = 2\left(1-\frac{1}{\sqrt{M}}\right)\left(1-\sqrt{\frac{g_{QAM}\bar{\gamma}_{sd}}{1+g_{QAM}\bar{\gamma}_{sd}}}\right)\left(1-\frac{1}{\sqrt{M}}\right)^2\left[\frac{4}{\pi}\sqrt{\frac{g_{QAM}\bar{\gamma}_{sd}}{1+g_{QAM}\bar{\gamma}_{sd}}} \times \tan^{-1}\left(\sqrt{\frac{1+g_{QAM}\bar{\gamma}_{sd}}{g_{QAM}\bar{\gamma}_{sd}}}\right)-1\right], \tag{6.11}$$

where $g_{QAM} = 1.5/(M-1)$, M is the modulation order and $\bar{\gamma}_{sd} = \mathbb{E}\langle|h_{sd}|^2\rangle\bar{\gamma}$. SER_{sr_i} is similar to (6.11) with the subscripts $S-D$ and $S-R_i$ reversed.

6.3.2 SER of the multi-relay DF cooperative networks

In this section, a closed-form expression for the SER in M-QAM multi-relay adaptive DF over non-identical Rayleigh fading channels by using the MGF approach is derived. The output SNR at the destination can be written as

$$\gamma_{total} = \gamma_{sd} + \sum_{i\in\mathcal{D}} \gamma_{r_i d}, \tag{6.12}$$

Similar to [82], (6.12) can be used to obtain the output MGF given by

$$\mathcal{M}_{\gamma_{total}}(s) = \left(1+s\bar{\gamma}_{sd}\right)^{-1} \cdot \prod_{i=1}^{L}\left[P_{e,sr_i}\left(1+\frac{1-P_{e,sr_i}}{P_{e,sr_i}}\left(1+s\bar{\gamma}_{sr_i}\right)^{-1}\right)\right], \tag{6.13}$$

where P_{e,sr_i} is the probability of an error occuring in the i^{th} $S-R$ link and is given by [57, Eq. (8.103)]

$$P_{e,sr_i} = A\left(1-\sqrt{\frac{B\bar{\gamma}_{sr_i}}{1+B\bar{\gamma}_{sr_i}}}\right), \tag{6.14}$$

where A and B depend on the type of modulation and are given by $A = (M-1)/M$ and $B = 3/(M^2-1)$.

It is assumed that the $S-R$ and $R-D$ links are i.n.i.d. Hence after some manipulations,

(6.13) can be given by

$$\mathcal{M}_{\gamma_{total}}(s) = \prod_{i=1}^{L} P_{e,sr_i}\left(1 + \sum_{n=1}^{L}\sum_{k_1=1}^{L-n+1}\sum_{k_2=k_1+1}^{L-n+2}\cdots\sum_{k_n=k_{n-1}+1}^{L}\prod_{j=1}^{n}\left(\frac{1-P_{e,sr_{k_j}}}{P_{e,sr_{k_j}}}\right)\left(1+s\bar{\gamma}_{r_{k_j}d}\right)^{-1}\right). \tag{6.15}$$

The average SER of the multi-relay M-QAM for adaptive DF can be obtained using [57, Eq. (9.20)] as

$$SER_{Retr} = \frac{4}{\pi}C_{QAM}\int_0^{\pi/2}\mathcal{M}_{\gamma_{total}}\left(\frac{g_{QAM}}{\sin^2\theta}\right)\mathrm{d}\theta - \frac{4}{\pi}C_{QAM}^2\int_0^{\pi/4}\mathcal{M}_{\gamma_{total}}\left(\frac{g_{QAM}}{\sin^2\theta}\right)\mathrm{d}\theta, \tag{6.16}$$

where $C_{QAM} = 1-1/\sqrt{M}$. After substituting (6.15) in (6.16), and performing some algebraic manipulations, with the aid of [57, Eqs. (5A.35)-(5A.56)], a closed-form expression for the SER is given by (6.17)

$$\begin{aligned}
SER_{Retr} = {} & 4C_{QAM}\left(\prod_{i=1}^{L}P_{e,sr_i}\right)\left[\frac{1}{2}\Big(1-\sqrt{\frac{g_{QAM}\bar{\gamma}_{sd}}{1+g_{QAM}\bar{\gamma}_{sd}}}\Big) + \sum_{n=1}^{L}\sum_{k_1=1}^{L-n+1}\sum_{k_2=k_1+1}^{L-n+2}\cdots\sum_{k_n=k_{n-1}+1}^{L}\right. \\
& \times\prod_{j=1}^{n}\left(\frac{1-P_{e,sr_{k_j}}}{P_{e,sr_{k_j}}}\right)\left(I_1\left(\phi,\bar{\gamma}_{r_{k_j}d}\right) - \frac{T\left(\frac{\pi}{2},g_{QAM}\bar{\gamma}_{sd}\right)}{\pi}\sqrt{\frac{g_{QAM}\bar{\gamma}_{sd}}{1+g_{QAM}\bar{\gamma}_{sd}}}\left(\frac{\bar{\gamma}_{sd}}{\bar{\gamma}_{sd}-\bar{\gamma}_{r_{k_j}d}}\right)\right. \\
& \left.\left. + \frac{T\left(\frac{\pi}{2},g_{QAM}\bar{\gamma}_{r_{k_j}d}\right)}{\pi}\sqrt{\frac{g_{QAM}\bar{\gamma}_{r_{k_j}d}}{1+g_{QAM}\bar{\gamma}_{r_{k_j}d}}}\left(\frac{\bar{\gamma}_{sd}}{\bar{\gamma}_{sd}-\bar{\gamma}_{r_{k_j}d}}\right)\right)\right] - 4C_{QAM}^2\left(\prod_{i=1}^{L}P_{e,sr_i}\right) \\
& \times\left[\frac{1}{4}\left(1-\sqrt{\frac{g_{QAM}\bar{\gamma}_{sd}}{1+g_{QAM}\bar{\gamma}_{sd}}}\left(\frac{4}{\pi}\tan^{-1}\left(\sqrt{\frac{1+g_{QAM}\bar{\gamma}_{sd}}{g_{QAM}\bar{\gamma}_{sd}}}\right)\right)\right) + \sum_{n=1}^{L}\sum_{k_1=1}^{L-n+1}\sum_{k_2=k_1+1}^{L-n+2}\cdots\right. \\
& \times\sum_{k_n=k_{n-1}+1}^{L}\prod_{j=1}^{n}\left(\frac{1-P_{e,sr_{k_j}}}{P_{e,sr_{k_j}}}\right)\left(I_1\left(\phi,\bar{\gamma}_{r_{k_j}d}\right)\frac{T\left(\frac{\pi}{4},g_{QAM}\bar{\gamma}_{sd}\right)}{\pi}\sqrt{\frac{g_{QAM}\bar{\gamma}_{sd}}{1+g_{QAM}\bar{\gamma}_{sd}}}\right. \\
& \left.\left.\left. + \left(\frac{\bar{\gamma}_{sd}}{\bar{\gamma}_{sd}-\bar{\gamma}_{r_{k_j}d}}\right)\frac{T\left(\frac{\pi}{4},g_{QAM}\bar{\gamma}_{r_{k_j}d}\right)}{\pi}\sqrt{\frac{g_{QAM}\bar{\gamma}_{r_{k_j}d}}{1+g_{QAM}\bar{\gamma}_{r_{k_j}d}}}\left(\frac{\bar{\gamma}_{sd}}{\bar{\gamma}_{sd}-\bar{\gamma}_{r_{k_j}d}}\right)\right)\right],
\end{aligned} \tag{6.17}$$

where

$$T(\phi,c)=\frac{1}{2}\tan^{-1}\left(\frac{N(\phi,c)}{D(\phi,c)}\right)+\frac{\pi}{2}\left[1-N(\phi,c)\left(\frac{1+D(\phi,c)}{2}\right)\right], \tag{6.18}$$

and

$$\begin{aligned} I_1(\phi,c) &= \frac{1}{\pi}\left(\phi-T(\phi,c)\sqrt{\frac{c}{1+c}}\right) && (6.19)\\ N(\phi,c) &= 2\sqrt{c(1+c)}\sin 2\phi, && (6.20)\\ D(\phi,c) &= (1+2c)\cos 2\phi-1. && (6.21) \end{aligned}$$

6.3.3 Asymptotic bounds

The derived closed-form expression for the SER given in (6.17) is not easy to analyze. Therefore, in this section the asympotic bounds expression for the SER of the multi-relay adaptive DF obtained in (6.17) is derived. It is noted that (6.16) can be rewritten as

$$\begin{aligned} SER_{Retr} = {} & \frac{4C_{QAM}}{\pi}\left(\prod_{i=1}^{L}P_{e,sr_i}\right)\int_0^{\frac{\pi}{2}}\left(1+\frac{g_{QAM}\bar{\gamma}_{sd}}{\sin^2\theta}\right)^{-1}\prod_{i=1}^{L}\left(1+\left(\frac{1-P_{e,sr_i}}{P_{e,sr_i}}\right)\right.\\ & \left.\times\left(1+\frac{g_{QAM}\bar{\gamma}_{r_id}}{\sin^2\theta}\right)^{-1}\right)\mathrm{d}\theta-\frac{4C_{QAM}^2}{\pi}\left(\prod_{i=1}^{L}P_{e,sr_i}\right)\int_0^{\frac{\pi}{4}}\left(1+\frac{g_{QAM}\bar{\gamma}_{sd}}{\sin^2\theta}\right)^{-1}\\ & \times\prod_{i=1}^{L}\left(1+\left(\frac{1-P_{e,sr_i}}{P_{e,sr_i}}\right)\left(1+\frac{g_{QAM}\bar{\gamma}_{r_id}}{\sin^2\theta}\right)^{-1}\right)\mathrm{d}\theta \end{aligned} \tag{6.22}$$

In (6.22), the following approximations can be made at high SNRs,

$$1+\frac{g_{QAM}\bar{\gamma}_{ij}}{\sin^2\theta}\approx\frac{g_{QAM}\bar{\gamma}_{ij}}{\sin^2\theta}, \tag{6.23}$$

and

$$1-P_{e,sr_i}\approx 1, \tag{6.24}$$

where $\bar{\gamma}_{ij}$ is the average SNR of the $i-j$ link, and after substituting (6.23) and (6.24) in (6.22), the asymptotic SER is given as

$$SER_{Retr} \approx \left(\prod_{i=1}^{L} P_{e,sr_i}\right) \frac{A_0}{g_{QAM}\bar{\gamma}_{sd}}\left[1+\sum_{n=1}^{L}\sum_{k_1=1}^{L-n+1}\sum_{k_2=k_1+1}^{L-n+2}\cdots\sum_{k_n=k_{n-1}+1}^{L}\prod_{j=1}^{n}\left(\frac{1}{P_{e,sr_{k_j}}}\right)\right. \\ \left.\times\left(\frac{1}{g_{QAM}\bar{\gamma}_{r_{k_j}d}}\right)\right], \tag{6.25}$$

where $P_{e,sr_i} \approx \frac{A}{2B\bar{\gamma}_{sr_i}}$ at high SNR and A_0, is given by

$$A_0 = \frac{4C_{QAM}}{\pi}\int_0^{\pi/2}\sin^2\theta \mathrm{d}\theta - \frac{4C_{QAM}^2}{\pi}\int_0^{\pi/4}\sin^2\theta\mathrm{d}\theta. \tag{6.26}$$

6.3.4 Power optimization

Due to the non-linear nature of the throughput function, finding the optimal throughput in (6.4) by using various optimizing techniques is not an easy task. However, we note that since the total power is distributed in the retransmission phase, emphasis should be on the SER of the retransmission. Fig. 6.1 shows the behaviour of the system throughput as the SER of the retransmission decreases. It is noted that as the SER of the retransmission decreases, the throughput increases. This implies that maximizing the throughput is equivalent to minimizing the SER of the retransmission.

In what follows, the optimal allocation between the source and the reliable relays that minimize the SER is determined. The asymptotic SER obtained in (6.25) can be rewritten by substituting $\bar{\gamma}_{sd} = \sigma_{sd}^2\alpha_0\frac{P}{N_0}$, $\bar{\gamma}_{sr_i} = \sigma_{sr_i}^2\alpha_0\frac{P}{N_0}$ and $\bar{\gamma}_{r_id} = \sigma_{r_id}^2\alpha_i\frac{P}{N_0}$ with $\sigma_{ij}^2 = \left(\frac{d_{sd}}{d_{ij}}\right)^{\nu}$, where d_{ij} represents the distance between node i and node j, ν is the pathloss coefficient and P/N_0 represents the average SNR. Without loss of generality, d_{sd} is normalized to $d_{sd}=1$. Hence,

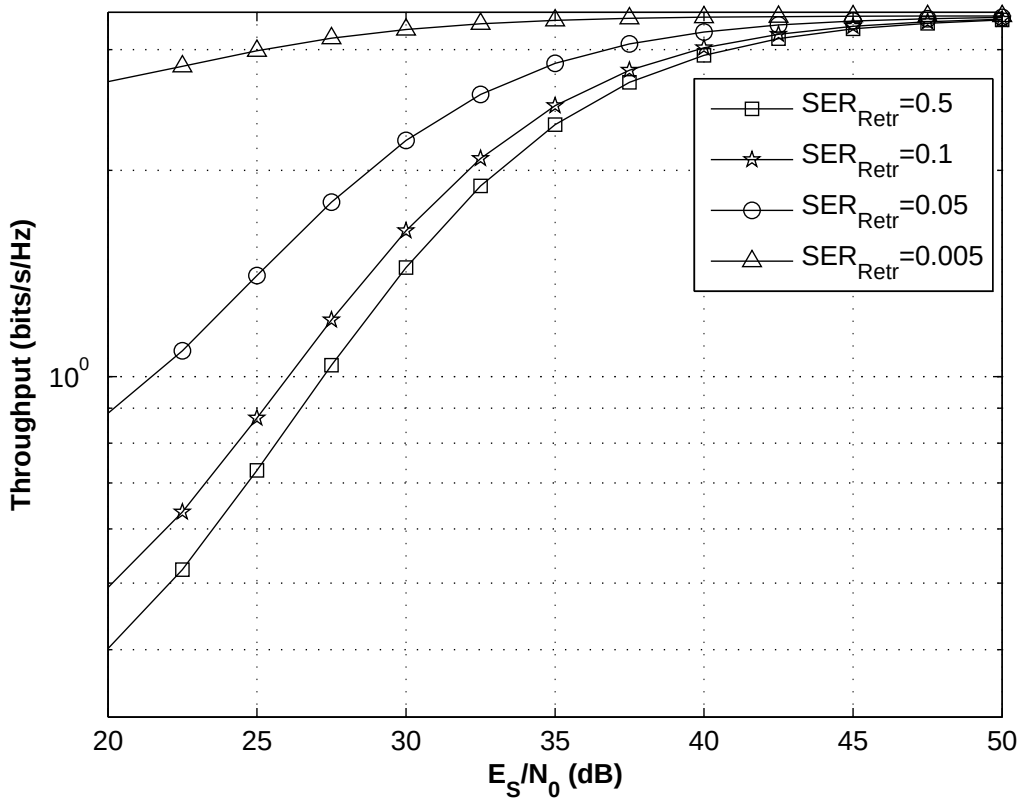

Figure 6.1: Throughput performance of the multi-relay adaptive DF as a function of SER using 16-QAM and $L = 3$.

the SER can be written as a function of power ratios and variances as

$$SER_{Retr} \approx \frac{(A/2B)^L A_0}{g_{QAM}\alpha_0^{L+1}\sigma_{sd}^2}\left(\frac{P}{N_0}\right)^{-(L+1)}\left(\prod_{i=1}^{L}\frac{1}{\sigma_{sr_i}^2}\right)\prod_{i=1}^{L}\left(1+\frac{(2B/A)\alpha_0}{g_{QAM}}\frac{\sigma_{sr_i}^2}{\sigma_{r_id}^2\alpha_i}\right). \quad (6.27)$$

As will be shown, the asymptotic SER derived in (6.27) yields tight bounds at high SNR. For this reason, it is employed to find the asymptotic optimum power allocation. The

optimization problem can then be formulated as follows,

$$\begin{aligned} \alpha_{opt} = \quad & \arg \min_{\alpha_0,\cdots,\alpha_L} SER_{Retr} \\ \text{subject to} \quad & \begin{cases} \alpha_i > 0, \\ \sum_{i=0}^{L} \alpha_i = 1. \end{cases} \end{aligned} \tag{6.28}$$

The second derivative test for multivariable case is used to determine the nature of the optimization problem in (6.28). The Hessian matrix of the objective function is defined as

$$\mathcal{H} = \begin{bmatrix} \frac{\partial^2 f}{\partial \alpha_0^2} & \frac{\partial^2 f}{\partial \alpha_0 \partial \alpha_1} & \cdots & \frac{\partial^2 f}{\partial \alpha_0 \partial \alpha_L} \\ \frac{\partial^2 f}{\partial \alpha_1 \partial \alpha_0} & \frac{\partial^2 f}{\partial \alpha_1^2} & \cdots & \frac{\partial^2 f}{\partial \alpha_1 \partial \alpha_L} \\ \vdots & \vdots & \ddots & \vdots \\ \frac{\partial^2 f}{\partial \alpha_L \partial \alpha_0} & \frac{\partial^2 f}{\partial \alpha_L \partial \alpha_1} & \cdots & \frac{\partial^2 f}{\partial \alpha_L^2} \end{bmatrix}, \tag{6.29}$$

where f denotes the objective function SER_{Retr}.

For $L = 1, 2$, it is noted that $\det(\mathcal{H})$ is positive definite for $\alpha_i > 0$ where $i = 0, 1, 2$. This confirms the convexity of the objective function in (6.28), by the second order conditions [94]. In Appendix E, $\det(\mathcal{H})$ is presented for $L = 2$.

This non-linear optimization problem can be solved using the Lagrange multiplier method. The Lagrangian of (6.28) can be written as

$$\mathrm{L}\left(\underline{\alpha}, \underline{\lambda}, \underline{\mu}\right) = SER_{Retr} - \left(\sum_{i=0}^{L} \lambda_i \alpha_i - 1\right) + \sum_{j=0}^{L} \mu_j \alpha_j, \tag{6.30}$$

where $\underline{\lambda}$ and $\underline{\mu}$ represent the Lagarange multipliers, $\underline{\alpha} = \{\alpha_0, \cdots, \alpha_L\}$, $\underline{\lambda} = \{\lambda_0, \cdots, \lambda_L\}$ and $\underline{\mu} = \{\mu_0, \cdots, \mu_L\}$

Since obtaining a closed-form expression of the optimal power allocation is intractable, this non-linear problem will be solved numerically using Newton's method [94]. Fig. 6.2 depicts the power distribution for 16-QAM and $L = 2$. It is noted that, as the relays get

close to the source(reliable $S-R$ links), more power is allocated to the relays. As the distance between the source and relays gets larger (i.e., less reliable $S-R$ links), less power is allocated to relays. For example, when $d_{sr_1}=0.1$ and $d_{sr_2}=0.5$, the allocated powers at the relays 1 and 2 are $\alpha_1 \approx 0.32$ and $\alpha_2 \approx 0.15$, respectively.

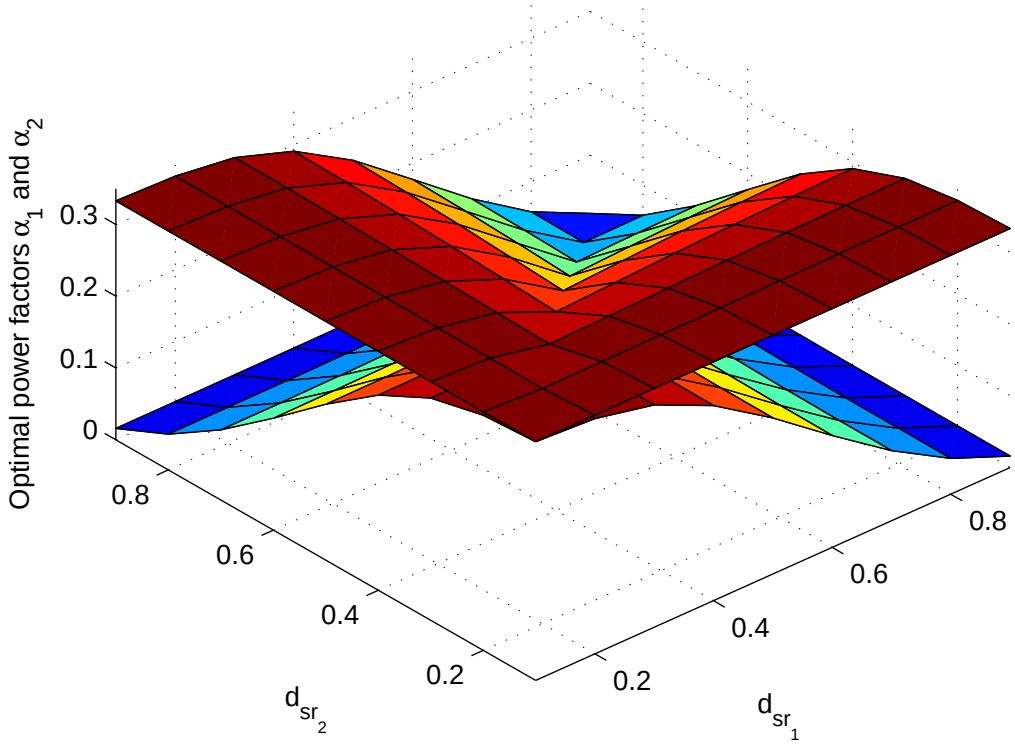

Figure 6.2: Optimal power distribution for 16-QAM and $L=2$ relays.

6.4 Numerical Results

In this section, some numerical results for the SER and throughput of the multi-relay adaptive DF are provided. The following parameters $K=100$, $C=16$, $N_{max}=3$, the pathloss coefficient $\nu=3$ are used and for the sake of simplicity we consider a cooperative scenario with $L=2$ is considered.

Fig. 6.3 shows SER comparison of the exact and asymptotic SER for the multi-relay

adaptive DF. It is noted that the approximated SER is in good agreement with the simulated one at high SNRs for different modulation schemes. In this figure, the distance between the source and relay one is $d_{sr_1} = 0.3$, whereas the distance between the source and relay two is $d_{sr_2} = 0.1$. Intuitively, relay two will be allocated more power than relay one, due to its close proximity to the source. For 4-QAM and 16-QAM, the power allocated at the nodes are found to be $\{\alpha_0, \alpha_1, \alpha_2\}$=$\{(0.357, 0.310, 0.333)\}$ and $\{(0.400, 0.268, 0.332)\}$, respectively.

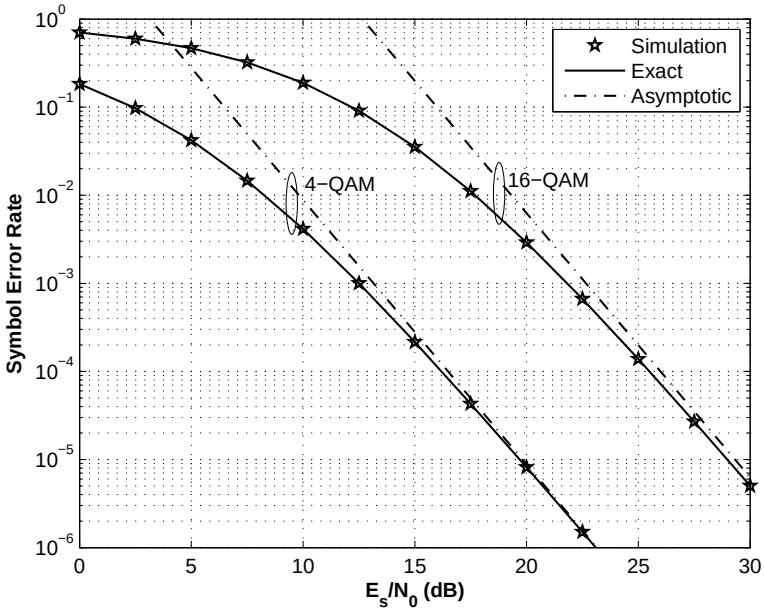

Figure 6.3: SER performance of multi-relay adaptive DF for 4-QAM and 16-QAM. $d_{sr_1} = 0.3, d_{sr_2} = 0.1$.

Fig. 6.4 shows the error rate performance of the multi-relay scenario when two relays participate in the retransmission. The power allocation at the relays was investigated and it can be seen that optimal power allocated to the relays yields the best performance in terms of symbol error rate performance. It can also be noted that equal power allocation (EPA) does not provide the best performance. This can also be observed when three users behave as relays during the retransmission process. The optimal power allocation (OPA) to the relays yields better error performance. This is illustrated in Fig. 6.5.

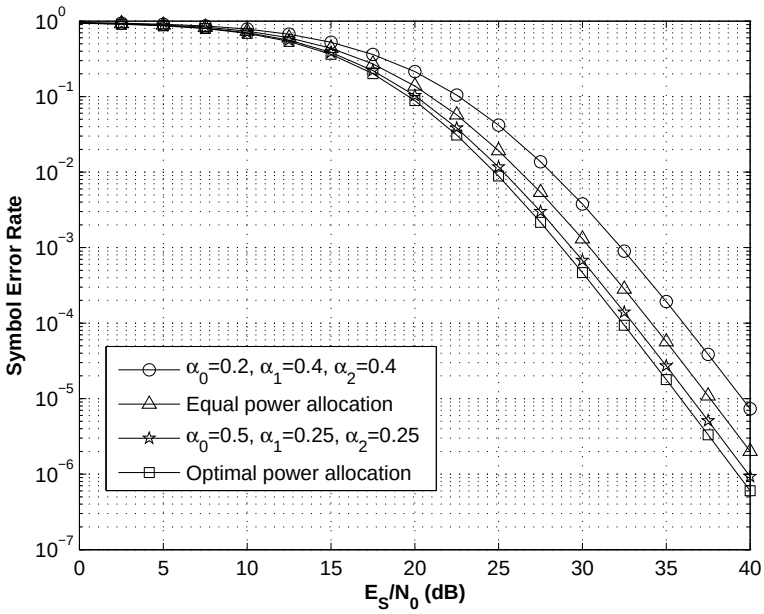

Figure 6.4: SER performance of multi-relay adaptive DF cooperative relaying for 64-QAM. $d_{sr_1} = 0.5, d_{sr_2} = 0.3$ with $L = 2$.

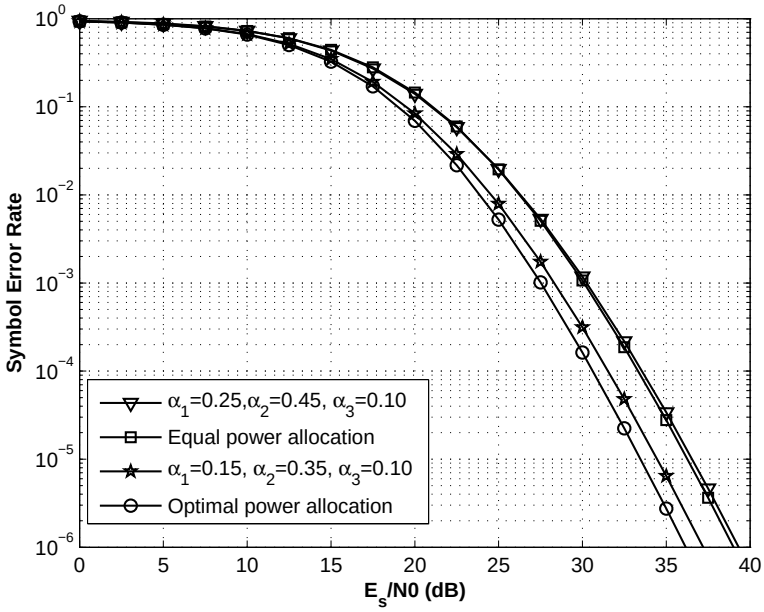

Figure 6.5: SER performance of multi-relay adaptive DF cooperative relaying for 64-QAM. $d_{sr_1} = 0.5, d_{sr_2} = 0.2$ and $d_{sr_3} = 0.8$ with $L = 3$.

Table 6.1 shows the power allocated at the source and relays for 16-QAM when d_{sr_1} is fixed and d_{sr_2} varies, whereas Table 6.2 shows the power allocated at the source and relays

for 64-QAM when d_{sr_1} is fixed while d_{sr_2} and d_{sr_2} vary.

Table 6.1: Optimal α_i values for 16-QAM when $L = 2$ and $d_{sr_1} = 0.25$.

d_{sr_2}	0.25	0.5	0.75
α_0	0.408	0.548	0.653
α_1	0.296	0.304	0.307
α_2	0.296	0.148	0.040

Table 6.2: Optimal α_i values for 64-QAM when $L = 3$ and $d_{sr_1} = 0.5$.

(d_{sr_2}, d_{sr_3})	$(0.1, 0.1)$	$(0.2, 0.8)$	$(0.6, 0.4)$
α_0	0.441	0.681	0.742
α_1	0.067	0.079	0.081
α_2	0.246	0.227	0.049
α_3	0.246	0.013	0.128

Fig. 6.6 shows the throughput of the system under study for 64-QAM when $d_{sr_1} = 0.5$ and $d_{sr_2} = 0.3$, respectively. It is noted that the system throughput with OPA is superior to other throughput performance obtained from non-optimized power assigment among which is the EPA. This has also been noted for different modulation schemes and relay topologies. In Fig. 6.7, there are three users that could potentially relay the source message in case of retransmission. The throughput performance for this scenario for 64-QAM and some relay positions is plotted. In this figure, $d_{sr_1} = 0.5, d_{sr_2} = 0.2$ and $d_{sr_3} = 0.8$. It can be noted that optimal allocated power to the relays yields better throughput performance that EPA and other relay positions.

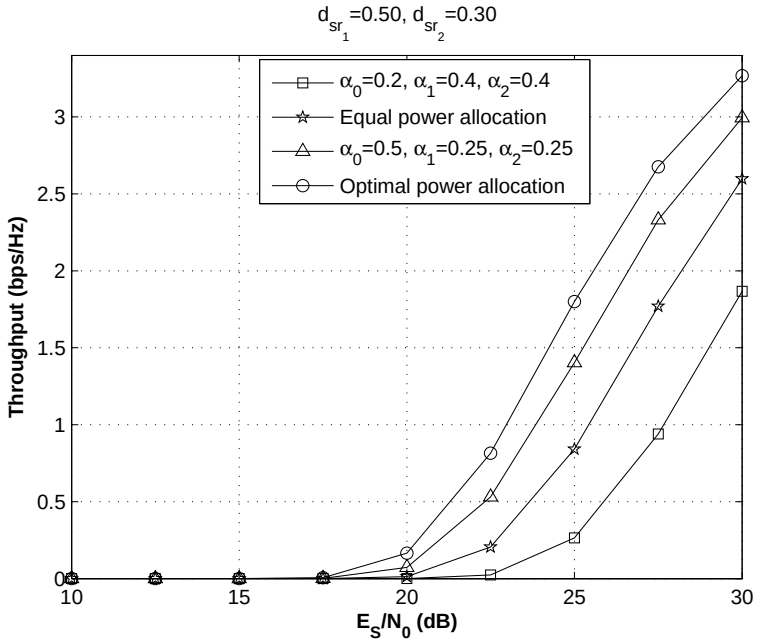

Figure 6.6: Throughput of multi-relay adaptive DF cooperative relaying for 64-QAM. $d_{sr_1} = 0.5, d_{sr_2} = 0.3$.

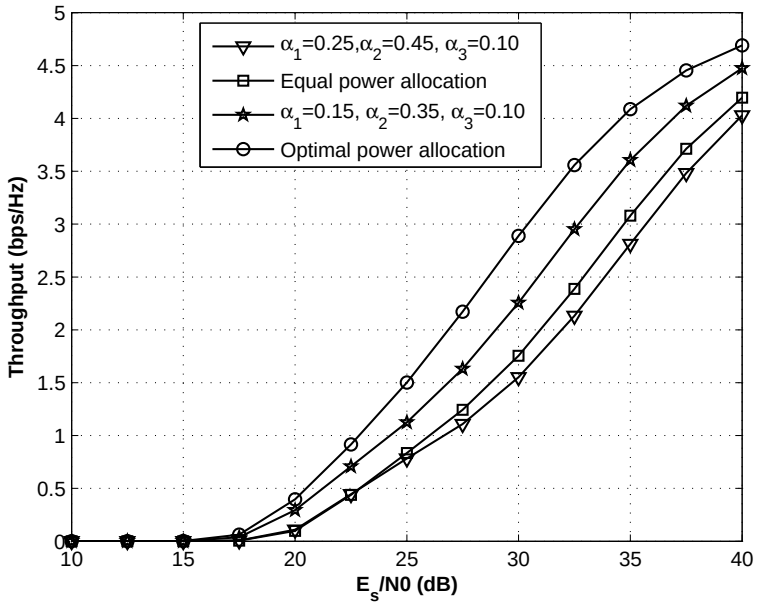

Figure 6.7: Throughput of multi-relay adaptive DF cooperative relaying for 64-QAM. $d_{sr_1} = 0.5, d_{sr_2} = 0.2$ and $d_{sr_3} = 0.8$ with $L = 3$.

6.5 Conclusion

In this chapter, a cross-layer design using multi-relay DF strategy at the physical layer and truncated ARQ at the link layer was investigated. The throughput maximization of the proposed scheme was studied. It was shown that, maximizing the throughput is similar to minimizing the SER of the cooperative scenario used in the retransmission. Results showed that the optimal power distribution yields maximum throughput. Furthermore, the power allocated at a relay is greatly affected by its location relative to the source and destination.

Chapter 7

Conclusions and Future Work

7.1 Conclusions

In this section, a summary of the work done is given as well as the contributions in this thesis.

In Chapter 2, a brief overview of the recent work on cooperative diversity was given since it is the focus of this thesis. Cooperative diversity techniques have been proposed since they mimic MIMO systems in a distributive manner. Due to their size and hardware constraints, mobile devices cannot adopt centralized MIMO technology. In order to keep the same structure but still reap the benefits of MIMO systems, cooperation among the mobiles or relay nodes is the only practical solution. A single or multiple relay node assist the source node by forwarding its message to the destination. The destination sees multiple replicas of the original message that have undergone different fading experiences, and combines them to create diversity. There are two main cooperative diversity strategies used at the relay nodes: AF and DF. In the former, no form of demodulation or decoding is required. The relay node simply amplifies the received signal prior to retransmitting it to the destination. On the other hand, a lot more is required by DF since demodulation or decoding is the core of the strategy. It is difficult to pinpoint which one of these two strategies is more advantageous

over the other. Since it is analogue, AF requires many radio frequency (RF) chains, and this can be difficult to implement especially when there are multiple relays. In the DF, it has been noted that decoding prior to retransmission is imperative. This causes some delays that could be prohibitive in a multi-relay scenario as far as synchronization is concerned. But DF is easy to implement. In order to improve DF, since it suffers from error propagation, channel coding has been integrated with cooperative communications. Convolutional codes, turbo codes have been implemented in cooperative communications and have shown to yield dramatic gains over uncoded DF.

In Chapter 3, a multi-relay algorithm for a variation of turbo-coded cooperation over Nakagami-m fading channels was proposed. In this scheme, the destination received the entire codeword from the source during the first phase, whereas the relays reveived a fragment of the codeword prior to performing decoding. This fragment of the codeword corresponds to the systematic bits and can be done in practice by puncturing all the parity bits. In the second phase, only the decoding relays forward the parity or punctured bits to the destination. The union bounds on the BER were derived using the transfer bounds and limit-before-average tehcniques. Furthermore, outage probability of the scheme under study was proposed and simulation results were presented to confirm the analytical work.

In Chapter 4, a cooperative ARQ system where a set of reliable relay nodes are selected based on the throughput maximization was proposed. This selection is performed at the destination through an exhaustive search and the selected relays are informed on this selection through a low-rate and error-free feedback channel. Furthermore, joint optimization of the packet length and constellation size was investigated and results showed that optimized values of the packet length and constellation size yield maximum throughput. Another advantage of the proposed scheme is better utilization of the bandwidth, since all the relays are not always used for retransmission.

In the previous chapter, bandwidth loss is an issue since all the relays could still be used

in the retransmission. In Chapter 5, a cooperative ARQ that combines best relay selection at the cooperative level and truncated ARQ at the link layer was proposed. It was shown that throughput maximization is equivalent to minimizing the SER of the retransmission phase. In what followed, the bounds on the asymptotic SER for the best relay selection in DF cooperative diversity were derived. Using the derived asymptotic SER, the optimal power distribution between the source node and the relay node was obtained.

A throughput maximization via power optimization in a multi-relay DF cooperative network over i.n.i.d. Rayleigh fading channels was proposed in chapter 6. Having noted that this optimization problem is equivalent to the minimization of the SER during the retransmission, the exact SER of the strategy used in the retransmission phase, as well as its bounds at high SNR were first derived.

7.2 Future Work

The following are some topics of interest for further investigations of this research:

1. In Chapter 2, a brief survey on LDPC codes in cooperative diversity is presented. In most of the aforementioned works, DF has been the preferred relaying protocol. Further works could investigate code designs for other relaying protocols such as estimate-and-forward or AF. Moreover, Gaussian has extensively been studied for LDPC-coded cooperative diversity. More general fading scenarios such as Rayleigh (that have barely been studied) and Nakagami-m can be investigated for LDPC codes in coded cooperation. Finally, multi-relay LDPC-coded cooperation can also be studied in future research works.

2. In Chapter 3, a multi-relay turbo-coded cooperative scheme was investigated. For better spectral efficiency, it would be better that only one relay, i.e., the best relay transmits in the second time slot. Most of the existing literature on relay selection has assumed that ideal CSI is used at the receiver side. However, in practice this

assumption is not viable as a feedback delay leading to outdated CSI may exist. A study of the impact of outdated CSI on turbo-coded cooperation with the best relay selection over Nakagami-m fading channels would be an attractive topic for future research. The effects of fading parameters on relay selection could also be studied, by analyzing the bit error and outage probabilities of the aforementioned scheme.

3. The multi-relay turbo coded cooperative networks were examined by assuming the simplified dual-hop relays. Further investigations need to be carried on a more general multi-hop relaying system. The latter scenario is more practical and encompasses the dual-hop scenario investigated in this thesis. In such a scenario, many questions arise such as: (a) what are the effects of unequal hops (the number of relays in a branch is not equal) on the performance of the system? (b) what is the diversity gain of the system?

4. The retransmission scheme considered in this work is similar to the *stop-and-wait* scheme. *Selective repeat* and/or *GO-BACK-N* can be investigated as well. Throughout this work, no delay for packet delivery was assumed, which is very unlikely in a practical scenario. Hence, an investigation of packet delay scenario analysis in ARQ cooperative systems could be undertaken in future work.

Bibliography

[1] V. Tarokh, N. Seshadri, and A.R Calderbank, "Space-time codes for high data rate wireless communications: performance criterion and code construction," *IEEE Transactions on Information Theory*, vol. 44, no. 2, pp. 744-765, March 1998.

[2] A. R. Calderbank, "The art of signaling: Fifty years of coding theory," *IEEE Transactions on Information Theory*, vol. 44, no. 6, pp. 2561-2595, October 1998

[3] A. F. Naguib, N. Seshadri, and A. R. Calderbank, "Increasing data rate over wireless channels," *IEEE Signal Processing Magazine*, vol. 17, no. 3, pp. 76-92, May 2000.

[4] J. Boutros and E. Viterbo, "Signal space diversity: a power and bandwith efficient diversity technique for the Rayleigh fading channel," *IEEE Transactions on Information Theory*, vol. 44, no. 4, pp. 1453-1467, July 1998.

[5] I. E. Telatar, "Capacity of multi-antenna Gaussian channels," *European Transactions on Telecommunications*, vol. 10, no. 6, pp. 585-595, November 1999.

[6] G. Foschini and M. Gans, "On limits of wireless communications in a fading environment when using multiple antennas," *Wireless Personal Communications*, vol. 6, no. 3, pp. 311-335, March 1998.

[7] S. M. Alamouti, "A simple transmit diversity technique for wireless communications," *IEEE Journal on Selected Areas in Communications*, vol. 16, no. 8, pp. 1451-1458, October 1998.

[8] V. Tarokh, H. Jafarkhani, and A. R. Calderbank, "Space-time block codes from orthogonal designs," *IEEE Transactions on Information Theory*, vol. 45, no. 5, pp. 1456-1467, July 1999.

[9] A. Sendonaris, E. Erkip, and B. Aazhang, "User cooperation diversity-Part I: System description," *IEEE Transactions on Communications*, vol. 51, no. 11, pp. 1927-1938, November 2003.

[10] A. Sendonaris, E. Erkip, and B. Aazhang, "User cooperation diversity-Part II: Implementation aspects and performance analysis," *IEEE Transactions on Communications*, vol. 51, no. 11, pp. 1939-1948, November 2003.

[11] J. N. Laneman, G. W. Wornell, and D. N. C. Tse, "An efficient protocol for realizing cooperative diversity in wireless networks," in Proc. *IEEE International Symposium on Information Theory (ISIT)*, Washington, DC, p. 294, June 2001.

[12] J.N. Laneman and G.W. Wornell, "Distributed space-time coded protocols for exploiting cooperative diversity in wireless networks," *IEEE Transactions on Information Theory*, vol. 49, no. 10, pp. 2415-2425, October 2003.

[13] J. N. Laneman, G. W. Wornell, and D. N. C. Tse, "Cooperative diversity in wireless networks: Efficient protocols and outage behavior," *IEEE Transactions on Information Theory*, vol. 50, no. 12, pp. 3062-3080, December 2004.

[14] J. N. Laneman and G. W. Wornell, "Energy-efficient antenna sharing and relaying for wireless networks," *IEEE Wireless Communications and Networking Conference (WCNC)*, vol. 1, Chicago, IL, pp. 7-12, September 2000.

[15] R. U. Nabar and H. Bolcskei, "Fading relay channels: performance limits and space-time signal design," *IEEE Journal on Selected Areas in Communications*, vol. 22, no. 6, pp. 1099-1109, August 2004.

[16] F. A. Onat, A. Adinoyi, Y. Fan, H. Yanikomeroglu and J. S. Thompson, "Threshold selection for SNR-based selective digital relaying in cooperative wireless networks," *IEEE Transactions on Wireless Communications*, vol. 7, no. 11, pp. 4226-4237, November 2008.

[17] P. Herhold, E. Zimmermann, and G. Fettweis, "A simple cooperative extension to wireless relaying," in Proc. *International Zurich Seminar on Communications*, pp. 36-39, August 2004.

[18] T.E. Hunter and A. Nosratinia, "Diversity through Coded Cooperation," *IEEE Transactions on Wireless Communications*, vol. 5, no. 2, pp. 283-289, February 2006.

[19] M. Janani, A. Hedayat, T.E. Hunter, A. Nosratinia, "Coded cooperation in wireless communications: space-time transmission and iterative decoding," *IEEE Transactions on Signal Processing*, vol. 52, no. 2, pp. 362-371, February 2004.

[20] L. Dai, and K. B. Lataeif , "Throughput maximization of ad-hoc wireless networks using adaptive cooperative diveristy and truncated ARQ," *IEEE Transactions on Communications* , vol. 56, no. 11, pp. 1907-1918, November 2008.

[21] A. Vosoughi and J. Yupeng, "Maximizing throughput in cooperative networks via cross-layer adaptive designs," *IEEE sarnoff Symposium*, pp. 1-6, April 2010.

[22] Q. Liu, S. Zhou and G. B. Giannakis, "Cross-layer combining of adaptive modulation and coding with truncated ARQ over wireless links," *IEEE Transactions on Wireless Communications*, vol. 3, no. 5, pp. 1746-1755, September 2004.

[23] E. C. Van Der Meulen, "Transmission of Information in a T-Terminal DiscreteMemory less Channel," *Technical report*, Department of Statistics, University of California, Berkeley, CA, 1968.

[24] B. Can, M. Portalski, H. Lebreton, S. Frattasi, and H. Suraweera, "Implementation issues for OFDM-based multihop cellular networks," *IEEE Communications Magazine*, vol. 45, no. 9, pp. 74-81, September 2007.

[25] R. Nabar and H. Bolcskei, "Space-time signal design for fading relay channels," in Proc. *IEEE Global Telecommunications Conference (GLOBECOM)*, vol. 4, December 2003.

[26] T. Hunter and A. Nosratinia, "Cooperation diversity through coding," *IEEE International Symposium on Information Theory (ISIT)*, Lausanne, Switzerland, p. 220, June 2002.

[27] A. Stefanov and E. Erkip, "Cooperative coding for wireless networks," *IEEE Transactions on Communications*, vol. 52, no. 9, pp. 1470-1476, September 2004.

[28] R. Liu, P. Spasojevic, and E. Soljanin, "User cooperation with punctured turbo codes," in Proc. of 41^{st} *Allerton Conference on Communications, Control and Computing*, Monticello, IL, October 2003.

[29] A. Stefanov and E. Erkip, "Cooperative space-time coding for wireless networks," *IEEE Transactions on Communications*, vol. 53, no. 11, pp. 1804-1809, November 2005.

[30] J. Hagenauer, "Rate-compatible punctured convolutional codes (RCPC codes) and their applications," *IEEE Transactions on Communications*, vol. 36, no. 4, pp. 389-400, April 1988.

[31] J. J. Boutros, A. Guilléen i Fàbregas and E. Calvanese, "Analysis of coding on non-ergodic block fading channels," In Proceeedings *Allerton Conference on Communication and Control*, Illinois, 2005.

[32] C. Li, G. Yue, M. A. Khojastepour, X. Wang, and M. Madihian, "LDPC-coded cooperative relay systems: Performance analysis and code design," *IEEE Transactions on Communications*, vol. 56, no. 3, pp. 485-496, March 2008.

[33] R. G. Gallager, Low-density parity-check codes, Cambridge, MA USA, MU Press, 1963. Also available online at http://justice.mit.edulpeople/pubs/ldpc.ps.

[34] R. G. Gallager, "Low-density parity-check codes," *IRE Transaction on Information Theory*, vol. 8, no. 1, pp. 21-28, January 1962.

[35] D. J. C MacKay and R. M. Neal, "Near-Shannon limit performance of low-density parity-check codes," *Electronics Letters*, vol. 32, pp. 1645-1646, August 1996.

[36] M. Sipser and D. A. Spielman, "Expander codes," *IEEE Transactions on Information Theory*, vol. 46, no. 6, pp. 1710-1722, November 1996.

[37] D. J. C. MacKay, "Good error-correcting codes based on very sparse matrices," *IEEE Transactions on Information Theory*, vol. 45, no. 2, pp. 399-431, March 1999.

[38] C. Li, G. Yue, X. Wang, and M. A. Khojastepour, "LDPC code design for half-duplex cooperative relay," *IEEE Transactions on Wireless Communications*, vol. 7, no. 11, pp. 4558-4567, November 2008.

[39] P. Razaghi and W. Yu, "Bilayer low-density parity-check codes for decode-and-forward in relay channels," *IEEE Transactions on Information Theory*, vol. 53, no. 10, pp. 3723-3739, October 2007.

[40] J. Hu and T. M. Duman, "Low density parity check codes over wireless relay channels," *IEEE Transactions on Wireless Communications*, vol. 6, no.9, pp. 3384-3394, September 2007.

[41] M. H. Azmi, J. Li, J. Yuan, and R. Malaney, "LDPC codes for soft decode-and-forward in half-duplex relay channels," To appear in *IEEE Journal on Selected Areas in Communications*, vol. 31, no. 8, August 2013.

[42] A. Chakrabarti, A. de Baynast, A. Sabharwal, and B. Aazhang, "Low density parity check codes for the relay channels," *IEEE Journal on Selected Areas in Communications*, vol. 25, no. 2, pp. 280-291, February 2007.

[43] S. Y. Chung, T. Richardson, and R. Urbanke, "Analysis of sum-product decoding of low-density parity-check codes using a Gaussian approximation," *IEEE Transactions on Information Theory*, vol. 47, no. 2, pp. 657-670, February 2001.

[44] C. Berrou and A. Glavieux, "Near optimum error correcting coding and decoding: Turbo codes," *IEEE Transactions on Communications*, vol. 44, no. 10, pp. 1261-1271, October 1996.

[45] G. D. Forney, *Concatenated codes.* Massachussetts Institute of Technology Press, 1966.

[46] P. Robertson, "Illuminating the structure of code and decoder of parallel concatenated recursive systematic (Turbo) codes," in Proc. *IEEE Global Telecommunications Conferende (GLOBEBOM'94)*, vol. 3, pp. 1298-1303, San Francisco, California, November 1994.

[47] L. R. Bahl, J. Cocke, F. Jelinek, and J.Raviv, "Optimal decoding of linear codes for minimizing symbol error rate," *IEEE Transactions on Information Theory*, vol. 20, no. 2, pp. 284-287, March 1974.

[48] S. Lin, D. J. Costello and M. J. Miller, "Automatic-repeat-request error control schemes," *IEEE Communications Magazine*, vol. 22, no. 12, pp. 5-17, December 984.

[49] S. Lin and P. Yu, "A hybrid ARQ scheme with parity retransmission for error control of satellite channels," *IEEE Transactions on Communications*, vol. 30, no. 7, pp. 1701-1719, July 1982.

[50] R. Comroe and D. J. Costello, Jr., "ARQ schemes for data transmission in mobile radio systems," *IEEE Journal on Selected Areas in Communications*, vol. 2, no. 4, pp. 472-481, July 1984.

[51] B. Zhao and M. C. Valenti, "Practical relay networks: a generalization of hybrid-ARQ," IEEE Journal on Selected Areas in Communications, vol. 23, no. 1, pp. 7-18, January 2005.

[52] S. Lee, W. Su, S. Batalama and J. D. Matyjas, "Cooperative decode-and-forward ARQ relaying: performance analysis and power optimization," *IEEE Transactions on Wireless Communications*, vol. 9, no. 8, pp. 2632-2642, August 2010.

[53] I. Krikidis, "Distributed truncated ARQ protocol for cooperative diversity networks," *IET Communications*, 2007, Vol. 1, Iss. 6, pp. 1212-1217, doi: 10.1049/iet-com.2007.0034.

[54] S. S. Ikki and M. H. Ahmed, "Performance analysis of cooperative diversity with incremental*best relay technique over Rayleigh fading channels," *IEEE Transactions on Communications*, vol. 59, no. 8, pp. 2152-2161, August 2011.

[55] T. E. Hunter, S. Sanayei, and A. Nosratinia, "Outage Analysis of Coded Cooperation," *IEEE Transactions on Information Theory*, vol. 52, no. 2, pp. 375-391, February 2006.

[56] M. Elfituri, W. Hamouda, and A. Ghrayeb, "A convolutional-based distributed coded cooperation scheme for relay channels," *IEEE Transactions on Vehicular Technology*, vol. 58, no. 2, pp. 655-669, February 2009.

[57] M. K. Simon and M. S. Alouini, *Digital Communication over Fading Channels: A Unified Approach to Performance Analysis.* New York: John Wiley & Sons, 2000.

[58] S. S. Ikki and M. H. Ahmed, "Multi-branch decode-and-forward cooperative diversity networks performance analysis over Nakagami-m fading channels," *IET Communications*, 2011, Vol. 5, Iss. 6, pp. 872-878, doi: 10.1049/iet-com.2010.0214.

[59] Y. Lee and M.-H. Tsai, "Performance of decode-and-forward cooperative communications with multiple dual-hop relays over Nakagami-m fading channels," *IEEE Transactions on Vehicular Technology*, vol. 8, no. 6, pp. 2853-2859, June 2009.

[60] C. K. Datsikas, N. C. Sagias, F. I. Lazarakis, and George S. Tombras, "Outage Analysis of Decode-and-Forward Relaying Over Nakagami-m Fading Channels," *IEEE Signal Processing Letters*, vol. 15, pp. 41-44, 2008.

[61] T. Duong, V.N.Q. Bao, and H.J. Zepernick, "On the performance of selection decode-and-forward relay networks over Nakagami-m fading channels," *IEEE Communications Letters*, vol. 13, no. 3, pp. 172-174, March 2009.

[62] H. Suraweera, P. J. Smith, and J. Armstrong, "Outage Probability of Cooperative Relay Networks in Nakagami-m Fading Channels," *IEEE Communications Letters*, vol. 10, no. 12, December 2006.

[63] A. Bansal, and P. Garg, "Performance analysis of coded cooperation under Nakagami-m fading channels," in *Proc. IEEE International Conference on Communications (ICC)*, Cape Town, South Africa, May 2010.

[64] C. Li, Y. Wang and D. Yang, "Performance analysis for coded cooperative multiple-relay in distributed turbo channels," in *Proc. IEEE 22nd International Symposium on Personal, Indoor and Mobile Radio Communications (PIRMC)*, Toronto, Canada, September 2011.

[65] J. Haghighat and W. Hamouda, "Decode-Compress-and-Forward with Selective-Cooperation for Relay Networks," *IEEE Communications Letters*, vol. 16, no. 3, pp. 378-381, March 2012.

[66] J. K. Proakis, *Digital Communications.* 3rd edition, New York: McGraw-Hill, 1995.

[67] J. W. Craig, "A new, simple, and exact result for calculating the probability of error for two-dimensional signal constellations," in Proc. *IEEE Military Communications Conference (MILCOM'91)*, McLean, VA, pp. 571-575, October 1991.

[68] M-S Alouini and A.J. Goldsmith, "A Unified Approach for Calculating Error Rates of Linearly Modulated Signals over Generalized Fading Channels," *IEEE Transactions on Communications*, Vol. 47, no. 9, pp. 1324-1334, September 1999.

[69] S. Benedetto and G. Montorsi, "Performance Evaluation of Turbo-Codes," *Electronics Letters*, vol. 31, no. 3, pp. 163-165, February 1995.

[70] D. Divsalar, S. Dolinar and F. Pollara, "Transfer function bounds on the performance of turbo codes," *Telecom and Data Acquisition Progress Report* 42-122, JPL, August 1995.

[71] R. P. Stanley, *Enumerative Combinatorics.* Monterey, California: Wadsworth & Brooks/Cole, 1986.

[72] E. Malkamaki and H. Leib, "Evaluating the performance of convolutional codes over block fading channels," *IEEE Transactions on Information Theory*, vol. 45, no. 5, pp. 1643-1646, July 1999.

[73] T. M. Cover and J. A. Thomas, *Elements of Information Theory.* New York: Wiley, 1991.

[74] N. C. Beaulieu and J. Hu, "A closed-form expression for the outage probability of decode-and-forward relaying in dissimilar Rayleigh fading channels," *IEEE Communications Letters*, vol. 10, no. 12, pp. 813-815, December 2006.

[75] I. S. Gradshteyn and I. M. Ryzhik, *Table of Integrals, Series, and Products.* 3rd ed. New York: Academic, 2007.

[76] A. Viterbi and J. K. Omura, *Principles of Digital Communication Coding.* New York: McGraw-Hill, 1979.

[77] J. L. Vicario, M. A. Lagunas and C. Anton-Haro, "A cross-layer approach to transmit antenna selection," *IEEE Transactions on Wireless Communications*, vol. 5, no. 8, pp. 1993-1997, August 2006.

[78] A. Milani, V. Tralli and M. Zorzi, "Improving protocol performance in BLAST-based wireless systems using channel adaptive antenna selection," in Proc.*IEEE Vehicular Technology Conference (VTC)*, vol. 1, pp. 409-413, Spring 2002.

[79] H. A. Abou-Saleh and W. Hamouda, "Cross-layer based transmit antenna selection for decision-feedback detection in correlated ricean MIMO channels," *IEEE Transactions on Wireless Communications*, vol. 8, no. 4, pp. 1677-1682, April 2009.

[80] M.S. Bazaraa, H.D. Sherali and C.M. Chetty , *Nonlinear programming: Theory and Algorithms.* Wiley, 1993.

[81] A. Bletsas, H. Shin, M. Z. Win, and A. Lippman, "A simple Cooperative diversity method based on network path selection," *IEEE Journal on Selected Areas in Communications*, vol. 24, no. 3, pp. 659-672, March 2006.

[82] S. Ikki and M. H. Ahmed, "Performance of multiple-relay cooperative diversity systems with best relay selection over Rayleigh fading channels," *EURASIP Journal on Advances in Signal Processing*, vol. 2008, no. 145, Article ID 580368, 7 pages, 2008.

[83] S. S. Ikki and M. H. Ahmed, "Performance analysis of adaptive decode-and-forward cooperative diversity networks with best-relay selection," *IEEE Transactions on Communications*, vol. 58, no. 1, pp. 68-72, January 2010.

[84] S. S. Ikki and M. H. Ahmed, "On the performance of cooperative-diversity networks with the N^{th} best relay selection scheme," *IEEE Transactions on Communications* , vol. 58, no. 11, pp. 3062-3069, November 2010.

[85] C. Yang, S. Zhao, W. Wang, and M. Peng, "Performance of decode-and-forward opportunistic cooperation with the N^{th} best relay selected," in *Proc. of the* 6^{th} *International Wireless Communications and Mobile Computing conference (IWCMC)*, pp. 1253-1257, Caen, France, June 28-July 02, 2010.

[86] F. A. Onat, Y. Fan, H. Yanikomeroglu, and V. Poor, "Threshold-based relay selection for detect-and-forward relaying in cooperative wireless networks," *EURASIP Journal on Wireless Communications and Networking*, vol. 2010, no. 43, Article ID 721492, 9 pages, 2010.

[87] S. S. Ikki and M. H. Ahmed, "Performance analysis of cooperative diversity with incremental-best-relay technique over Rayleigh fading channels," *IEEE Transactions on Communications*, vol. 59, no. 8, pp. 2152-2161, August 2011.

[88] J. S. Harsini, F. Lahouti, M. Levorato and M. Zorzi, "Analysis of non-cooperative and cooperative type II Hybrid ARQ protocols with AMC over correlated fading channels," *IEEE Transactions on Wireless Communications*, vol. 10, no. 3, pp. 877-889, March 2011.

[89] Z. Wang and G. B. Giannakis, "A simple and general parameterization quantifying performance in fading channels," *IEEE Transactions on Communications*, vol. 51, no. 8, pp. 1389-1398, August 1998.

[90] A. Jeffrey and H. -H. Dai, *Handbook of Mathematical Formulas and Integrals.* 4th ed. San Diego, CA: Elsevier, 2008.

[91] A. Ribeiro, X. Cai, and G. B. Giannakis, "Symbol error probabilities for general cooperative links," *IEEE Transactions on Communications*, vol. 4, no. 3, pp. 1264-1273, May 2005.

[92] J. R. Magnus and H. Neudecker, "Matrix differential calculus with applications in statistics and econometrics," 3^{rd} edition, New York: John Wiley and Sons, 1988.

[93] H. Boujemaa, "Delay analysis of cooperative truncated HARQ with opportunistic relaying," *IEEE Transactions on Vehicular Technology*, vol. 58, no. 9, pp. 4795-4804, November 2009.

[94] S. Boyd and L. Vandenberghe, *Convex Optimization.* Cambridge University Press, 2004.

Appendix A

Evaluation of the code fragment $(1, \frac{17}{13})_{octal}$ by the recursion method

The evaluation of the code fragment by the recursion formula can be done through mathematical software. In this work, MATLAB was used to derive it and only the resulting expression is presented, given by

$$
\begin{aligned}
t(j,i,d) = {} & t(j-1,i,d) + t(j-1,i-1,d) - t(j-3,i-1,d) - t(j-3,i-2,d) \\
& + t(j-3,i-1,d-2) + t(j-3,i-2,d-2) + 2t(j-4,i-2,d) \\
& - t(j-4,i-1,d-2) - 2t(j-4,i-2,d-2) - t(j-4,i-3,d-2) \\
& + t(j-4,i-1,d-4) + t(j-4,i-3,d-4) - t(j-5,i-2,d) \\
& - t(j-5,i-3,d) + t(j-5,i-1,d-2) + t(j-5,i-2,d-2) \\
& - t(j-5,i-1,d-4) + t(j-5,i-3d-2) + t(j-5,i-4,d-2) \\
& - t(j-5,i-4,d-4) + t(j-7,i-3,d) + t(j-7,i-4,d) \\
& - t(j-7,i-1,d-2) - 2t(j-7,i-2,d-2) - 2t(j-7,i-5,d-2) \\
& - t(j-7,i-6,d-2) + t(j-7,i,d-4) + 2t(j-7,i-3,d-4) \\
& + 2t(j-7,i-4,d-4) + t(j-7,i-7,d-4) - t(j-7,i-2,d-6) \\
& - t(j-7,i-5,d-6) - t(j-8,i-4,d) + 2t(j-8,i-2,d-2) \\
& + 2t(j-8,i-6,d-2) - t(j-8,i,d-4) - 4t(j-8,i-4,d-4) \\
& - t(j-8,i-8,d-4) + 2t(j-8,i-2,d-6) + 2t(j-8,i-6,d-6) \\
& - t(j-8i-4,d-8) + \delta(j,i,d) - \delta(j-1,i-1,d) \\
& - \delta(j-2,i-1,d) + \delta(j-3,i-2,d) - \delta(j-3,i-1,d-2) - \delta(j-3,i-1,d-2) \\
& - \delta(j-4,i-2,d) + \delta(j-4,i-2,d-2) + \delta(j-4,i-3,d-2) - \delta(j-4,i-1,d-4) \\
& + \delta(j-5,i-3,d) - \delta(j-5,i-1,d-2) + \delta(j-6,i-3,d) - \delta(j-6,i-1,d-2) \\
& - \delta(j-6,i-5,d-2) + \delta(j-6,i-3,d-4) - \delta(j-7,i-4,d) + 2\delta(j-7,i-2,d-2) \\
& + \delta(j-7,i-6,d-2) - \delta(j-7,i,d-4) - 2\delta(j-7,i-4,d-4) + \delta(j-7,i-2,d-6),
\end{aligned}
\tag{A.1}
$$

where $\delta(j,i,d) = 1$ if $j = i = d = 1$ and $\delta(j,i,d) = 0$ otherwise, and $t(j,i,d) = 0$ for any negative index.

Appendix B

Derivation of $I(\mu, \nu, \beta)$ in (3.42)

The lower incomplete gamma function can be rewritten using its alternative representation [75, Eq. (8.352.4)] as

$$\varphi\left(m_{r_jd}, \frac{m_{r_jd}}{\bar{\gamma}_{r_jd}}\left(\frac{2^{R_c\beta}}{(1+\gamma_{sd})^{\beta}}-1\right)\right) = (m_{r_jd}-1)!\left[1-\exp\left(\frac{m_{r_jd}}{\bar{\gamma}_{r_jd}}\left(1-\frac{2^{R_c\beta}}{\left(1+\gamma_{sd}\right)^{\beta}}\right)\right)\right. \\ \left.\times \sum_{n=0}^{m_{r_jd}-1} \frac{(m_{r_jd}/\bar{\gamma}_{r_jd})^n}{n!}\left(\frac{2^{R_c\beta}}{\left(1+\gamma_{sd}\right)^{\beta}}-1\right)^n\right]. \tag{B.1}$$

Using (B.1) in (3.42) and after some manipulations, $I(\mu, \nu, \beta)$ can be written as

$$I(\mu,\nu,\beta) = \prod_{j=1}^{\vartheta} \frac{m_{sd}^{m_{sd}}}{\Gamma(m_{sd})\bar{\gamma}_{sd}}\left[\underbrace{\int_0^{2^{R_c}-1} \gamma_{sd}^{\mu}\exp\left(-\nu\gamma_{sd}\right)\mathrm{d}\gamma_{sd}}_{I_1}\right. \\ \left.\underbrace{-\int_0^{2^{R_c}-1} \gamma_{sd}^{\mu}\exp\left(-\nu\gamma_{sd}\right)\exp\left(\frac{m_{r_jd}}{\bar{\gamma}_{r_jd}}-\frac{2^{R_c\beta}\left(\frac{m_{r_jd}}{\bar{\gamma}_{r_jd}}\right)}{\left(1+\gamma_{sd}\right)^{\beta}}\right)\sum_{n=0}^{m_{r_jd}-1}\frac{m_{r_jd}^n}{\bar{\gamma}_{r_jd}^n n!}\left(\frac{2^{R_c\beta}}{\left(1+\gamma_{sd}\right)^{\beta}}-1\right)^n}_{I_2}\right]. \tag{B.2}$$

I_1 can easily be obtained from [75, Eq. (3.351.1)] and given by

$$I_1 = \nu^{-m_{sd}} \varphi\Big(m_{sd}, \nu\big(1-2^{R_c}\big)\Big). \tag{B.3}$$

In order to obtain I_2, its form is expanded in (B.2), and the Binomial expansion $(1-x)^k = \sum_{j=0}^{k} \binom{k}{j}(-1)^j x^j$ is applied and performing some algebraic manipulations yields

$$I_2 = \exp\left(\frac{m_{r_j d}}{\bar{\gamma}_{r_j d}} + 1\right) \sum_{n=0}^{m_{r_j d}-1} \sum_{m=0}^{n} \frac{(-1)^{n+m} m_{r_j d}^n}{\bar{\gamma}_{r_j d}^n n!} \binom{n}{m} 2^{R_c \beta m} \int_0^{2^{R_c}-1} \gamma_{sd}^{\mu} \exp\left(-\nu\gamma_{sd} - \frac{2^{R_c\beta}\left(\frac{m_{r_j d}}{\bar{\gamma}_{r_j d}}\right)}{\big(1+\gamma_{sd}\big)^{\beta}}\right) \times \frac{1}{\big(1+\gamma_{sd}\big)^{\beta}} \mathrm{d}\gamma_{sd}. \tag{B.4}$$

Using the following series

$$\exp(-x) = \sum_{k=0}^{\infty} \frac{(-1)^k}{k!} x^k, \tag{B.5}$$

and applying the binomial expansion $(g+h)^k = \sum_{j=0}^{k} \binom{k}{j} g^{k-j} h^j$ and after some manipulations (B.4) is given by

$$I_2 = \exp\left(\frac{m_{r_j d}}{\bar{\gamma}_{r_j d}} + 1\right) \sum_{n=0}^{m_{r_j d}-1} \sum_{m=0}^{n} \frac{(-1)^{n+m} m_{r_j d}^n}{\bar{\gamma}_{r_j d}^n n!} \binom{n}{m} 2^{R_c \beta m} \sum_{k=0}^{\infty} \sum_{l=0}^{k} \frac{(-1)^k}{k!} \binom{k}{l} 2^{R_c \beta (k-l)} \times \left(\frac{m_{r_j d}}{\bar{\gamma}_{r_j d}}\right)^{k-l} \left(\frac{m_{sd}}{\bar{\gamma}_{sd}}\right)^{l} \int_0^{2^{R_c}-1} \frac{\gamma_{sd}^{\mu+l}}{\big(1+\gamma_{sd}\big)^{\beta(k-l)}} \mathrm{d}\gamma_{sd}. \tag{B.6}$$

Using [75, Eq. (3.194.1)] in (B.6) and the fact that ${}_2F_1(a,b;c;x) = {}_2F_1(b,a;c;x)$, I_2 can be

obtained as

$$I_2 = \exp\left(\frac{m_{r_j d}}{\bar{\gamma}_{r_j d}} + 1\right) \sum_{n=0}^{m_{r_j d}-1} \sum_{m=0}^{n} \frac{(-1)^{n+m} m_{r_j d}^n}{\bar{\gamma}_{r_j d}^n n!} \binom{n}{m} 2^{R_c \beta m} \sum_{k=0}^{\infty} \sum_{l=0}^{k} \frac{(-1)^k}{k!} \binom{k}{l} 2^{R_c \beta (k-l)} \\ \times \left(\frac{m_{r_j d}}{\bar{\gamma}_{r_j d}}\right)^{k-l} \left(\frac{m_{sd}}{\bar{\gamma}_{sd}}\right)^{l} \frac{\left(2^{R_c}-1\right)^{m_{sd}+l}}{m_{sd}+l} {}_2F_1\Big(m_{sd}+l, \beta(j-l); m_{sd}+l+1; 1-2^{R_c}\Big). \tag{B.7}$$

where ${}_2F_1(b, a; c; x)$ denotes the Gauss hypergeometric function defined in [75, Eq. (9.111)].

Using (B.7), (B.3) and (B.2) in (3.41) yields the closed-form expression for the outage probability shown in (3.43).

Appendix C

Proof of Equation (5.15)

The asymptotic SER of the $S-R$ link denoted as $P_{e,sr}(e)$ is found. This was restricted to a single $S-R$ link which can be considered as a single-user uncoded transmission over Rayleigh fading channel. The instantaneous SER of the $S-R$ link can be given by

$$P_{e,sr}(e|\gamma_{sr}) = A \cdot Q(\sqrt{B\gamma_{sr}}), \tag{C.1}$$

where $\gamma_{sr} = \eta\bar{\gamma}_{sr}$ with $\eta = |h|^2$, and $\bar{\gamma}_{sr}$ represents the average SNR per symbol.

Since the $S-R$ channel is Rayleigh distributed, and by assuming that $\mathbb{E}\langle|h|^2\rangle = 1$, the RV $|h|^2$ follows an exponential distribution. Hence its PDF can be written as $p(\eta) = e^{-\eta}$ and using the Maclaurin series as $p(\eta) = 1 + \sum_{k=1}^{\infty} \frac{(-\eta)^k}{k!}$, where according to [89], $p(\eta) \approx 1$.

The average SER is obtained by averaging the instantaneous SER over the RV η as

$$P_{e,sr}(e) = \int_0^{\infty} A \cdot Q\left(\sqrt{B\eta\bar{\gamma}_{sr}}\right) p(\eta)\, d\eta. \tag{C.2}$$

The Gaussian Q-function in (C.2) can be rewritten using the one-to-one mapping of the

Gaussian Q-function with the complementary error function given in [57] by

$$Q(x) = \frac{1}{2}\text{erfc}\left(\frac{x}{\sqrt{2}}\right), \tag{C.3}$$

where the complementary error function is defined as

$$\text{erfc}(x) = \frac{2}{\sqrt{\pi}}\int_{x}^{\infty} e^{-t^2}\text{d}t, \tag{C.4}$$

obtained from [90, Eqs. (13.2.1.1.1)-(13.2.1.1.4)].

Hence, the average SER in (C.2) is given by

$$\begin{aligned} P_{e,sr}(e) &= \frac{A}{2}\int_{0}^{\infty} \text{erfc}\left(\sqrt{\frac{B\eta\bar{\gamma}_{sr}}{2}}\right) d\eta \\ &= \frac{A}{2B\bar{\gamma}_{sr}}. \end{aligned} \tag{C.5}$$

Appendix D

Determinant of the Hessian Matrix corresponding to (5.21)

Here it is shown that the objective function in (5.21) is positive semi-definite given the constraints. Without loss of generality, it is assumed that $L = 2$. Let $\mathcal{W} = g(-1)\left(\frac{N_0^3}{P}\right)$, $\mathcal{X} = g(0)\left(\frac{N_0^3}{P}\right)$ and $\mathcal{Y} = g(1)\left(\frac{N_0^3}{P}\right)$ and for the sake of notation, $x = d_{sr}$ is used. The objective function for this case can be written as:

$$SER_r = x^{-1}\left(\mathcal{W}\frac{(1-x)^{2\alpha}}{(P-P_s)^2} + \mathcal{X}\frac{x^\alpha}{P_s}\frac{(1-x)^\alpha}{P-P_s} + \mathcal{Y}\frac{x^{2\alpha}}{P_s^2}\right). \tag{D.1}$$

The Hessian matrix is defined as

$$\mathcal{H} = \begin{bmatrix} \chi & \epsilon \\ \epsilon & \iota \end{bmatrix} \tag{D.2}$$

where $\chi = \frac{\partial^2 SER_r}{\partial P_s^2}$, $\epsilon = \frac{\partial^2 SER_r}{\partial P_s \partial x}$ and $\iota = \frac{\partial^2 SER_r}{\partial x^2}$ respectively. That is,

$$\chi = x^{-1}\left[\mathcal{W}\left(\frac{6(1-x)^{2\alpha}}{(P-P_s)^4}\right)+\mathcal{X}\left(\frac{2(1-x)^{\alpha}x^{\alpha}}{P_s^3(P-P_s)}-\frac{2(1-x)^{\alpha}x^{\alpha}}{P_s^2(P-P_s)^2}+\frac{2(1-x)^{\alpha}x^{\alpha}}{P_s(P-P_s)^3}\right)+\mathcal{Y}\left(\frac{6x^{2\alpha}}{P_s^4}\right)\right], \tag{D.3}$$

$$\begin{aligned}\epsilon = \mathcal{W}&\left(-\frac{2(1-x)^{2\alpha}x^{-2}}{(P-P_s)^3}-\frac{4\alpha(1-x)^{2\alpha-1}x^{-1}}{(P-P_s)^3}\right)+\mathcal{X}\left(-\frac{(1-x)^{\alpha}x^{\alpha-2}}{(P-P_s)P_s^2}+\frac{(1-x)^{\alpha}x^{\alpha-2}}{(P-P_s)^2P_s}\right.\\ &\left.-\frac{\alpha(1-x)^{\alpha}x^{\alpha-2}}{(P-P_s)P_s^2}+\frac{\alpha(1-x)^{\alpha}x^{\alpha-2}}{(P-P_s)^2P_s}+\frac{\alpha(1-x)^{\alpha-1}x^{\alpha-1}}{(P-P_s)P_s^2}-\frac{\alpha(1-x)^{\alpha-1}x^{\alpha-1}}{(P-P_s)^2P_s}\right)\\ &+\mathcal{Y}\left(-\frac{2x^{2\alpha-2}}{P_s^3}-\frac{4\alpha x^{2\alpha-2}}{P_s^3}\right),\end{aligned} \tag{D.4}$$

$$\begin{aligned}\iota = \mathcal{W}&\left(\frac{2(1-x)^{2\alpha}x^{-3}}{(P-P_s)^2}+\frac{2\alpha(2\alpha-1)(1-x)^{2\alpha-2}x^{-1}}{(P-P_s)^2}+\frac{4\alpha(1-x)^{2\alpha-1}x^{-2}}{(P-P_s)^2}\right)+\mathcal{X}\left(\frac{(1-x)^{\alpha}x^{\alpha-3}}{(P-P_s)P_s}\right.\\ &+\frac{\alpha(\alpha-1)(1-x)^{\alpha}x^{\alpha-3}}{(P-P_s)P_s}-\frac{2\alpha^2(1-x)^{\alpha-1}x^{\alpha-2}}{(P-P_s)P_s}+\frac{\alpha(\alpha-1)(1-x)^{\alpha-2}x^{\alpha-1}}{(P-P_s)P_s}-\frac{2\alpha(1-x)^{\alpha}x^{\alpha-3}}{(P-P_s)P_s}\\ &\left.+\frac{2\alpha(1-x)^{\alpha-1}x^{\alpha-3}}{(P-P_s)P_s}\right)+\mathcal{Y}\left(\frac{x^{2\alpha-3}}{P_s^2}+\frac{2\alpha(2\alpha-1)x^{2\alpha-3}}{P_s^2}-\frac{2\alpha x^{2\alpha-3}}{P_s^2}\right).\end{aligned} \tag{D.5}$$

The determinant of $\mathcal{H}\left(SER_r\right)$ is given by $\chi\iota - \epsilon^2$. It is noted that χ and ι are positive, hence $\chi\iota > 0$. Using the expressions of χ, ϵ and ι and after some manipulations, it can be concluded that $\det\left(\mathcal{H}(P_{ser})\right) > 0$ based on the conditions $P_s \in \{0, P\}$, $x \in \{0, 1\}$, $\alpha \geq 3$ and $P > 0$.

Appendix E

Determinant of the Hessian Matrix for $L = 2$ in (6.29)

Using (6.27) for $L = 2$ and for the sake of clarity let:

$$k = \frac{(A/2B)^2 A_0}{g_{QAM}\sigma_{sd}^2\sigma_{sr_1}^2\sigma_{sr_2}^2}\left(\frac{P}{N_0}\right)^{-3}, \tag{E.1}$$

$$\Psi_i = \frac{2B\sigma_{sr_i}^2}{Ag_{QAM}\sigma_{r_id}^2}, \tag{E.2}$$

where $i = \{1, 2\}$. Henceforth, the equation in (6.29) can be written as

$$SER_{Retr} \approx \frac{k}{\alpha_0^3}\left(1 + \Psi_1\frac{\alpha_0}{\alpha_1}\right)\left(1 + \Psi_2\frac{\alpha_0}{\alpha_2}\right) \triangleq f(\alpha_0, \alpha_1, \alpha_2). \tag{E.3}$$

For $L = 2$, the Hessian matrix $\mathcal{H}$ is given by

$$\mathcal{H} = \begin{bmatrix} \frac{\partial^2 f}{\partial\alpha_0^2} & \frac{\partial^2 f}{\partial\alpha_0\partial\alpha_1} & \frac{\partial^2 f}{\partial\alpha_0\partial\alpha_2} \\ \frac{\partial^2 f}{\partial\alpha_1\partial\alpha_0} & \frac{\partial^2 f}{\partial\alpha_1^2} & \frac{\partial^2 f}{\partial\alpha_1\partial\alpha_2} \\ \frac{\partial^2 f}{\partial\alpha_2\partial\alpha_0} & \frac{\partial^2 f}{\partial\alpha_2\partial\alpha_1} & \frac{\partial^2 f}{\partial\alpha_2^2} \end{bmatrix}, \tag{E.4}$$

and using some linear algebra the determinant of $\mathcal{H}$ (3×3 matrix) can be found and expressed as

$$\det(\mathcal{H}) = k^3\Psi_1\Psi_2\left(\frac{4\Psi_1^2\Psi_2^2}{\alpha_0^5\alpha_1^5\alpha_2^5} + \frac{20\Psi_1\Psi_2^2}{\alpha_0^6\alpha_1^4\alpha_2^5} + \frac{16\Psi_2^2}{\alpha_0^7\alpha_1^3\alpha_2^5} + \frac{20\Psi_1^2\Psi_2}{\alpha_0^6\alpha_1^5\alpha_2^4} + \frac{84\Psi_1\Psi_2}{\alpha_0^7\alpha_1^4\alpha_2^4} + \frac{64\Psi_2}{\alpha_0^8\alpha_1^3\alpha_2^4} + \frac{16\Psi_2^2}{\alpha_0^7\alpha_1^5\alpha_2^3} + \frac{64\Psi_1}{\alpha_0^8\alpha_1^4\alpha_2^3} + \frac{64}{\alpha_0^9\alpha_1^3\alpha_2^3}\right). \tag{E.5}$$

It can be noted that for $\alpha_i > 0$ for $i = \{0, 1, 2\}$ and since k and Ψ are positive, $\det(\mathcal{H}) > 0$.